Ice Jams in Lower St. Regis River Akwesasne, NY

Report submitted to
Water Resources Program, Environment Division
The Saint Regis Mohawk Tribe
(Contract No. 19-0015)

Fengbin Huang and Hung Tao Shen

Department of Civil and Environmental Engineering
Clarkson University
Potsdam, NY 13699-5710

July 2020

Executive Summary

In 2016 the Saint Regis Mohawk Tribe decommissioned and removed the Hogansburg Dam on the lower St. Regis River and restored over 555 miles of migratory fish access. During winter months, ice jams occurred on this river prior to construction in 1929, during dam operation and after its removal. Dr's. Hung Tao Shen and Fengbin Huang of the internationally renowned river ice research group of Clarkson University present a numerical model on the ice transport and ice jam processes in the Lower St. Regis River, to evaluate pre- and post-dam removal conditions at this site. Diagnostic simulations for water flow and ice movement characteristics are simulated with the model for discharges ranging from a low flow of 850 ft^3/s to a high flow of 7,000 ft^3/s. These simulation results indicate that under the lowest flow conditions of 850 ft3/s, the dam reduced the surface ice run from being transported downstream, and allowed the ice cover accumulation to form upstream of the dam. However, at moderately higher flows of 1,400 ft^3/s and 4,000 ft^3/s, both pre-removal and post-removal conditions, allow the ice run to move through this section of the river and form a thick accumulation of ice immediately downstream.

Although the removal of the dam does allow for increased water flow and surface ice transport capacity downstream at low flows, this change is effectively negated as flow increases to 1,400 ft^3/s and beyond. Downstream of the former dam location flow slows down due to a backwater effect from the St. Lawrence River. At this point, the ice discharge through the former dam site forms a thick ice jam downstream regardless of the presence or absence of the former Hogansburg Dam because the solid ice cover in the backwater zone blocks the ice and promotes the jam formation. Historical and recorded measurements of past ice jam flooding events and weather conditions are reviewed to aid in developing a forecasting method for assisting in emergency management.

A potential mitigation scheme for reducing ice jam flooding in the Hogansburg area with the use of ice booms is evaluated using the model. The use of one and two strategically located ice booms at the upstream of the former dam site are evaluated and compared to those models without ice booms installed in an effort to determine the local effects within the study reach. Although the ice booms could reduce the ice supply to the area downstream of the dam and alleviate the ice jam flooding potential in Hogansburg during periods of low water flow, at the same time, ice accumulation against the ice boom will result in high water levels and potential flooding in the upstream reach. This could cause additional areas of isolated flooding, property damage, and potential environmental harm due to the severe erosional forces of ice flows on shorelines that have not previously experienced this type of wear.

Ultimately, the effect of dam removal decreases as the flow discharge increases, which is typical of ice cover breakup conditions. Similarly, the addition of one or two ice booms may have a beneficial effect on the area downstream of the former dam site during times of low flow. However, this effect could be counteracted by the flooding that would be experienced within the upstream reach areas under these similar conditions. It is of value to note that based on these simulations, neither the existence of the former Hogansburg Dam, nor the installation of ice booms would adequately negate the potential for flooding situations either above or below the location of the former dam. In fact, it is illustrated that under a scenario where two ice booms are installed and high water flow conditions are present, that significant flooding can occur at both

locations above and below the former dam site location. Based on these scenarios and the modeling presented within this report, a case could be made that by installing a single well placed and designed ice boom in the area upstream of the former dam location that a reasonable amount of ice jam flood protection could be provided to the Hogansburg area downstream of the former dam. It could also be suggested that in doing so, a reasonable amount of water level rise would be experienced within areas upstream of the installed ice boom.

Tiernan W. Smith

Table of Contents

List of Figures

List of Tables

Unit Coversion

Length:
1 in = 0.0254 m
1 ft = 0.3048 m
1 mi = 1.60934 km

Area:
1 in^2 = 645.16 mm^2
1 ft^2 = 0.092903 m^2

Volume:
1 ft^3 = 0.02831681 mm^3

Temperature:
T_C =(5/9)(T_F-32°)

Force:
1 lb = 4.448 N

1. Introduction

The Hogansburg Dam in the St. Regis River was located upstream of the St. Regis Mohawk Reservation. The dam was initially built in the late 1890s for mill and small electric production. After damaged by ice floes in 1921, the dam was replaced by the concrete dam and powerhouse in 1929. The dam blocked migratory patterns of fish from hundreds of miles of upstream habitat. The dam was removed during the period between July and November 2016, when the flow rate was low. Removal of this dam is the first of its kind, a historic accomplishment for tribal sovereignty and a success for ecological restoration in the St. Lawrence River basin (David 2016). The dam removal will improve the water quality and create the passage for the fish from the St. Lawrence River to the St. Regis River. However, ice jam conditions will likely change after the dam removal, as indicated by ice conditions reported before the dam was in place (Erie 2012). A two-dimensional river ice dynamic model (Shen et al. 2000, Shen 2010) is employed to evaluate the effect of the dam removal on the ice jam flooding potential near the dam site in the Lower St. Regis River. Based on the historical monthly average flows during winter and spring (SRMT, 2015), and higher mechanical breakup flow conditions based on the Feb. 2018 ice jam event, four discharges ranging from 24.07 m^3/s (850 ft^3/s) to 198.22 m^3/s (7000 ft^3/s) with different ice thickness are used to simulate breakup and related ice jam conditions. A preliminary model study (Huang and Shen 2016) was carried out based on the bathymetry of a 1.3 km reach near the dam surveyed in 2012 shown in Figure 1 (Fisher Associates 2015) together with approximated bathymetry beyond this short reach. An additional bathymetric survey was conducted in 2016 for an extended river reach between Highway 37C Bridge in Helena and the confluence with the St. Lawrence River (Fisher Associates 2017), which is used in the present study.

2. The Study Reach

The study reach is the St. Regis River extending upstream (southerly) from the confluence with the St. Lawrence River, to Highway 37C Bridge in Helena, including the low-lying floodplain areas. Figure 1 shows the pre-dam removal bathymetry within a distance of 1.3 km provided by CH2M, which was surveyed in 2012 (Fisher Associates 2015) and the post-dam removal bathymetry surveyed in 2016 (Thew Associates, 2016). The powerhouse on the east side of the Dam in Figure 2 remains. The datum of the bed elevation and horizontal survey is referenced to NAVD 88 and NAD 83, respectively. The simulation domain covers a distance of 13.5 km as shown in Figure 3 and the floodplains in the Hogansburg area. The red line in Figure 3 shows the river thalweg. Figure 4 shows the longitudinal profile of channel thalweg. Figure 5 shows the river kilometer from Helena in the study reach. The hydraulic boundary conditions include the inflow discharge at upstream and water level downstream.

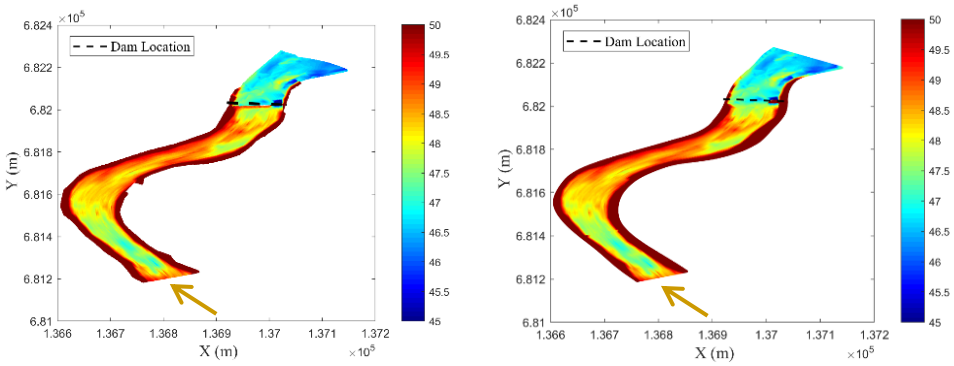

Figure 1. Pre- and Post-dam removal bathymetries (Left: Pre-removal; Right: Post-removal).

Figure 2. Hogansburg Dam.
(https://www.arcgis.com/apps/Cascade/index.html?appid=21952c937eb84b08addedd2ee0a933ff).

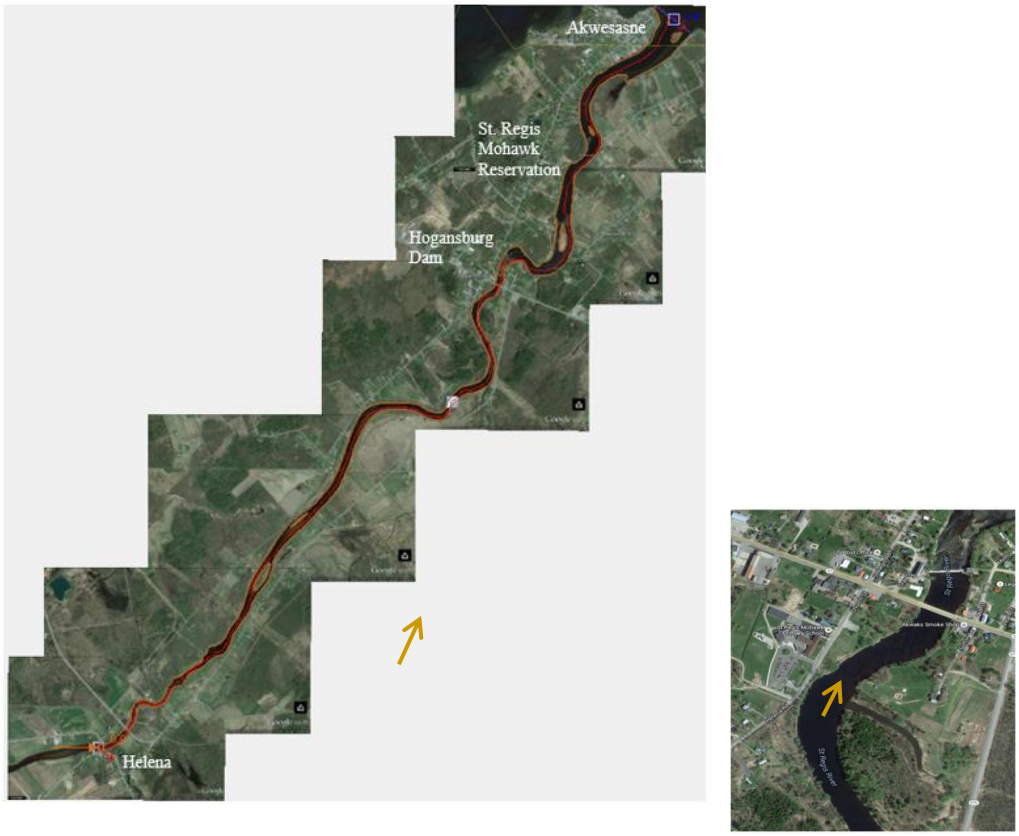

Figure 3. Simulation domain extending from the St. Lawrence River to Helena, NY, and the vicinity of the Dam.

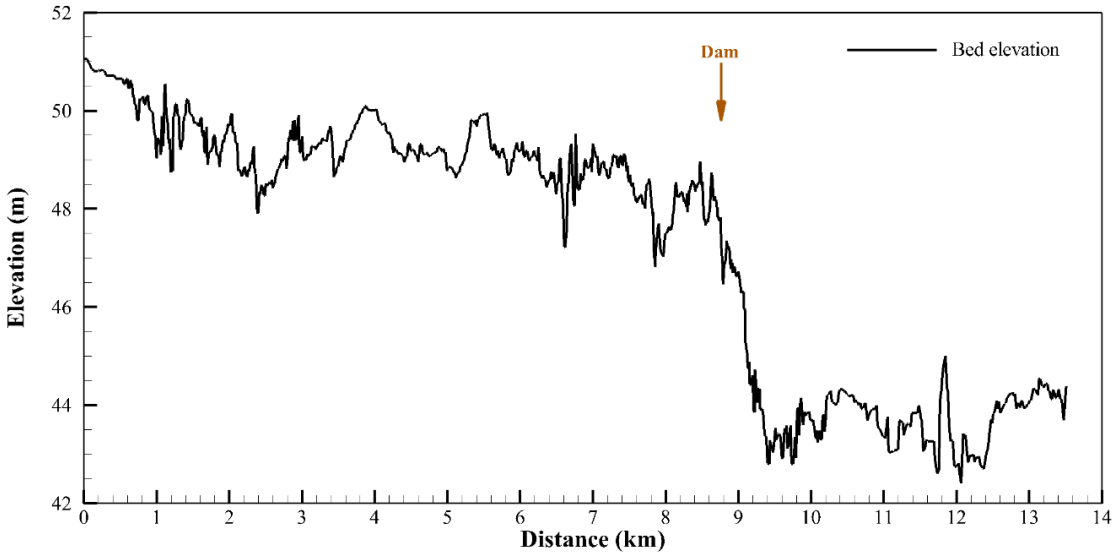

Figure 4. longitudinal profile of channel thalweg starting from Helena at km 0 to the confluence at km 13.5.

The post-removal survey of the area around the dam site was conducted in 2016 (Thew Associates 2016). An additional bathymetric survey on the cross sections upstream and downstream of the dam was conducted in 2017 (Fisher Associates 2017). Figure 6 shows the the surveyed cross sections between Helena and the St. Lawrence River confluence in 2017 for the post-dam-removal condition. The survey included 386 cross sections in the portion of the upstream of the dam towards Helena and downstream of the dam towards St. Lawrence River. The spacing of the cross sections is approximately every 30.48m (100 ft), except for the reach near the confluence where the spacing is 152.4 m (500 ft). The fine sediment at the upstream of the dam site is likely to be transported and deposited at the dam site after the dam removal. The major bed change is at the dam site and its proximity. The post-removal survey of the dam site captured the bed change. The bed change in the reaches upstream and downstream of the dam is limited. Thus, it is assumed that the pre-removal bathymetry in the reaches upstream and downstream of the dam is the same as the surveyed data. Two sets of bathymetry, i.e. the pre-removal and post-removal bathymetries, will be used in the simulations. Figure 7 shows the post-dam-removal bathymetry. Figure 8 shows the comparison of the bed elevation at the dam site between pre-removal and post-removal conditions. Figure 9 shows the bed elevation of floodplains.

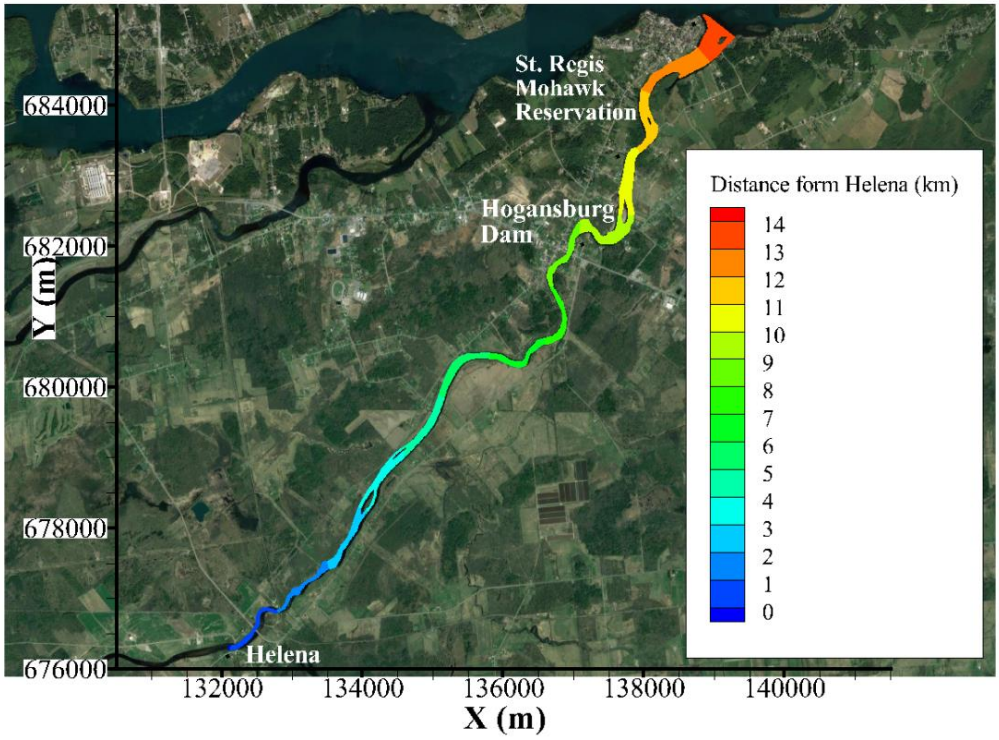

Figure 5. River kilometer from Helena of the study reach.

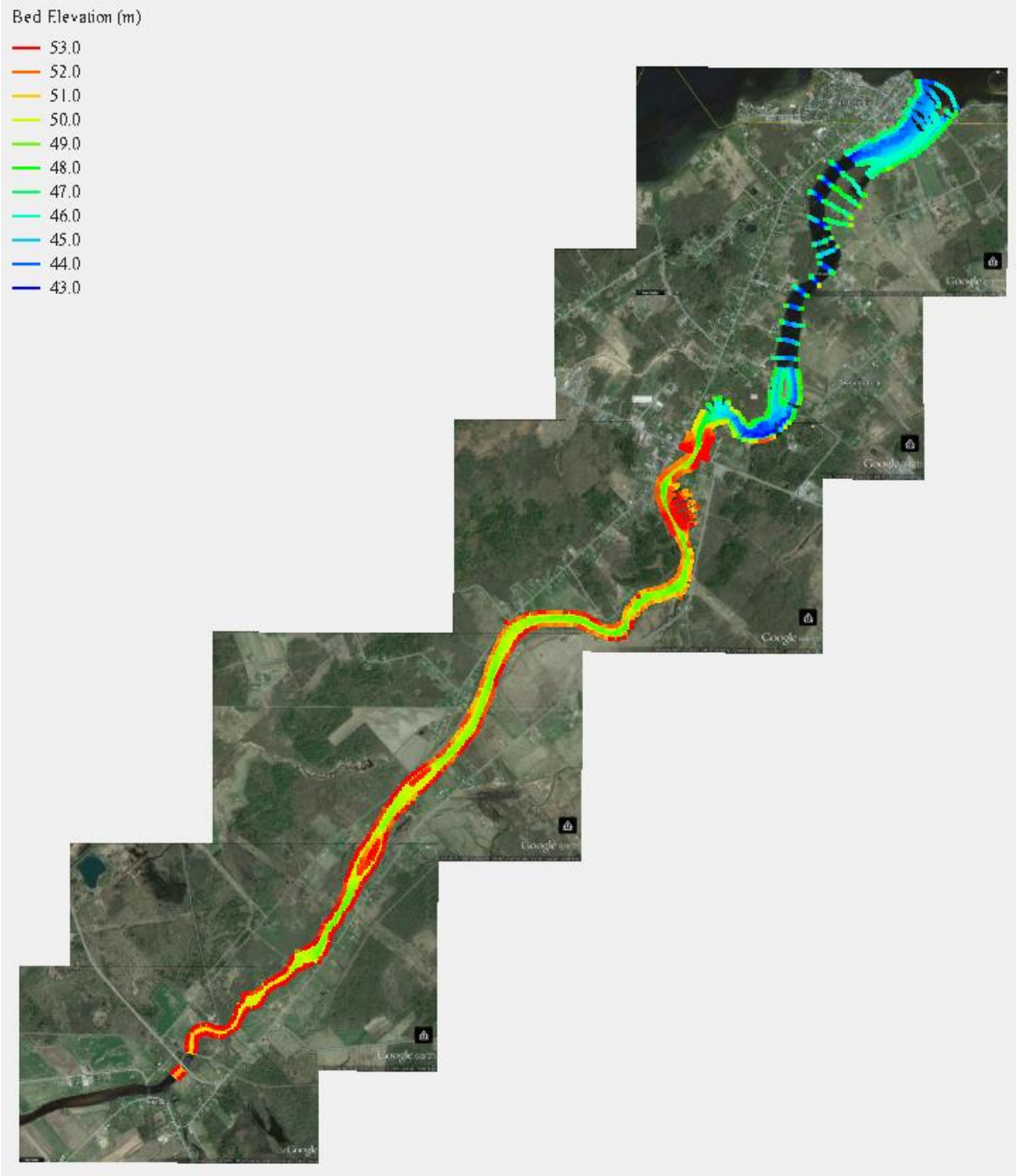

Figure 6. The 2017 surveyed cross sections.

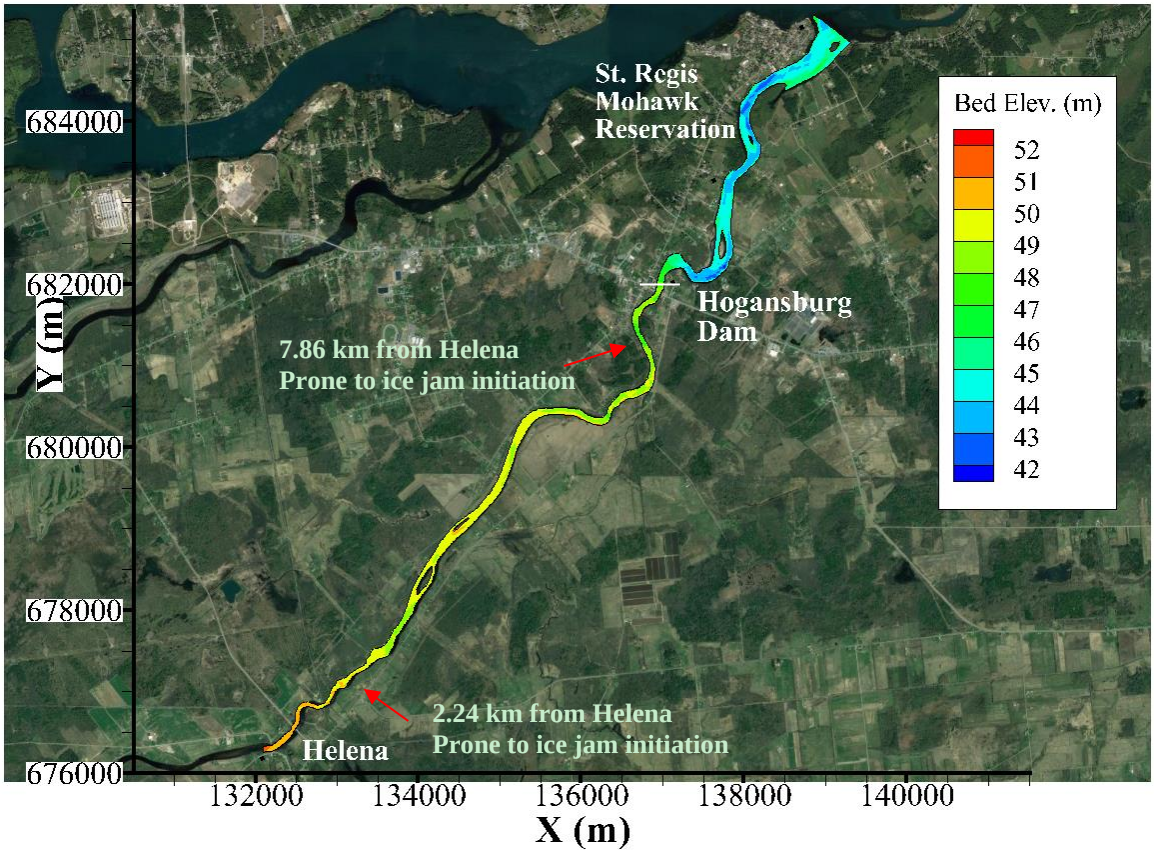

Figure 7. Bed elevation distribution based on the 2017 surveyThe red arrows in the figure point out the locations that are prone to the ice jam initiation.

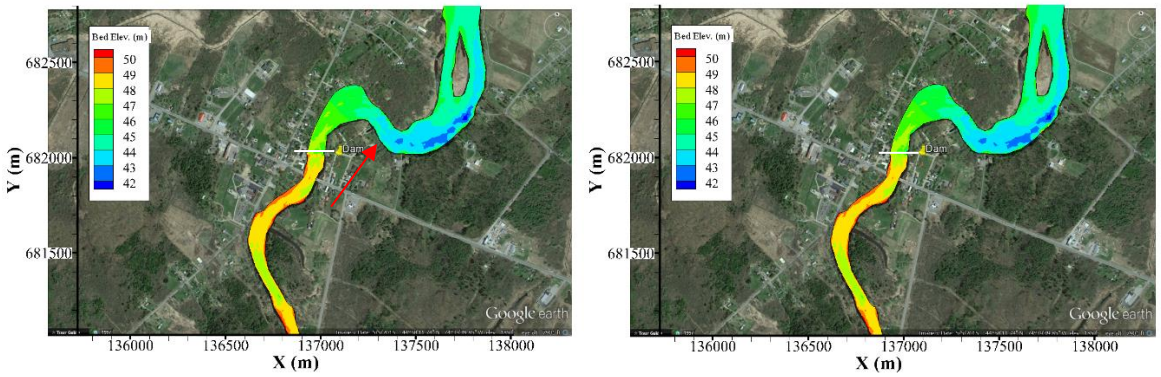

Figure 8. Bed elevation near the dam site (Left: pre-removal; Right: post-removal). The red arrow in the figure points to the channel bend exit that is prone to ice jam initiation, followed by a pool with larger flow depth due to the backwater from the St. Lawrence River.

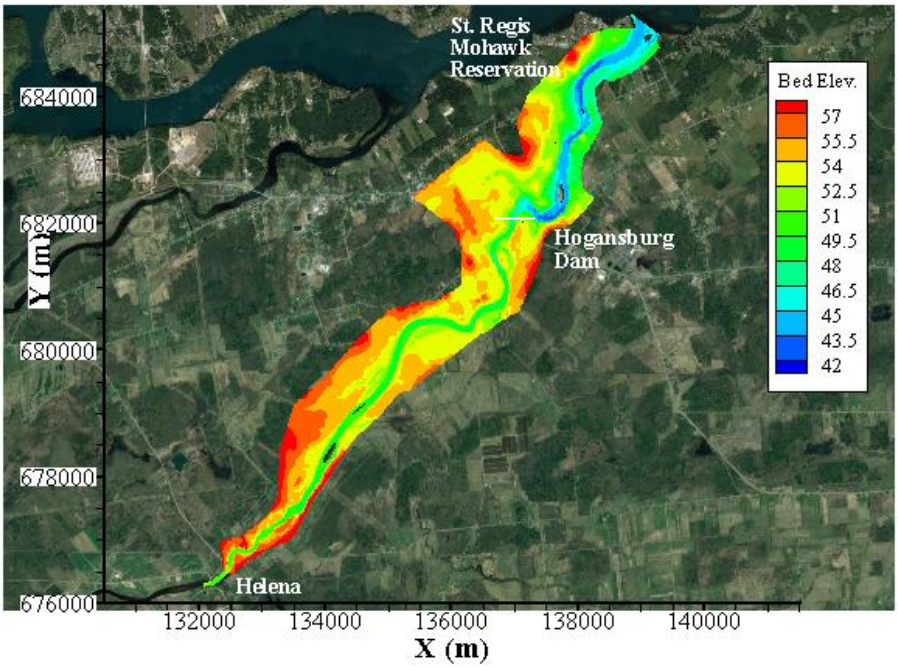

Figure 9. Bed elevation distribution based on the 2017 survey with the floodplain.

The channel geometry plays a vital role in the flow and ice movement, as well as the jamming potential. Figure 7 shows two locations with contraction and large increase in flow depth that are prone to the ice jam initiation upstream of the dam site. Figure 8 shows the width contraction and the increase flow depth at the exit of the channel bend downstream of the dam. The effective passage for ice movement is relatively narrow because of the shallow area at the outer bank and a small island near the inner bank downstream of the powerhouse.

3. Ice Transport Characteristics

In this section, diagnostic simulations are made to investigate the flow and ice movement characteristics in the lower St. Regis under different flow conditions and the effect of dam removal, assuming no ice cover in the reach. Four scenarios with low and high inflow discharges are simulated for pre- and post-dam removal conditions. The water level at the downstream boundary is assumed to be 47.0 m, which is the mean historical water level at the St. Lawrence River confluence. For this study, the bed roughness in the channel is assumed to be 0.025, since the main bed material is coarse sand. The bed roughness on the floodplain is 0.07. The ice supply from the upstream boundary at Helena consists of a moderate ice concentration of 0.4 with a thickness of 0.2 m. The ice Manning's roughness coefficient varies linearly from a minimum value of 0.02 for a single layer ice run to a maximum value of 0.06 for thick ice jams.

3.1 Pre-Dam-Removal, Q = 24.07 m^3/s (850 ft^3/s)

The surface ice movement with a steady inflow discharge of 24.07 m^3/s (850 ft^3/s) from the upstream boundary at Helena was simulated for the pre-dam removal condition. Figure 10 shows the initial ice-free flow condition near the Hogansburg Dam. The flow depth increases rapidly from the immediate downstream of the dam to the bend, creating a pool where the flow velocity decreases to less than 0.1 m/s. Figure 11 shows the simulated surface ice arrival at the dam from Helena at hour 6 and the ice condition at hour 24. The ice run stopped at the dam and formed a juxtaposed ice accumulation due to the low flow velocity. Figure 12 shows the stabilized ice condition at hour 36. The surface ice movement stopped at the dam pool, and the ice accumulation extends upstream with the incoming ice. The small amount of the ice floes passing the dam through the stop-log gate spillway stopped at the exit of the sharp bend downstream.

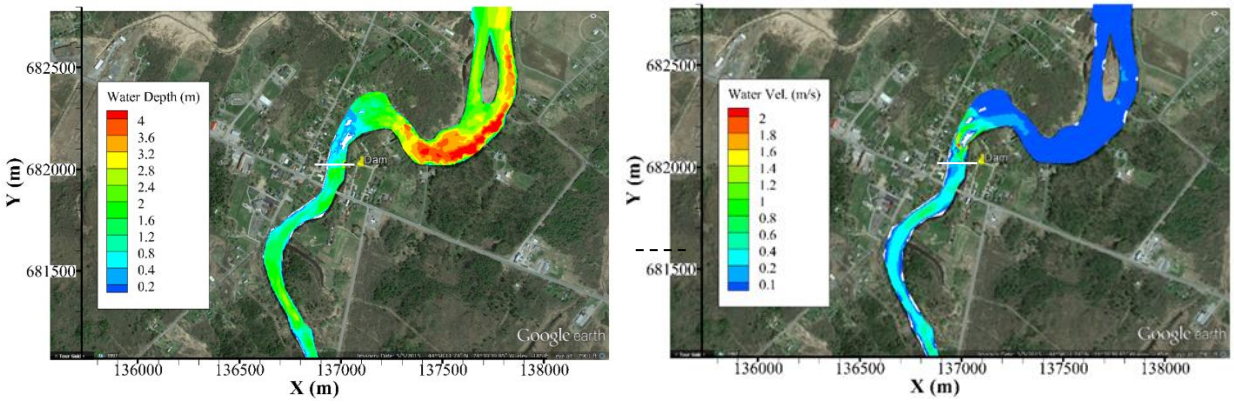

Figure 10. Simulated initial flow condition, Q = 24.07 m^3/s (850 ft^3/s) – Pre-dam-removal. White color indicates zero value.

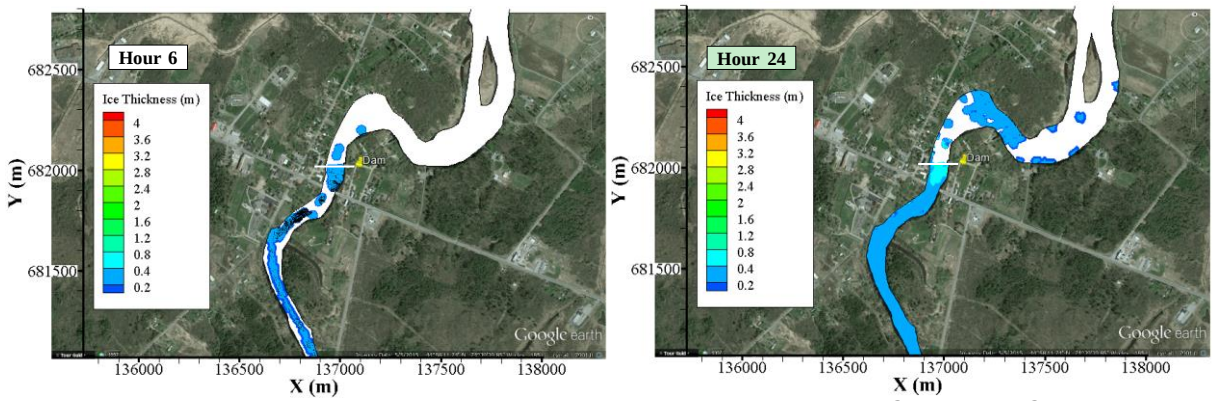

Figure 11. Ice thickness distribution at hrs 6 and 24, Q = 24.07 m^3/s (850 ft^3/s) – Pre-dam-removal.

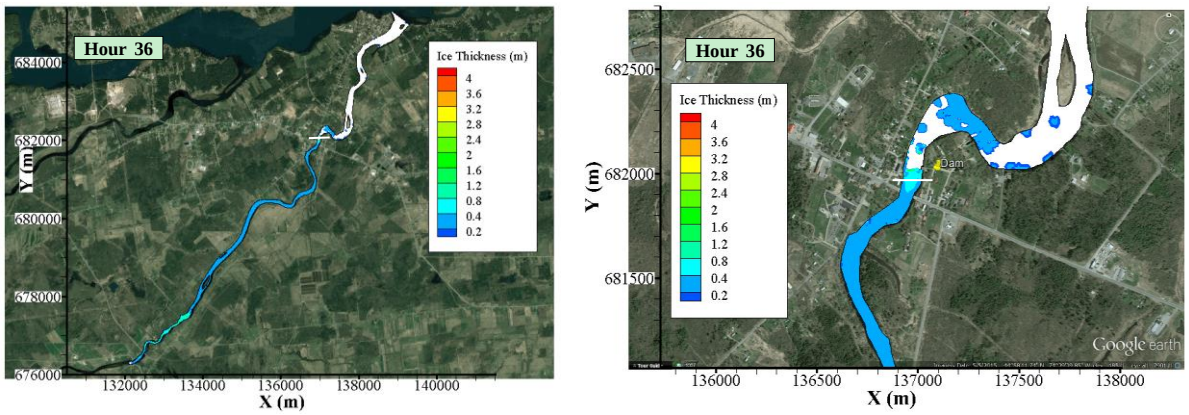

Figure 12. Ice thickness distribution at hr 36, Q = 24.07 m^3/s (850 ft^3/s) – Pre-dam-removal.

3.2 Post-Dam-Removal, Q = 24.07 m^3/s (850 ft^3/s)

Figure 13 shows the initial ice-free flow condition with a steady discharge of 24.07 m^3/s (850 ft^3/s) from the upstream boundary for the post-dam removal condition. Figure 14 shows the ice conditions at hours 5, 24, and 48. The ice run reaches the dam site in 5 hours, one hour faster than the pre-removal condition. The removal of the dam enhanced flow and ice transport. Comparing with the pre-dam -removal scenario, the ice discharge past the dam site increased and exceeds the ice transport capacity at the bend exit downstream. Ice jam formed in the bend due to the narrowing of the flow passage and the rapid reduction of the flow velocity at the bend exit. The jam expands towards the island downstream during its upstream progression, along with a small ice discharge to downstream. Figure 15 shows the ice thickness distribution at hour 72. The jam in the bend grows with a small ice discharge to downstream.

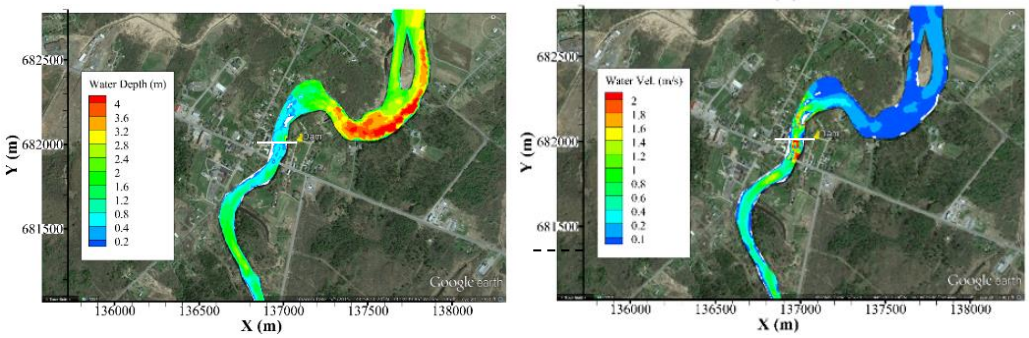

Figure 13. Simulated initial flow condition, Q = 24.07 m^3/s (850 ft^3/s) – Post-dam-removal.

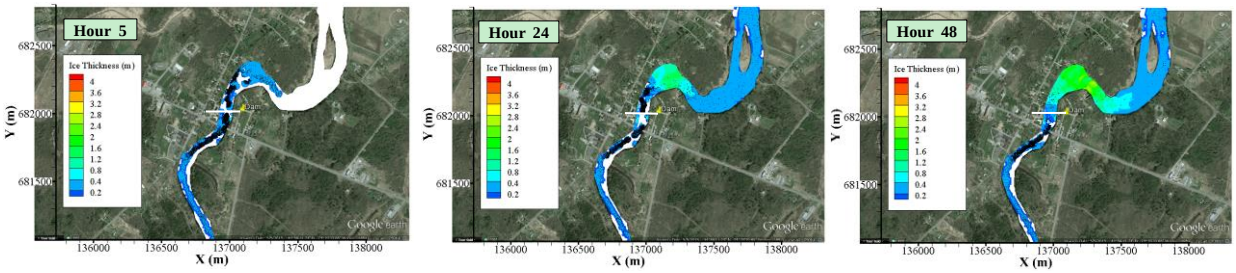

Figure 14. Ice thickness distribution at hrs 5, 24, and 48, Q = 24.07 m^3/s (850 ft^3/s) – Post-dam-removal.

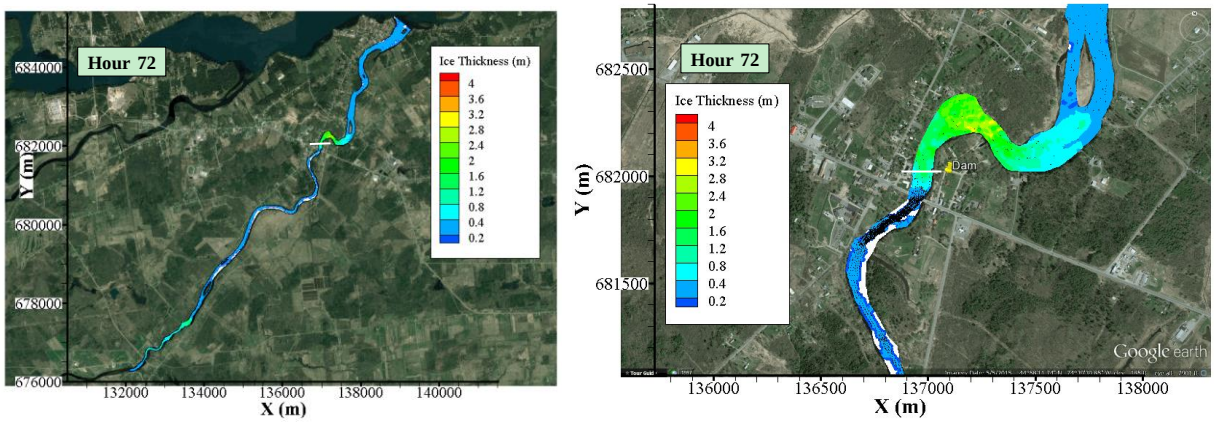

Figure 15. Ice thickness distribution at hour 72, Q = 24.07 m^3/s (850 ft^3/s) – Post-dam-removal. (The vectors represent ice velocities.)

3.3 Pre-Dam-Removal, Q = 39.64 m^3/s (1400 ft^3/s)

Figure 16 shows the initial ice-free flow condition with a steady discharge of 39.64 m^3/s (1400 ft^3/s) for the pre-dam removal condition. The water velocity downstream of the dam is generally more than 1.5 m/s but quickly decreases along the channel bend due to the increasing flow depth. Figure 17 shows the ice conditions at hours 5, 24, 48, and 72.

- Hour 5: The travel time for the surface ice run from Helena to the dam is about 5 hours.
- Hour 24: Ice started to accumulate in the channel bend.

- Hour 48: An ice jam formed near the exit of the bend due to the narrowing of the flow pass and the rapid reduction of the flow velocity at the bend exit.
- Hour 72: The jam in the bend remains and grows, with some ice moving to downstream due to the high water discharge.

This downstream ice movement decreases with time, as shown in Figure 18. Figure 18 also shows the ice accumulation in the entire reach at hour 96.

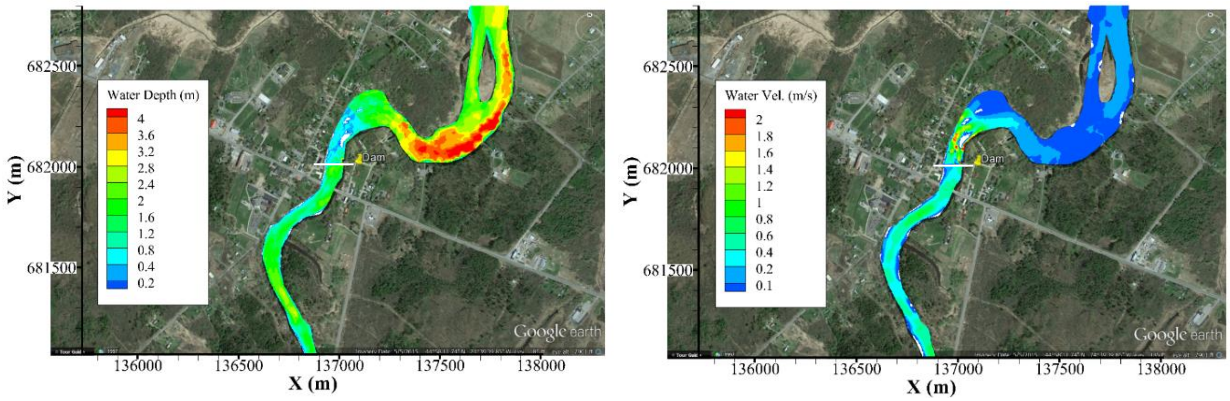

Figure 16. Simulated initial flow condition, Q = 39.64 m^3/s (1400 ft^3/s) – Pre-dam-removal.

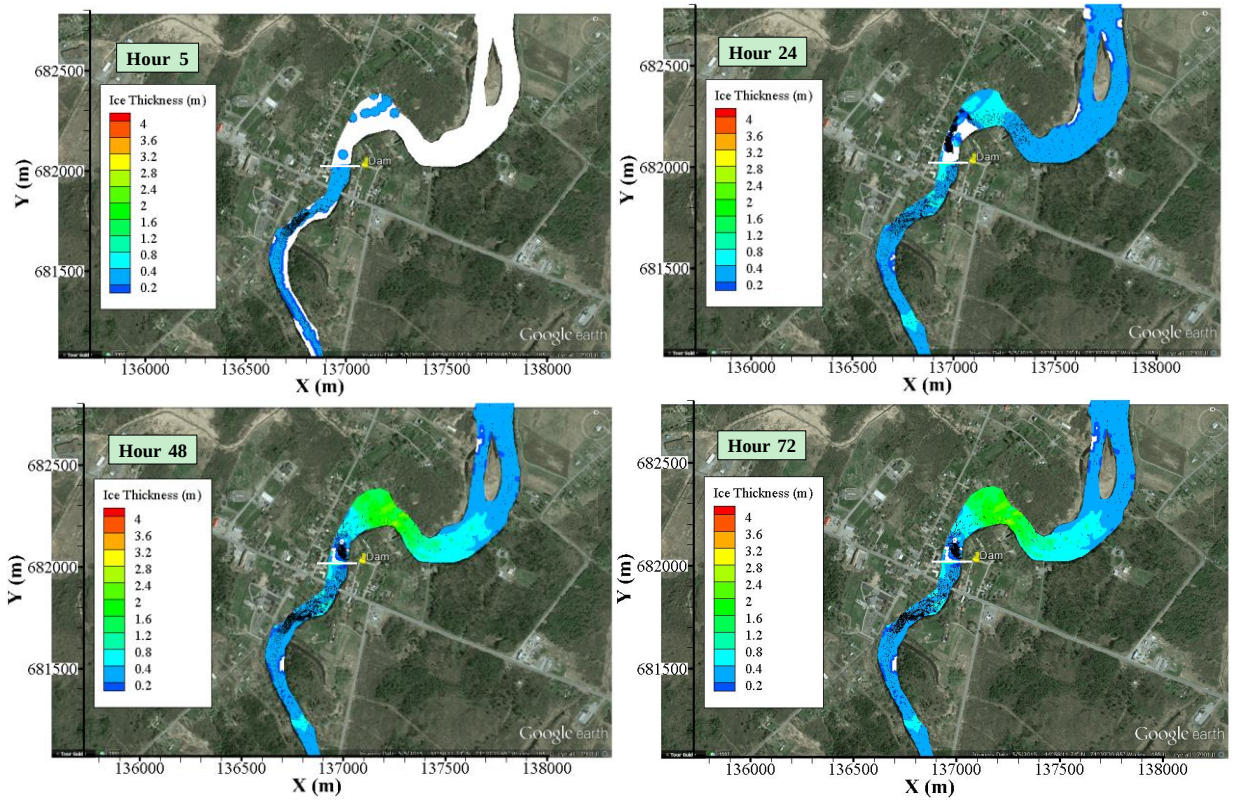

Figure 17. Ice thickness distribution at hrs 5, 24, 48, and 72, Q = 39.64 m^3/s (1400 ft^3/s) – Pre-dam-removal.

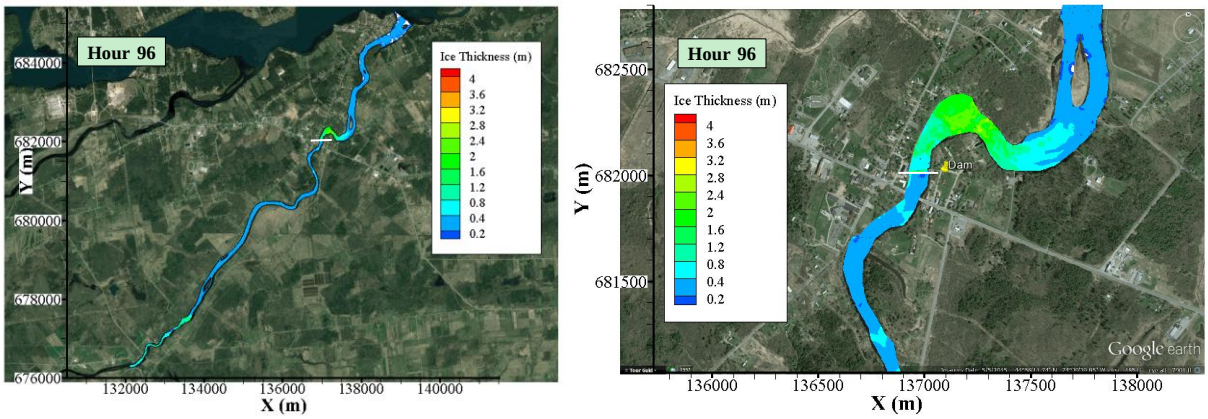

Figure 18. Ice thickness distribution at hour 96, Q = 39.64 m^3/s (1400 ft^3/s) – Pre-dam-removal.

3.4 Post-Dam-Removal, Q = 39.64 m^3/s (1400 ft^3/s)

Figure 19 shows the initial ice-free flow condition with a steady discharge of 39.64 m^3/s (1400 ft^3/s) for the post-dam removal condition. Figure 20 shows the ice condition at hours 5, 24, 48, and 72.

- Hour 5: The travel time for the ice run from Helena to the former dam site is little less than 5 hours. The removal of the dam enhanced the flow and ice transport passing the dam site.
- Hour 24: The ice jam starts to form at the bend exit due to the narrowing of the flow pass and the rapid reduction of the flow velocity.
- Hour 48 and 72: The jam develops in the pool and progress towards upstream, with a small amount of ice breeding to downstream.

Figure 21 shows the ice accumulation in the entire reach at hour 96. The jam in the bend grew, and the small ice discharge to downstream stopped.

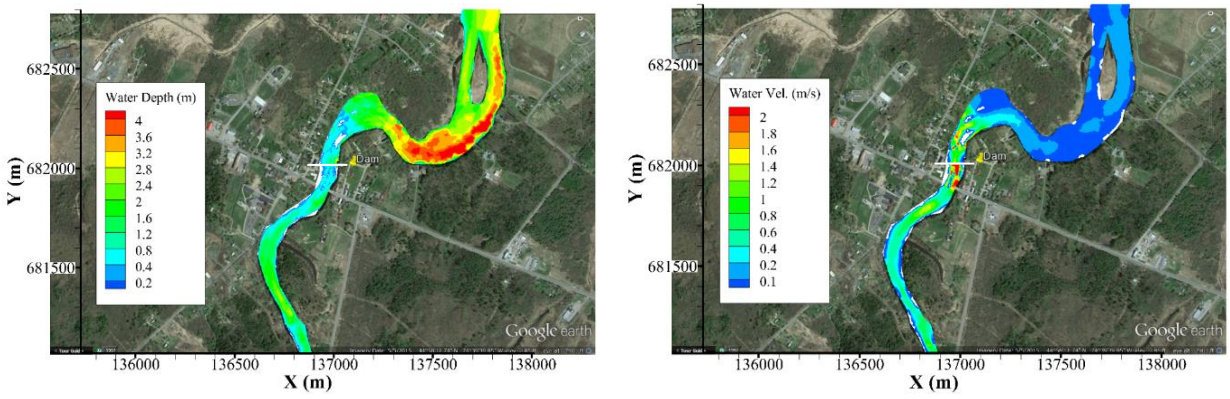

Figure 19. Simulated initial flow condition, Q = 39.64 m^3/s (1400 ft^3/s) – Post-dam-removal.

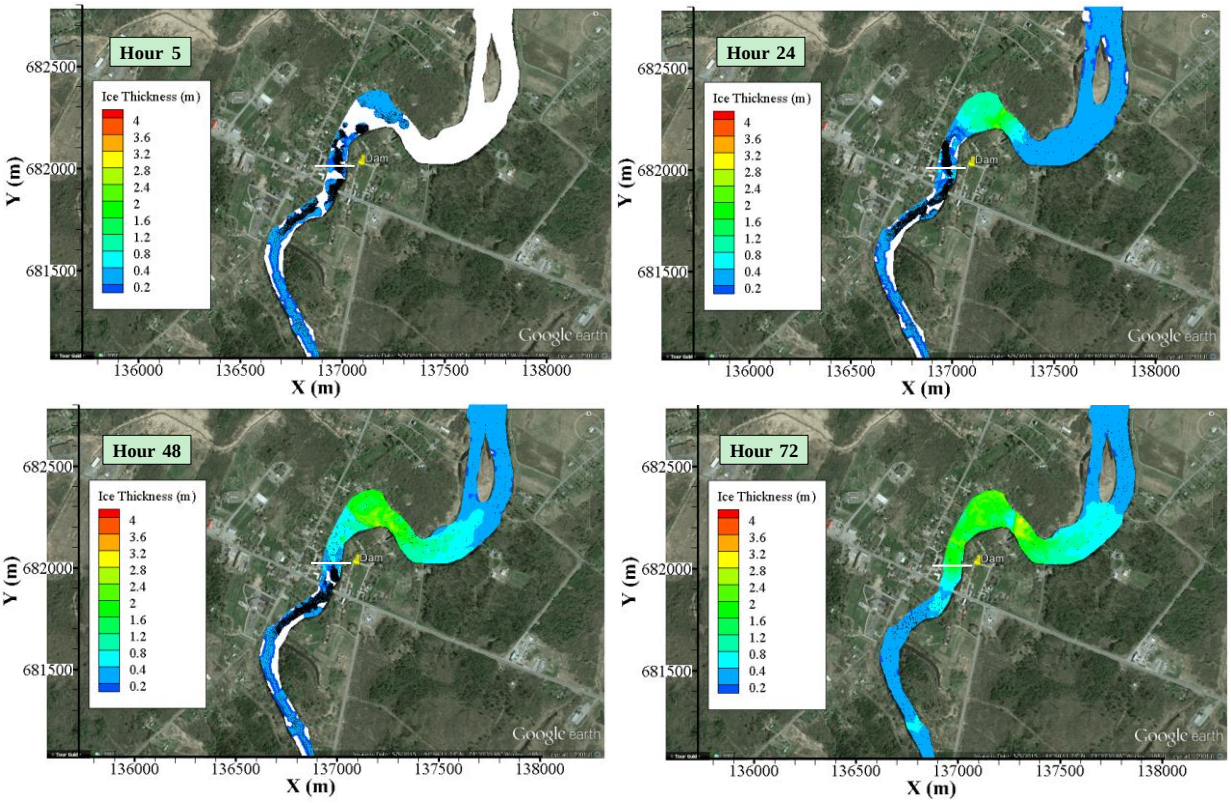

Figure 20. Ice thickness distribution at hrs 5, 24, 48, and 72, Q = 39.64 m^3/s (1400 ft^3/s) – Post-dam-removal.

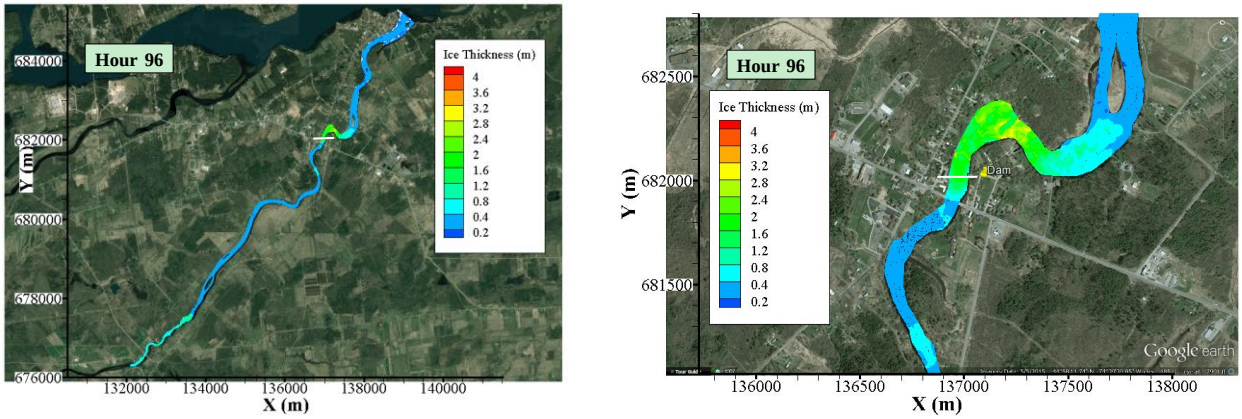

Figure 21. Ice thickness distribution at hour 96, Q = 39.64 m^3/s (1400 ft^3/s) – Post-dam-removal.

3.5 Summary

Diagnostic simulations of the ice transport and jamming processes are conducted for both pre-removal and post-removal bathymetries. The simulated results indicate that the dam blocked most surface ice and lead to the ice accumulation towards upstream under pre-removal conditions. The enhanced flow condition and the ice transport capacity due to the dam removal increased the ice discharge passing the dam site. The collective impact of the channel geometry and the abrupt change of the flow condition in the pool area increased the potential of the ice

accumulation/jam near the bend exit. Figure 22, 23, 24, and 25 show the ice accumulation and the water surface profiles of the four scenarios when the flow and ice conditions are stabilized. The pre-dam-removal case showed ice accumulation at the dam under the lower flow condition of 24.07 m^3/s (850 ft^3/s). The removal of the dam allows more ice transport to downstream. Ice jamming occurs in the downstream pool and results in an increase in the water level downstream of the dam. This also occurs for the pre-dam-removal case under the high flow condition of 39.64 m^3/s (1400 ft^3/s). At the discharge of 24.07 m^3/s (850 ft^3/s), the dam removal leads to lower water levels upstream of the dam site and a mild jam formation in the bend. Another ice jam located near downstream of Helena at km 2.24 brings about the head loss and contributes to the lower water levels between the jam and Hogansburg. However, at the discharge of 39.64 m^3/s (1400 ft^3/s), the dam removal enhances the flow and ice transport past the dam site and results in a larger ice jam in the downstream pool. As a result, the water level at Hogansburg is higher than that of the pre-dam-removal condition. The localized thick ice accumulations at the upstream of the dam site increase the upstream water levels. Therefore, the water levels between the upstream jam and the dam site are higher than those for the pre-dam-removal conditions. Figure 26 shows the comparison of the water surface profiles for the four simulated cases.

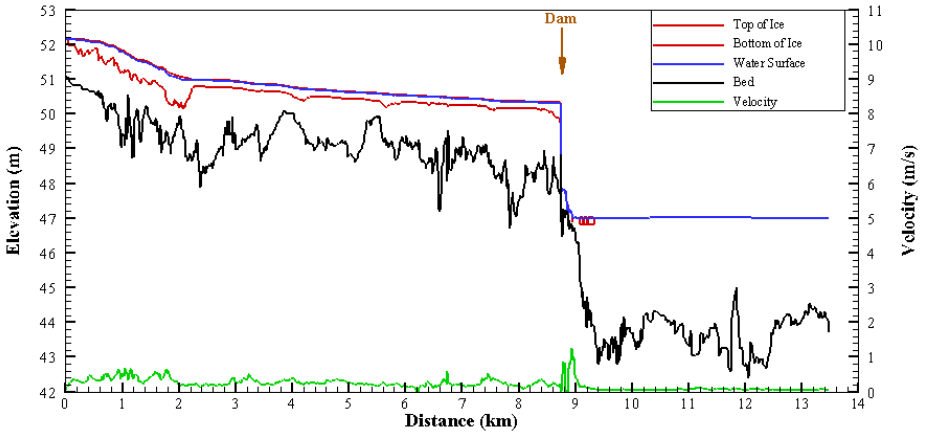

Figure 22. Longitudinal profiles of flow and ice conditions at hour 48, 24.07 m^3/s (850 ft^3/s) – Pre- dam-removal.

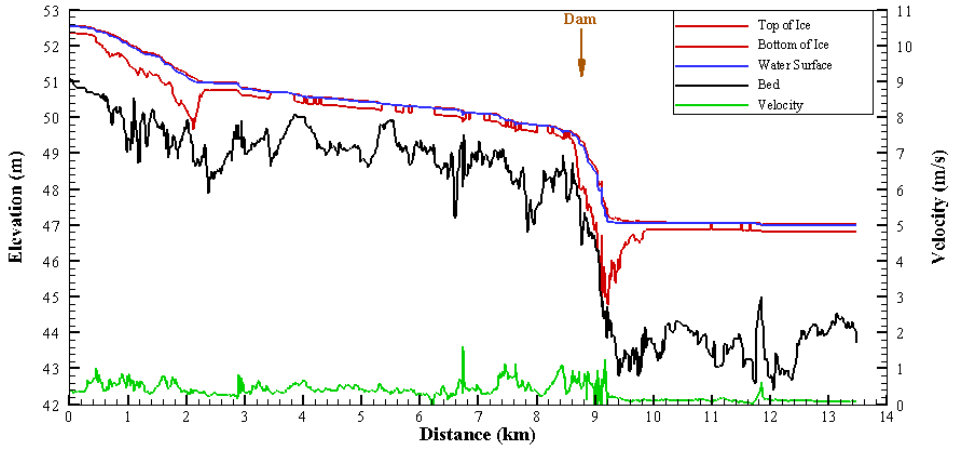

Figure 23. Longitudinal profiles of flow and ice conditions at hour 72, 24.07 m^3/s (850 ft^3/s) – Post-dam-removal.

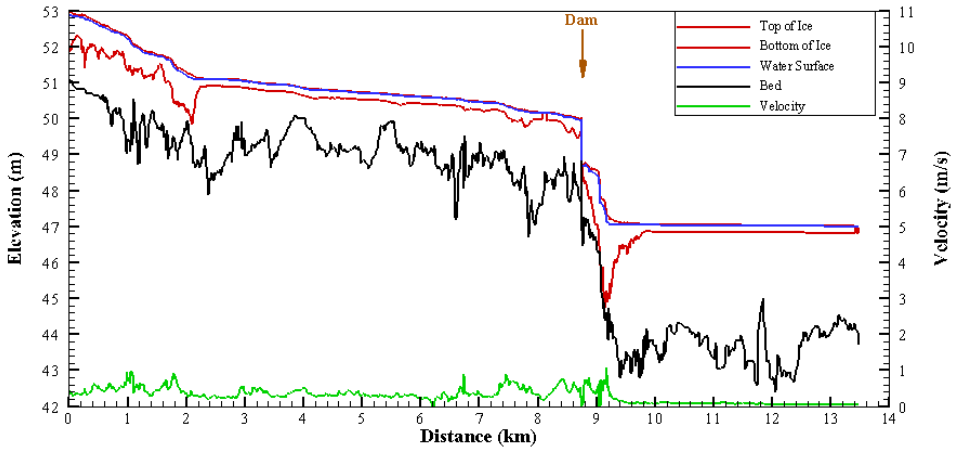

Figure 24. Longitudinal profiles of flow and ice conditions at hour 96, Q = 39.64 m^3/s (1400 ft^3/s) – Pre-dam-removal.

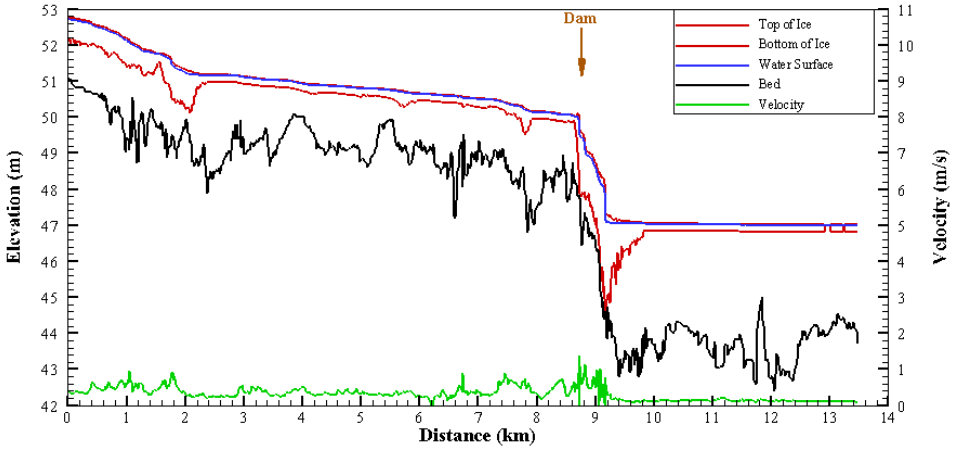

Figure 25. Longitudinal profiles of flow and ice conditions at hour 96, Q = 39.64 m^3/s (1400 ft^3/s) – Post-dam-removal.

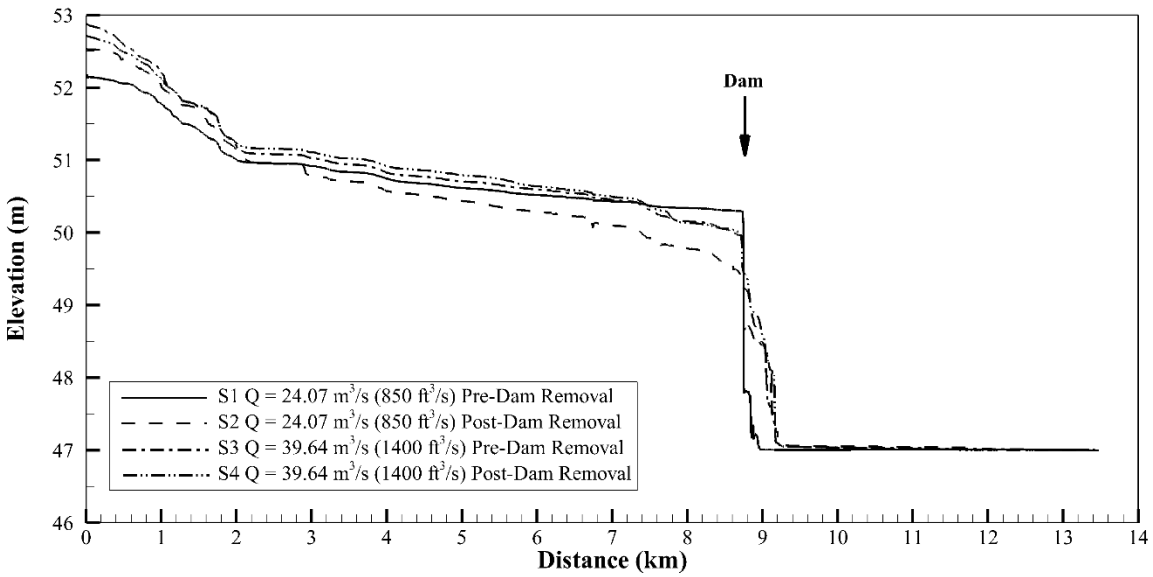

Figure 26. Comparison of water surface profiles.

The maximum water level and ice thickness at key locations shown in red circles in Figure 27 are summarized in Table 1. The two locations near the banks at Hogansburg were flooded in 2018 and 2020 ice-jam flooding events. The third one is at the dam site. The fourth one is at the NY State Route 37 Bridge (NY 37 Bridge). In addition, the location at NY State Route 37C Bridge (NY 37C Bridge) at Helena is also selected. The maximum jam thickness at Hogansburg at locations indicated in Figure 28 are also included in Table 1.

Figure 27. Key locations selected to summarize the ice thickness and peak water surface elevation.

Table 1. Summary of ice and flow conditions at the key locations – ice run simulations

Locations	Pre-Dam-Removal Q = 24.07 m^3/s (850 ft^3/s)		Post-Dam-Removal Q = 24.07 m^3/s (850 ft^3/s)	
	$h_{i,max}$ (m)	$H_{w,max}$ (m)	$h_{i,max}$ (m)	$H_{w,max}$ (m)
Left Bank at Hogansburg	0	47.032	1.016	48.499
Right Bank at Hogansburg	0	47.017	1.223	48.495
Dam Site	1.08	50.28	1.113	49.217
NY 37 Bridge	0.335	50.297	0.201	49.395
NY 37C Bridge	0.225	52.080	0.355	52.402
Ice Jam at Hogansburg	No Ice Jam	No Ice Jam	3.128	46.514

Locations	Pre-Dam-Removal Q = 39.64 m^3/s (1400 ft^3/s)		Post-Dam-Removal Q = 39.64 m^3/s (1400 ft^3/s)	
	$h_{i,max}$ (m)	$H_{w,max}$ (m)	$h_{i,max}$ (m)	$H_{w,max}$ (m)
Left Bank at Hogansburg	0.890	48.183	1.350	48.878
Right Bank at Hogansburg	1.011	48.172	1.798	48.845
Dam Site	0.935	50.518	1.804	49.771
NY 37 Bridge	0.354	50.518	0.403	50.058
NY 37C Bridge	0.735	52.620	0.625	52.549
Ice Jam at Hogansburg	2.774	45.520	3.071	45.265

Note: $h_{i,max}$ is the maximum ice thickness in meter; $H_{w,max}$ is the maximum water surface elevation in meter.

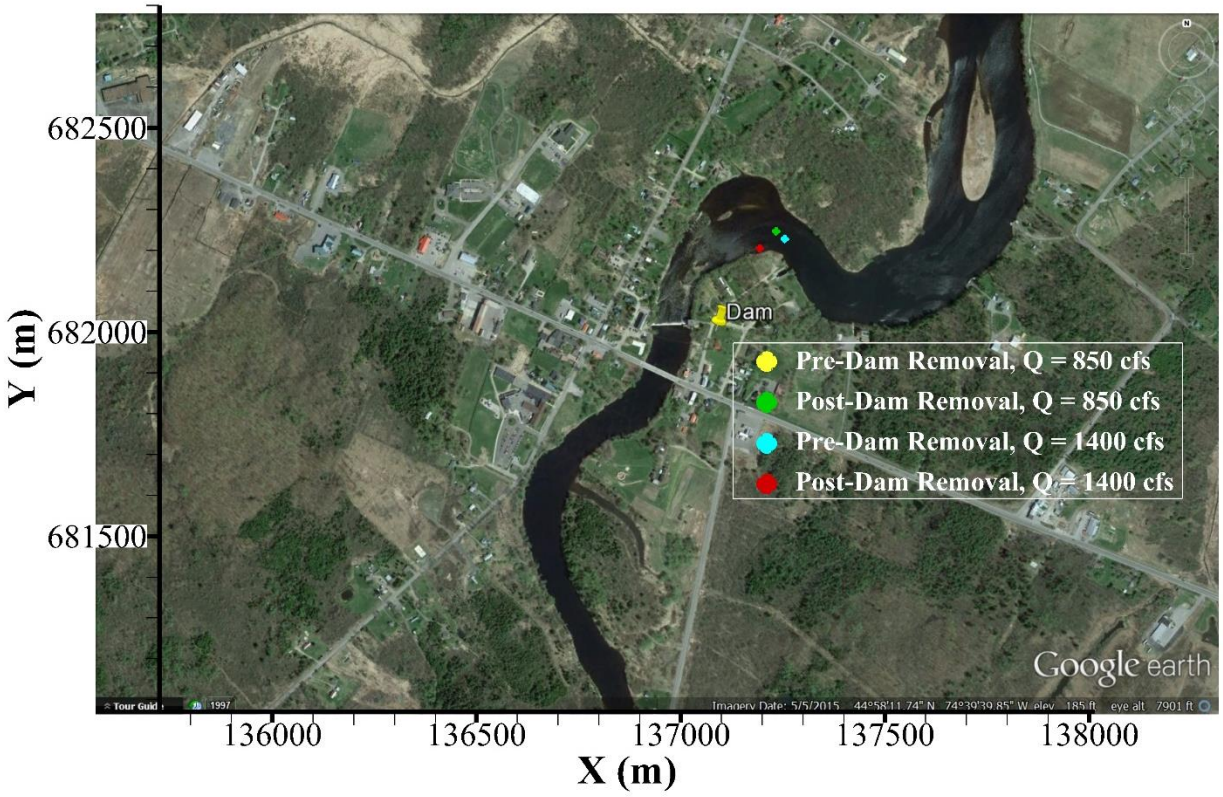

Figure 28. The location of the maximum ice jam thickness at Hogansburg. No ice jam occurred in the case with pre-dam removal and discharge of 24.07 m^3/s (850 ft^3/s).

4. Breakup Ice Jam Simulations

Historically, breakup ice jam flooding has occurred in the Lower St. Regis River in the area near the Hogansburg Dam site (HDR, Inc. 2012). This section presents simulations on the evolution of ice breakup cases to illustrate the ice jam flooding processes for both pre- and post-dam-removal conditions. The breakup ice run and jamming processes are simulated for four discharge conditions ranging from 24.07 m^3/s (850 ft^3/s) to 198.22 m^3/s (7000 ft^3/s). The higher discharges are typical for mechanical breakups associated with ice jam flooding. The highest discharge of 198.22 m^3/s (7000 ft^3/s) is the peak discharge that occurred in 2018 February ice jam event. The steady discharges for three days in the breakup simulation aims to evaluate the possible worst scenarios of the ice jam processes and its impact on the water levels. For cases with low flow conditions, the simulations assume the breakup of the ice cover between Helena and Hogansburg with a thickness of 0.3 m. The surface ice supply continues at Helena with an ice concentration of 0.4 and a thickness of 0.3 m. For cases with high flow conditions, the simulations assume the breakup of the ice cover between Helena and Hogansburg with a thickness of 0.43 m (17 inches). This is based on the observed ice thickness in Feb. 2018 ice jam events (David 2018). The surface ice supply continues at Helena with a thickness of 0.43 m (17 inches) and an ice concentration of 0.4. The cover downstream from the dam site remains unbroken initially. This is because it is in the backwater zone of the confluence with the St. Lawrence River with a nearly horizontal water surface. However, it is allowed to break from the action of the incoming moving ice jam, as have been observed in recent ice jam events shown in Figure 29 and Figure 30. All simulations continue until a stable ice condition is reached.

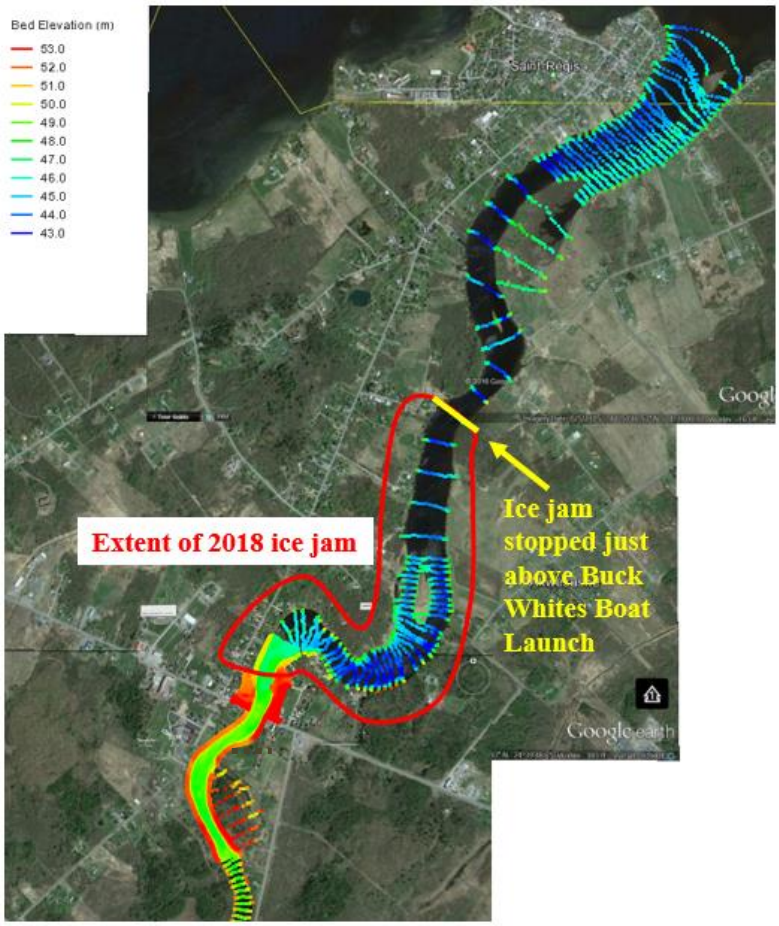

Figure 29. Observed ice jam toe location in the 2018 ice jam event (Courtesy of David Tracy, SRMT-Environmental Division).

Figure 30. Aerial view of the ice jam toe on Jan. 30, 2020.

4.1 Pre-Dam-Removal, Q = 24.07 m^3/s (850 ft^3/s)

Figure 31 shows simulated ice thickness distribution in the Lower St. Regis River and the vicinity of the dam. Some thick ice accumulation developed in the bend downstream of the dam. The ice movement is stopped by the unbroken ice cover downstream. The ice accumulation upstream of the dam is mainly in the juxtaposition mode, with a few minor thickening along the channel.

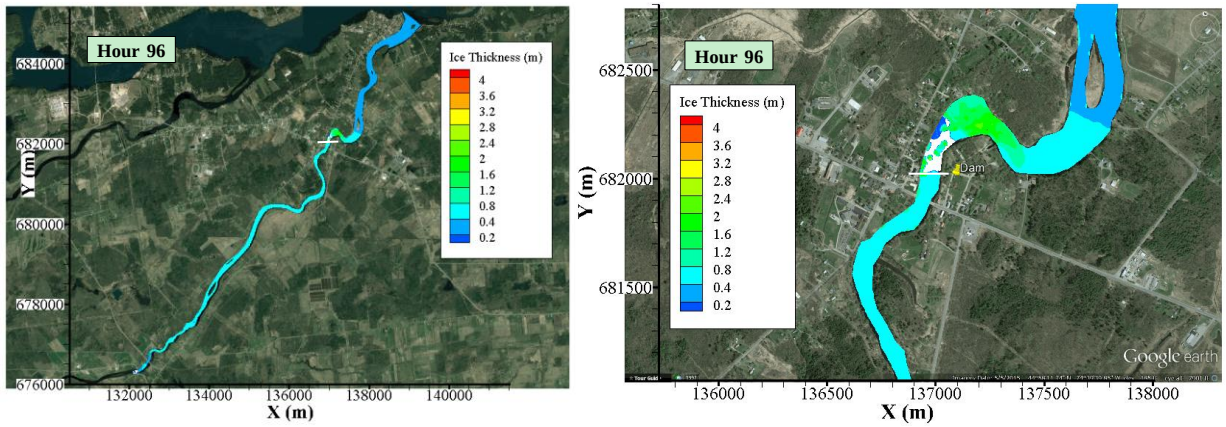

Figure 31. Simulated ice thickness distribution at hour 96 - Pre-dam-removal, 24.07 m^3/s (850 ft^3/s).

4.2 Post-Dam-Removal, Q = 24.07 m^3/s (850 ft^3/s)

Figure 32 shows simulated ice thickness distribution in the Lower St. Regis River and the vicinity of the former dam site. The breakup of ice cover between Helena and Hogansburg forms an ice jam in the channel bend downstream of the dam site. The removal of the dam enhanced the flow and ice run through the dam site. As a result, a thicker ice jam formed in the channel bend downstream of the former dam site in comparison to the pre-dam-removal case.

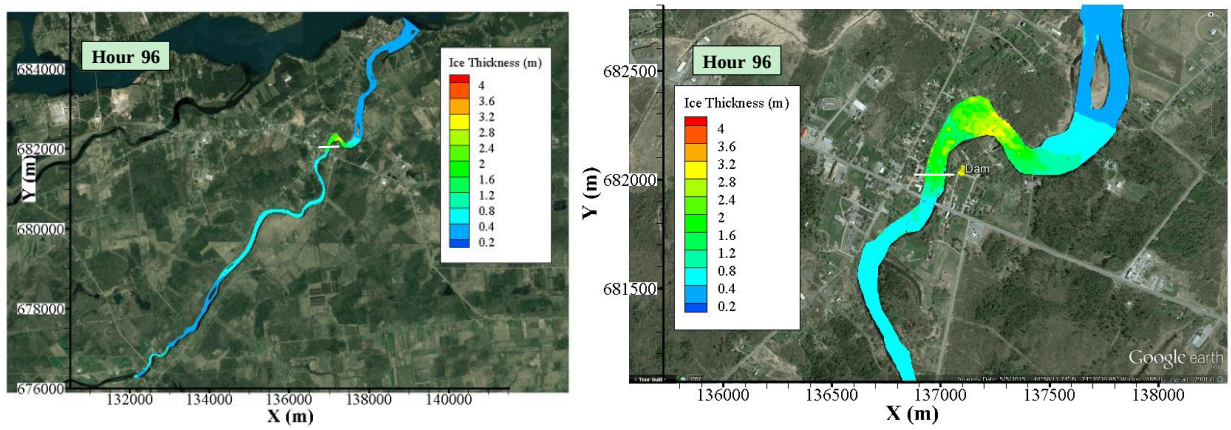

Figure 32. Simulated ice thickness distribution at hour 96 - Post-dam-removal, 24.07 m^3/s (850 ft^3/s).

4.3 Pre-Dam Removal, Q = 39.64 m^3/s (1400 ft^3/s)

Figure 33 shows simulated ice thickness distribution in the Lower St. Regis River and the vicinity of the dam. Under this discharge condition, more ice can pass the dam site, which results in a thick ice accumulation in the bend downstream. The ice movement was stopped against the downstream ice cover. The thickening of the surface ice mainly occurred in the channel bend at the downstream of the dam. With ice supply from upstream, another ice jam formed near Helena. The ice jam toe is located at the channel contraction 1.45 km downstream of Helena. This prevented additional ice coming in from upstream.

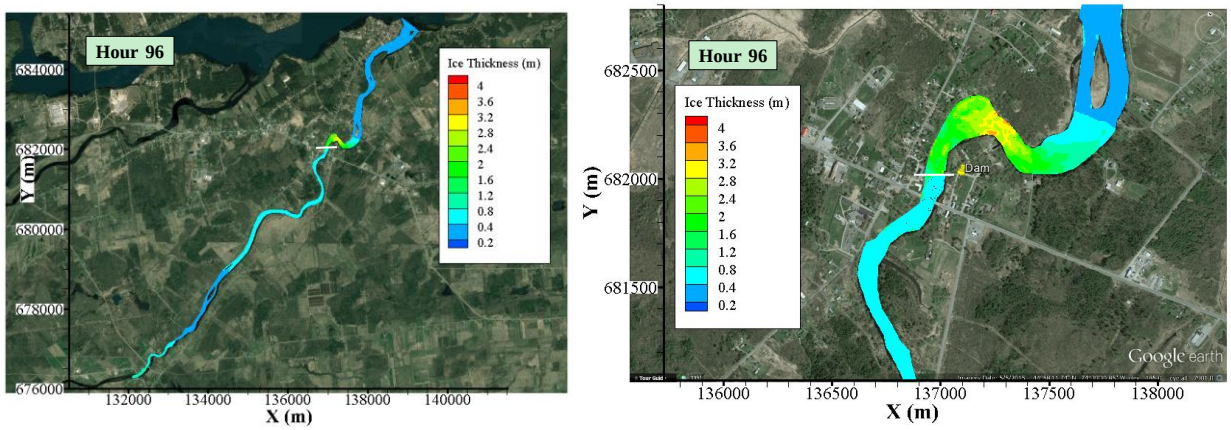

Figure 33. Simulated ice thickness distribution at hour 96 - Pre-dam-removal, Q = 39.64 m^3/s (1400 ft^3/s).

4.4 Post-Dam-Removal, Q = 39.64 m^3/s (1400 ft^3/s)

Figure 34 shows simulated ice thickness distribution in the Lower St. Regis River and the vicinity of the Dam site. The removal of the dam enhanced the flow and ice run through the dam site. As a result, a larger ice jam formed in the channel bend downstream of the dam site in comparison to the pre-dam removal case. The ice movement is again stopped by the downstream ice cover. With the ice supply from upstream, a thick ice accumulation occurs at the channel contraction downstream of Helena. However, the ice movement towards the former dam site continues due to the high water discharge and result in the growth of the ice jam downstream of the dam site.

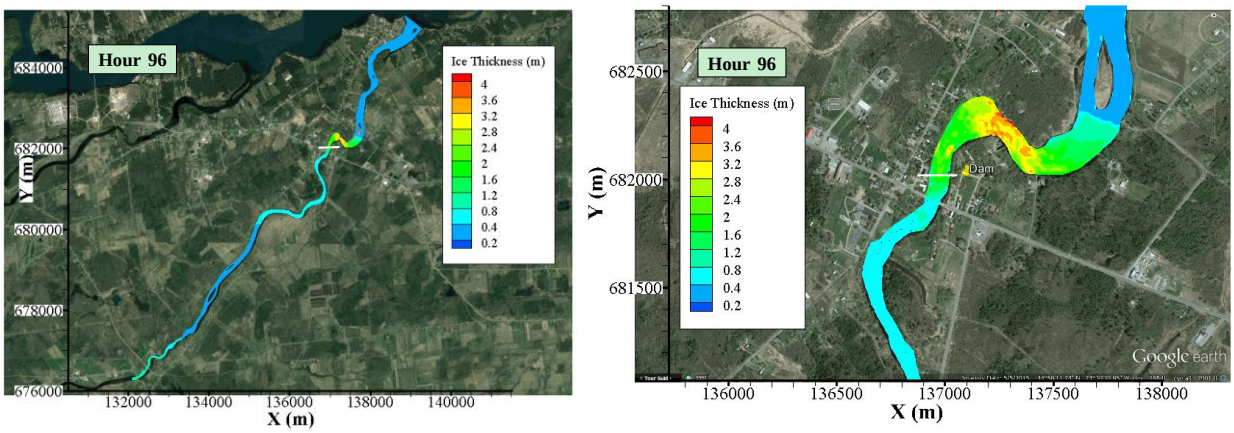

Figure 34. Simulated ice thickness distribution at hour 96 - Post-Dam Removal, Q = 39.64 m^3/s (1400 ft^3/s).

4.5 Pre-Dam-Removal, Q = 113.27 m^3/s (4000 ft^3/s)

Figure 35 shows simulated ice thickness distribution in the Lower St. Regis River and near the dam. The larger flow depth due to the large discharge allows the surface ice from the broken ice cover between Helena and Hogansburg to move past the former dam site to form an ice jam against the downstream cover. The backwater effect of the ice jam led to a mild water surface slope and large flow depth to allow the formation of the jam at the channel contraction 2.24 km downstream of Helena.

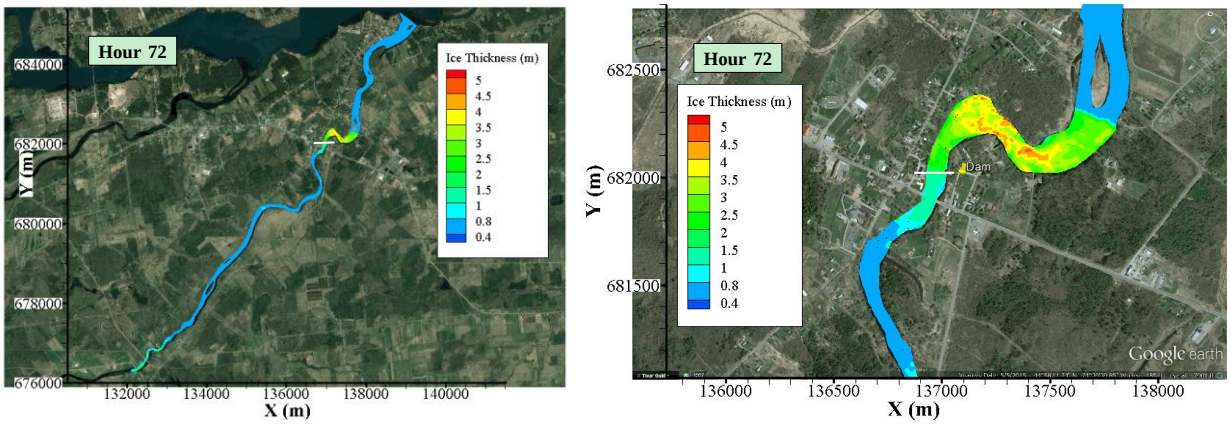

Figure 35. Simulated ice thickness distribution at hour 72 - Pre-dam-removal, Q = 113.27 m^3/s (4000 ft^3/s). (Note: The legend of the ice thickness increases to 0-5 m because much thicker ice jam forms in at the downstream of the dam)

4.6 Post-Dam-Removal, Q = 113.27 m^3/s (4000 ft^3/s)

Figure 36 shows simulated ice thickness distribution in the Lower St. Regis River and near the dam. Ice jam formed in the bend downstream of the dam site. The continuous ice supply resulted in another ice jam formation at the channel contraction 1.45 km downstream of Helena.

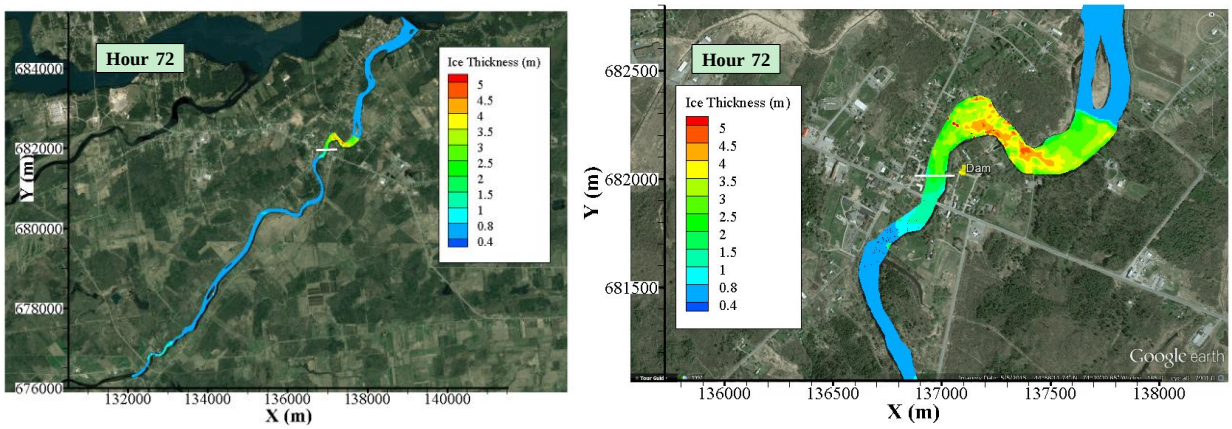

Figure 36. Simulated ice thickness distribution at hour 72 - Post-Dam-Removal, Q = 113.27 m^3/s (4000 ft^3/s).

4.7 Pre-Dam Removal, Q = 198.22 m^3/s (7000 ft^3/s)

Figure 37 shows simulated ice thickness distribution in the Lower St. Regis River and near the dam. The ice from the breakup of the ice cover between Helena and Hogansburg moved to the downstream quickly with this high discharge. The ice jam formed against the downstream ice cover within 6 to 7 hours. The ice jam in the bend downstream of the dam is thicker with this high discharge. The surface ice at either side of the bank in the upstream reach of Hogansburg remained because the release of the channel storage together with the ice cover breakup resulted in the sudden decrease of the water levels. The ice-jam flooding occurred at Hogansburg as shown in Figure 38. Some surface ice rested over the left bank at Hogansburg due to the local flooding. Figure 38 also shows the flooded area at the upstream of Hogansburg resulting from the development of the ice jam. The flooded sub-channel led to a small amount of surface ice entering and being rested there. With the continuous ice supply from upstream, another ice jam formed with the ice jam toe located at the channel contraction 2.24 km downstream of Helena. With the exceptionally high discharge increased the ice transport capacity at the channel contractions. Therefore, this jam is located further downstream than the cases with lower discharge.

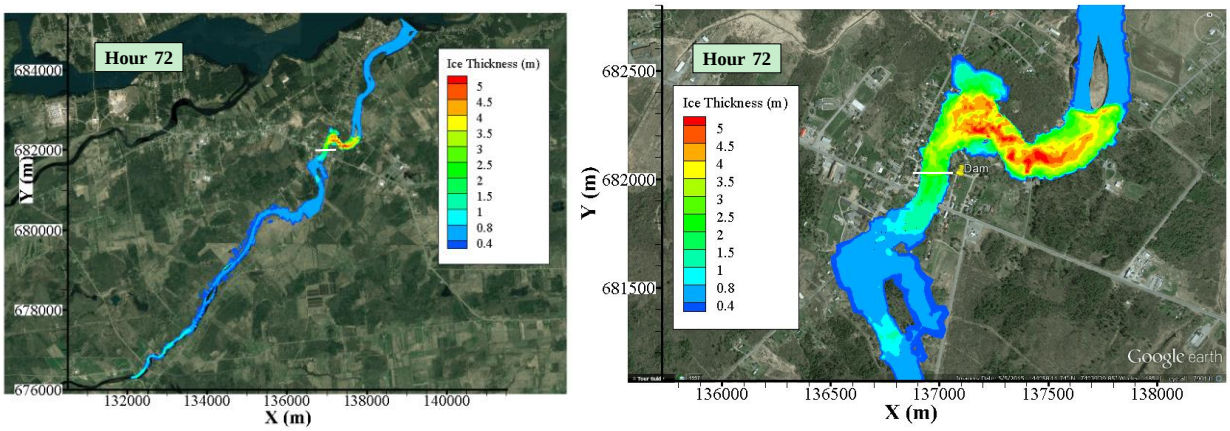

Figure 37. Simulated ice thickness distribution at hour 72 - Pre-Dam-Removal, Q = 198.22 m^3/s (7000 ft^3/s).

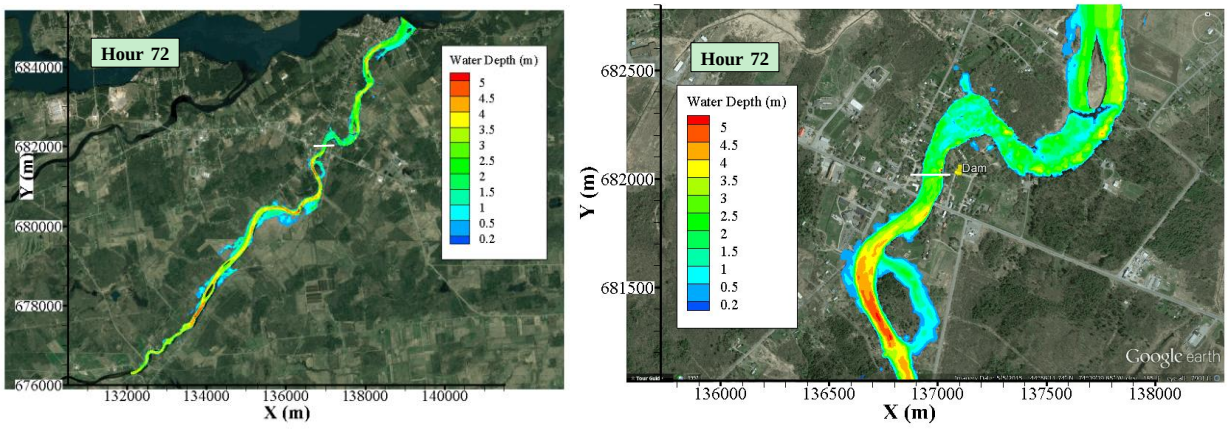

Figure 38. Simulated water depth distribution at hour 72 - Pre-Dam-Removal, Q = 198.22 m^3/s (7000 ft^3/s).

4.8 Post-Dam Removal, Q = 198.22 m^3/s (7000 ft^3/s)

Figure 39 shows simulated ice thickness distribution in the Lower St. Regis River and near the dam. The ice jam formed in the bend at the downstream of the dam and caused the flooding at Hogansbur. The development of the ice jam further led to the flooding in the upstream reach. The removal of the dam increased the ice discharge into Hogansburg. This promoted the speedy ice accumulation from the jam towards upstream and the upstream flooding as shown in Figure 39 and Figure 40. It is noted that some surface ice were transported on the banks in the upstream reach caused by the backwater effect of the ice accumulation before the ice jam near Helena developed. Another ice jam formed at the channel contraction 2.24 km downstream of Helena. This jam led to the decrease of the downstream water levels. By comparison with the case of pre-dam removal, more surface ice remained on the banks in the upstream reach of Hogansburg.

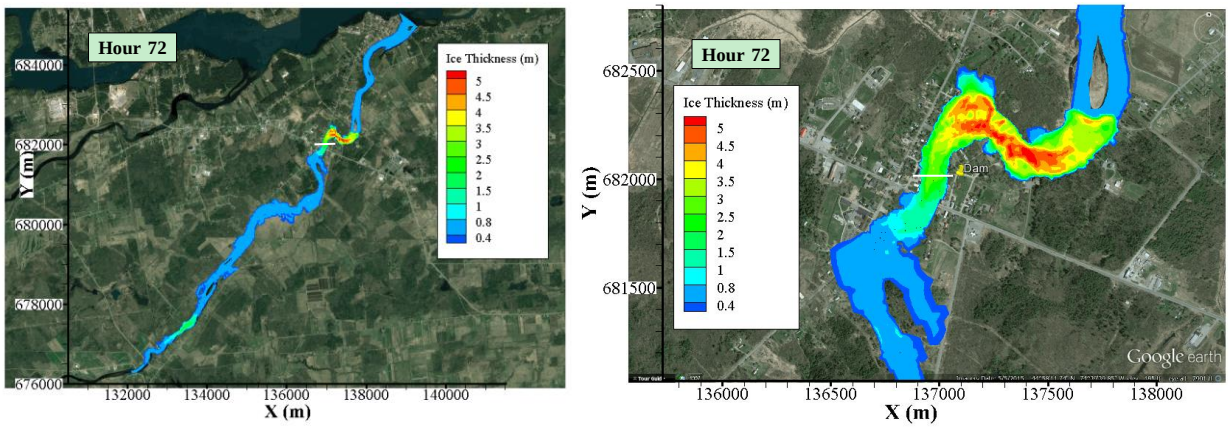

Figure 39. Simulated ice thickness distribution at hour 72 - Post-dam-removal, Q = 198.22 m^3/s (7000 ft^3/s).

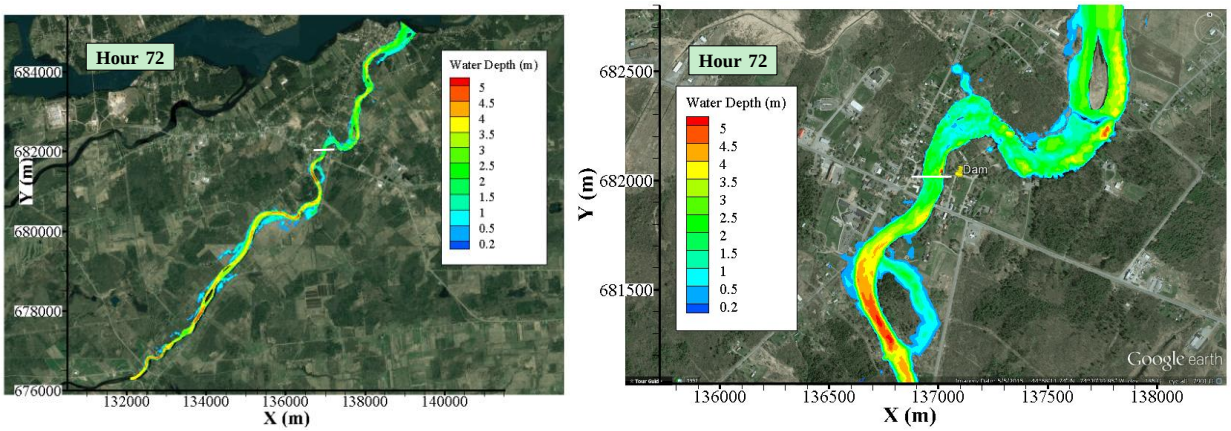

Figure 40. Simulated water depth distribution at hour 72 - Post-dam-Removal, Q = 198.22 m^3/s (7000 ft^3/s).

4.9 Summary

Simulations of the breakup ice jams are made for both pre- and post-dam-removal conditions for four discharge conditions ranging from a low flow of 24.07 m^3/s (850 ft^3/s) to a high flow of 198.22 m^3/s (7000 ft^3/s). The simulated results showed that the dam removal enhanced the flow and ice transport passing the dam site, resulting in increasing ice amount for a larger ice jam in the bend downstream of the dam site. In all cases, the ice movement stopped by the ice cover downstream in the backwater zone from the confluence of the St. Lawrence River. This leads to a possible mitigation method of removing the ice cover before the breakup. However, it is impractical for the extensive work and cost it will involve. Figure 41 to Figure 44 show the ice accumulation and the water surface profiles of the four scenarios of low flow conditions when the flow and ice conditions are stabilized. Figure 45 shows the comparison of the water surface profiles for these four low flow discharge cases. The post-dam-removal conditions have higher water levels downstream of the dam and lower water levels in the upstream reach, especially for low flow conditions. Figure 46 to Figure 49 show the ice accumulation and the water surface profiles of the four scenarios of high flow conditions when the flow and ice conditions are

stabilized. Figure 50 shows the comparison of the water surface profiles for the four simulated cases with high flow discharges. The high discharges cause a larger increase in the backwater caused by the ice jam than the low discharges. Similarly, the post-dam-removal conditions have a higher water level downstream of the dam and lower water level in the upstream reach. The water levels at Helena is affected by the ice jam formed near downstream. Thicker ice jam resulted in higher water levels at Helena. The difference in the water levels between the channel contraction near Helena and Hogansburg is small between pre-removal and post-removal cases for high discharges. This indicates that the impact of the removal of the dam on the ice jam processes and flow conditions at Hogansburg is limited if the flow discharge is high.

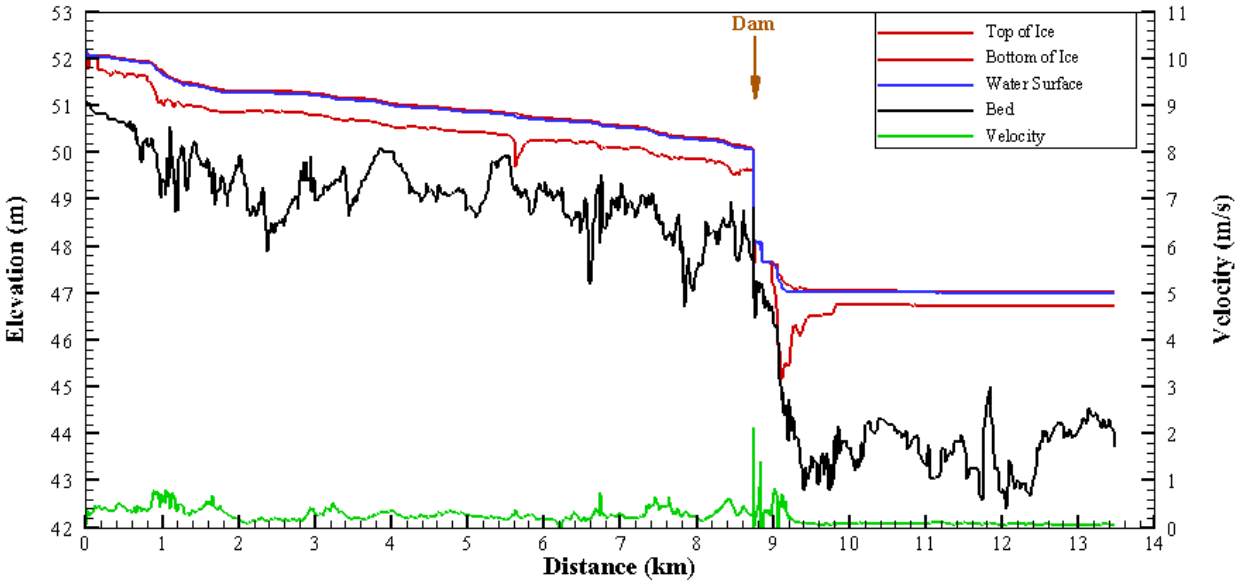

Figure 41. Simulated longitudinal profiles of flow and ice conditions at hour 96 - Pre-dam-removal, Q = 24.07 m^3/s (850 ft^3/s) .

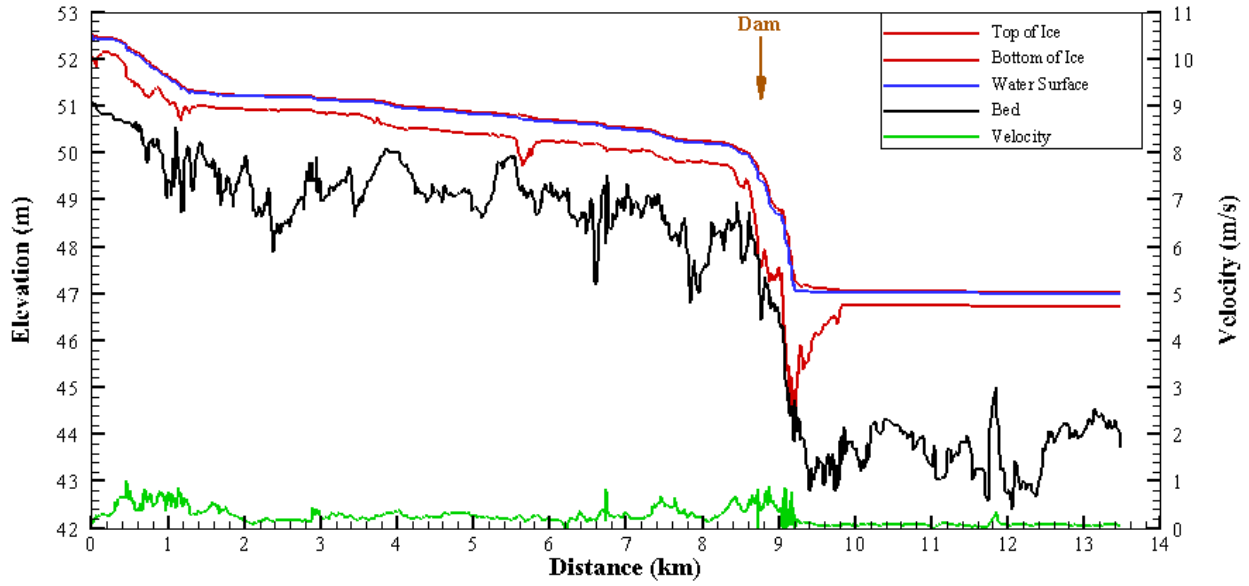

Figure 42. Simulated longitudinal profiles of flow and ice conditions at hour 96 - Post-dam-removal, Q = 24.07 m^3/s (850 ft^3/s).

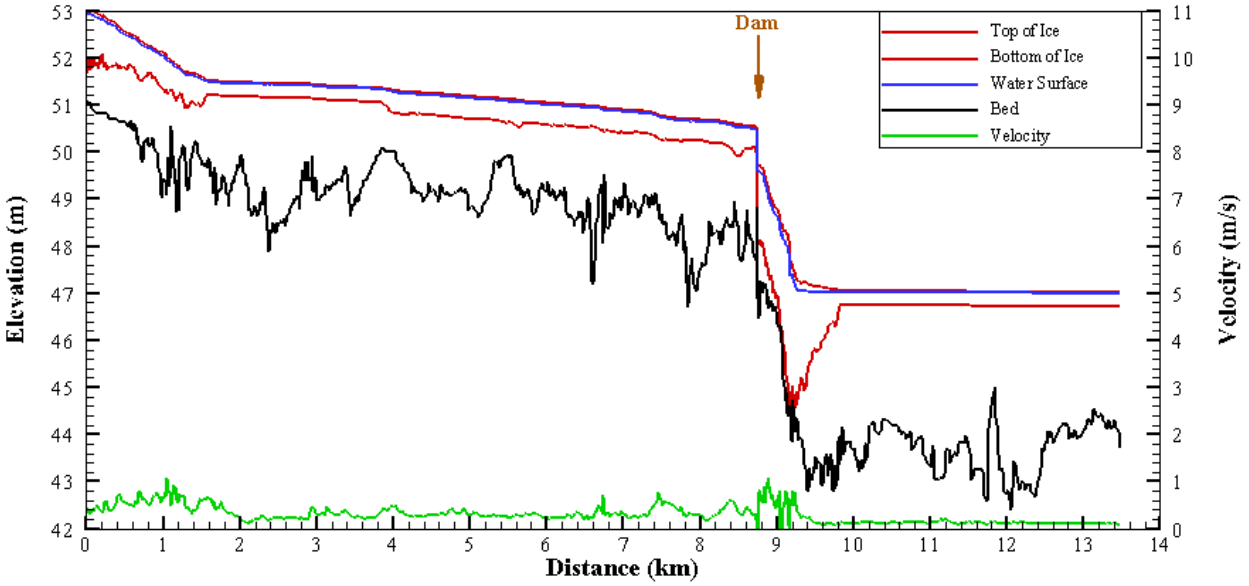

Figure 43. Simulated longitudinal profiles of flow and ice conditions at hour 90 - Pre-dam-removal, 39.64 m^3/s (1400 ft^3/s).

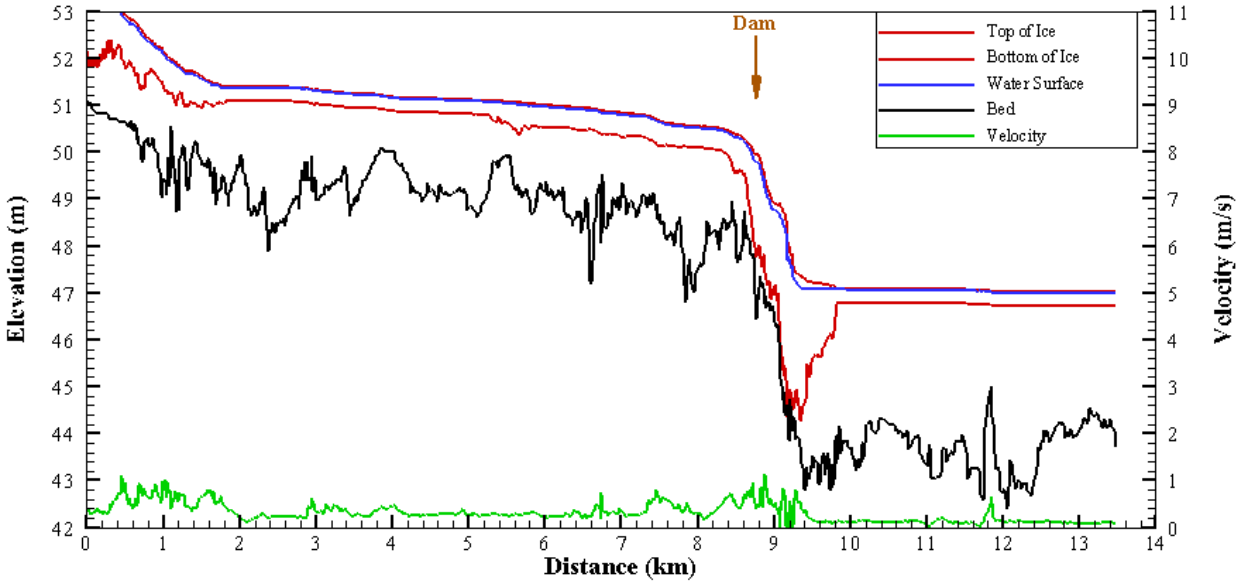

Figure 44. Simulated longitudinal profiles of flow and ice conditions at hour 96 - Post-dam-removal, 39.64 m^3/s (1400 ft^3/s).

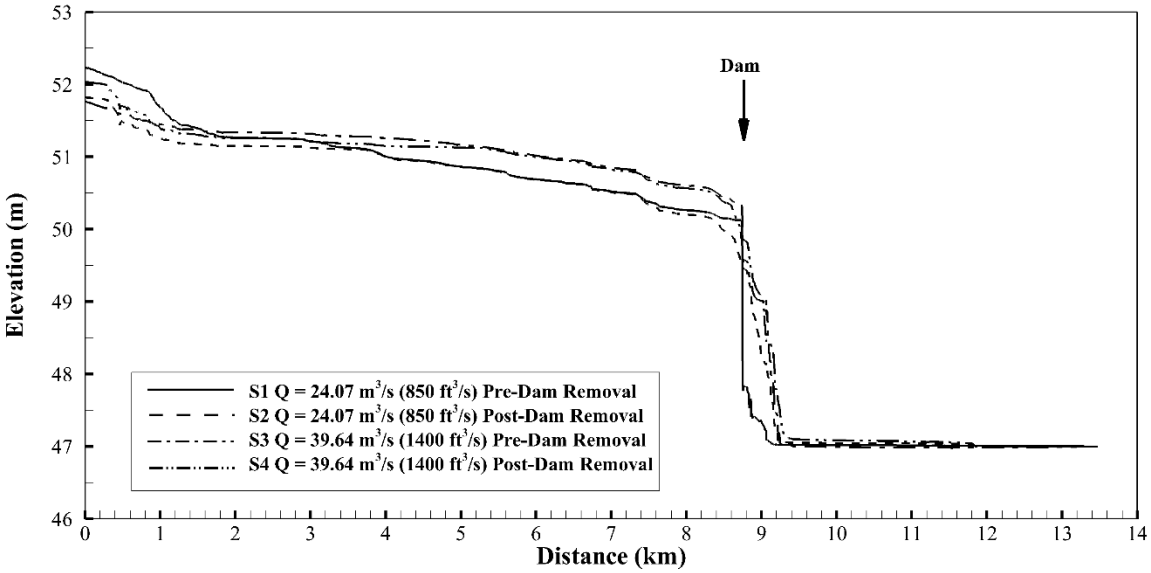

Figure 45. Comparison of water surface profiles – low discharge cases (24.07 and 39.64 m^3/s).

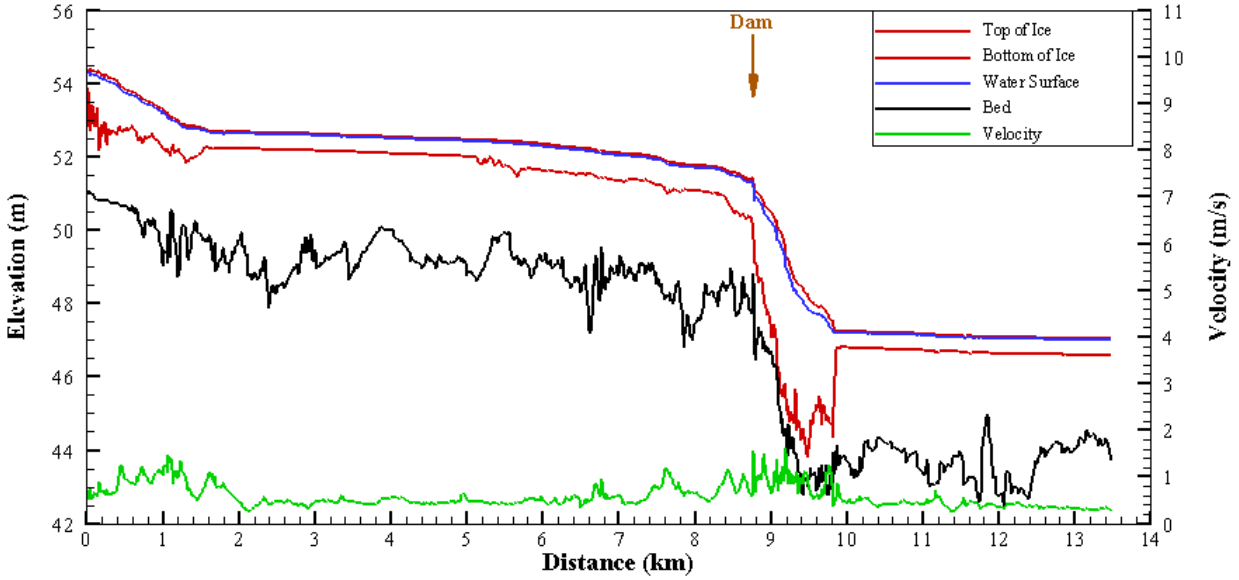

Figure 46. Simulated longitudinal profiles of flow and ice conditions at hour 72 - Pre-dam-removal, Q = 113.27 m^3/s (4000 ft^3/s).

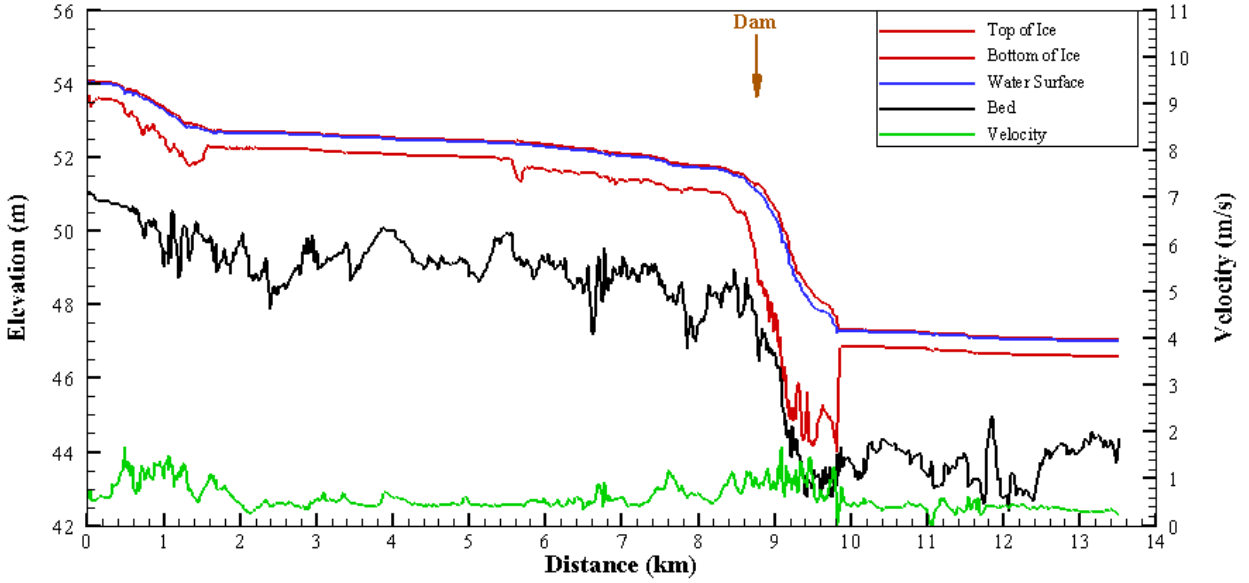

Figure 47. Simulated longitudinal profiles of flow and ice conditions at hour 72 - Post-dam-removal, Q = 113.27 m^3/s (4000 ft^3/s).

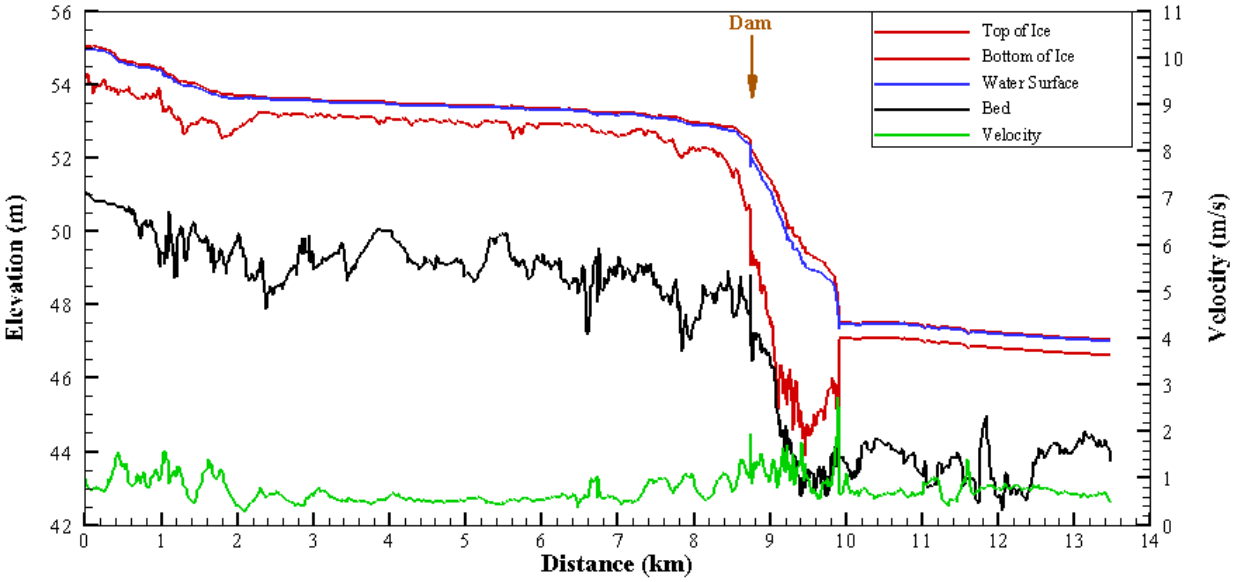

Figure 48. Simulated longitudinal profiles of flow and ice conditions at hour 72 - Pre-dam-removal, Q = 198.22 m^3/s (7000 ft^3/s).

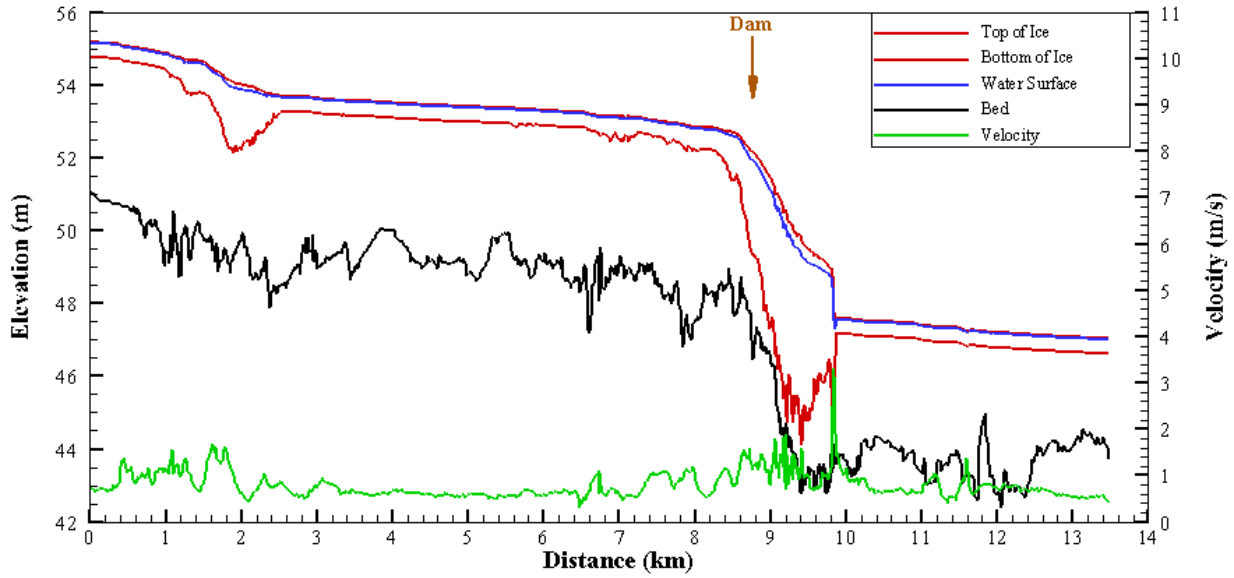

Figure 49. Simulated longitudinal profiles of flow and ice conditions at hour 72 - Post-dam-removal, Q = 198.22 m^3/s (7000 ft^3/s).

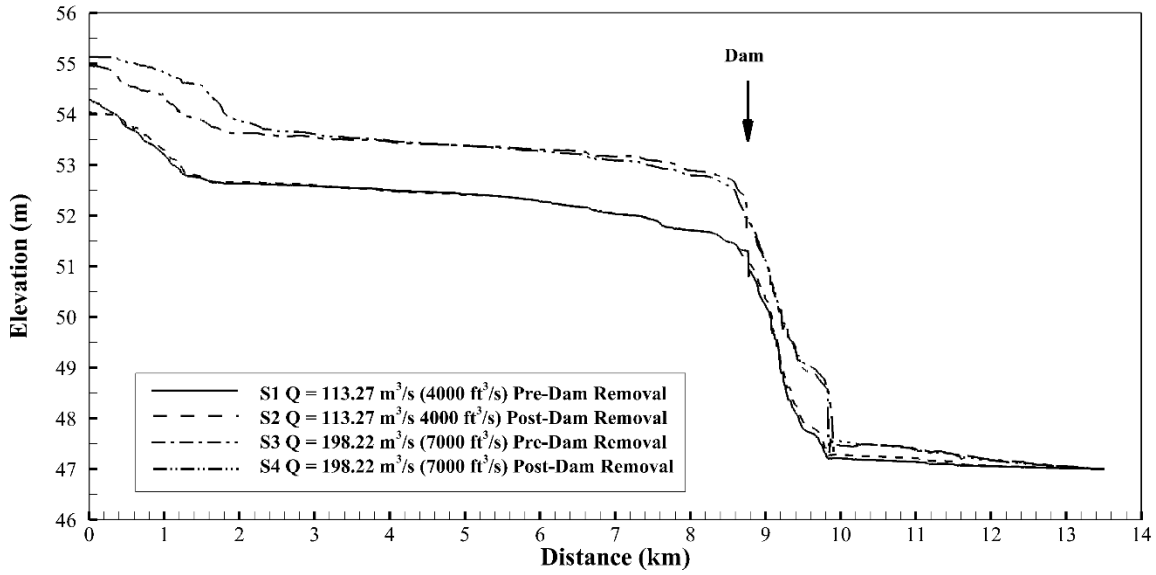

Figure 50. Comparison of water surface profiles – high discharge cases (113.27 and 198.22 m^3/s).

The maximum water level and ice thickness at key locations shown in red circles in Figure 27 are summarized in Table 2. The maximum jam thickness at Hogansburg at locations indicated in Figure 51 and Figure 52 are also included in Table 2.

Table 2. Summary of ice and flow conditions at the key locations – breakup simulations

Locations	Pre-Dam Removal Q = 24.07 m^3/s (850 ft^3/s)		Post-Dam Removal Q = 24.07 m^3/s (850 ft^3/s)	
	$h_{i,max}$ (m)	$H_{w,max}$ (m)	$h_{i,max}$ (m)	$H_{w,max}$ (m)
Left Bank at Hogansburg	0.114	47.665	1.057	48.712
Right Bank at Hogansburg	0.000	47.651	1.163	48.691
Dam Site	0.441	49.896	1.911	49.425
NY 37 Bridge	0.504	50.079	0.698	49.902
NY 37C Bridge	0.368	51.964	0.661	52.183
Ice Jam at Hogansburg	2.092	47.124	3.116	47.669

Locations	Pre-Dam Removal Q = 39.64 m^3/s (1400 ft^3/s)		Post Dam Removal Q = 39.64 m^3/s (1400 ft^3/s)	
	$h_{i,max}$ (m)	$H_{w,max}$ (m)	$h_{i,max}$ (m)	$H_{w,max}$ (m)
Left Bank at Hogansburg	1.158	48.849	1.561	48.802
Right Bank at Hogansburg	1.678	48.793	1.621	48.843
Dam Site	0.786	50.405	2.098	49.805
NY 37 Bridge	0.491	50.412	0.770	50.227
NY 37C Bridge	0.786	52.516	1.113	52.864
Ice Jam at Hogansburg	3.352	44.924	3.755	45.161

Locations	Pre-Dam Removal Q = 113.27 m^3/s (4000 ft^3/s)		Post Dam Removal Q = 113.27 m^3/s (4000 ft^3/s)	
	$h_{i,max}$ (m)	$H_{w,max}$ (m)	$h_{i,max}$ (m)	$h_{i,max}$ (m)
Left Bank at Hogansburg	2.126	50.125	Left Bank at Hogansburg	2.126
Right Bank at Hogansburg	2.175	50.224	Right Bank at Hogansburg	2.175
Dam Site	1.624	51.255	Dam Site	1.624
NY 37 Bridge	1.074	51.356	NY 37 Bridge	1.074
NY 37C Bridge	1.109	53.751	NY 37C Bridge	1.109
Ice Jam at Hogansburg	4.783	48.151	Ice Jam at Hogansburg	4.783

Locations	Pre-Dam Removal Q = 198.22 m^3/s (7000 ft^3/s)		Post Dam Removal Q = 198.22 m^3/s (7000 ft^3/s)	
	$h_{i,max}$ (m)	$H_{w,max}$ (m)	$h_{i,max}$ (m)	$H_{w,max}$ (m)
Left Bank at Hogansburg	2.757	51.154	3.464	51.161
Right Bank at Hogansburg	3.122	51.175	3.231	51.203
Dam Site	2.519	52.296	2.763	51.954
NY 37 Bridge	1.663	52.562	1.915	52.420
NY 37C Bridge	0.805	54.567	0.417	55.029
Ice Jam at Hogansburg	5.930	50.503	5.781	49.474

Note: $h_{i,max}$ is the maximum ice thickness; $H_{w,max}$ is the maximum water surface elevation.

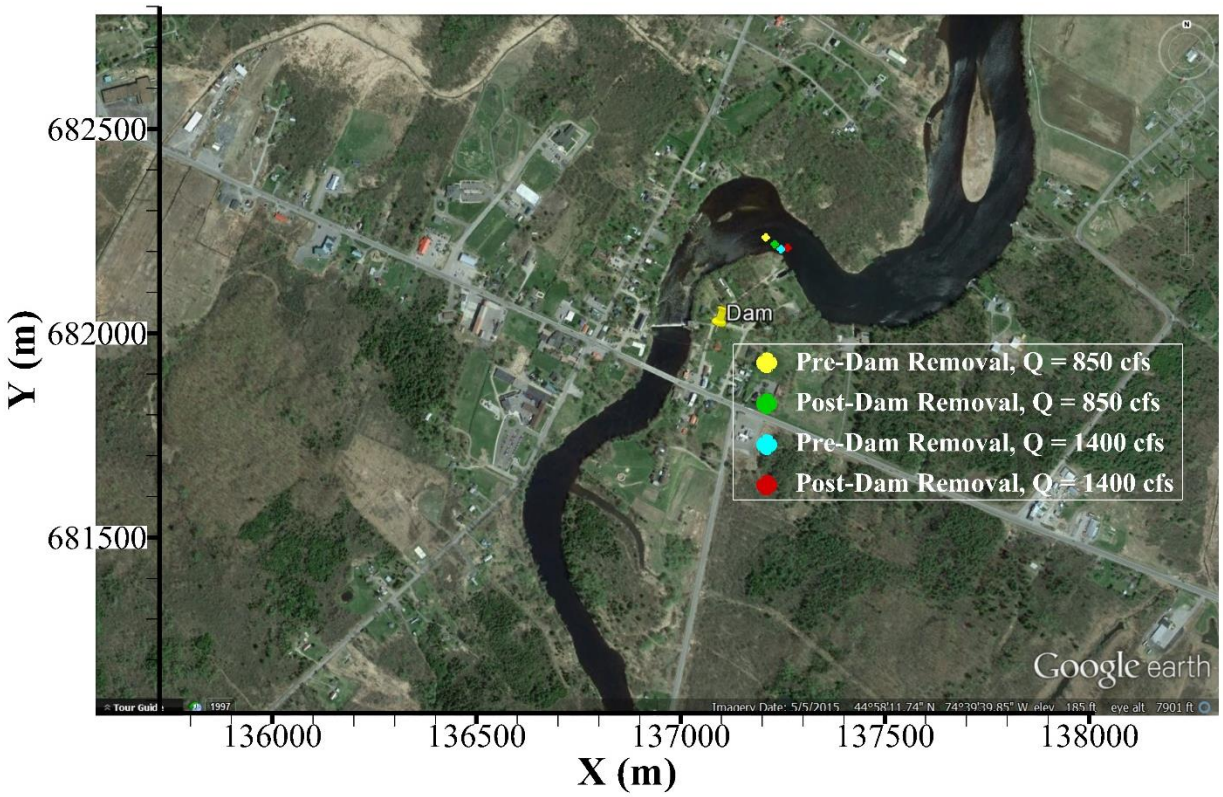

Figure 51. The location of the maximum ice jam thickness at Hogansburg – breakup simulations with discharges of 24.07 m^3/s (850 ft^3/s) and 39.64 m^3/s (1400 ft^3/s).

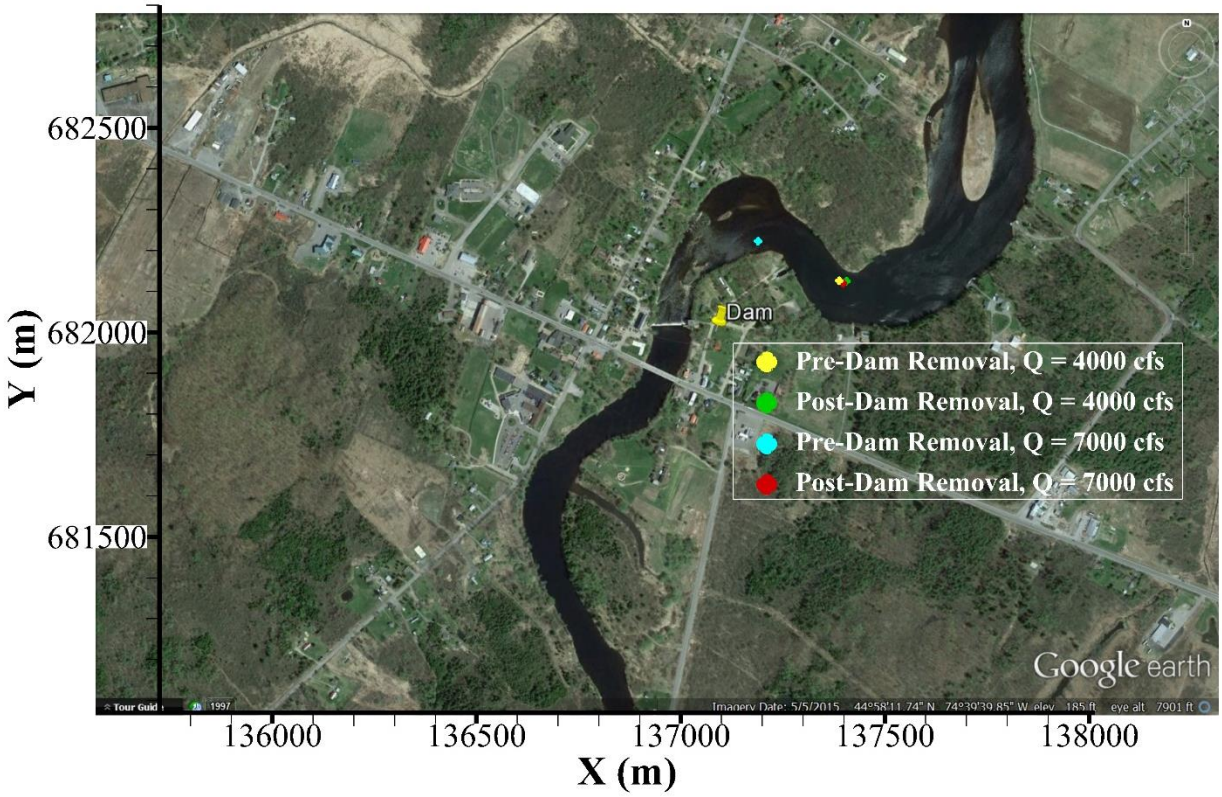

Figure 52. The location of the maximum ice jam thickness at Hogansburg – breakup simulations with discharges of 113.27 m^3/s (4000 ft^3/s) and 198.22 m^3/s (7000 ft^3/s). The locations of the maximum ice jam thickness for the cases of pre-dam removal are very close, including Q = 113.27 m^3/s (4000 ft^3/s), post-dam removal, Q = 113.27 m^3/s (4000 ft^3/s), and post-dam removal, Q = 198.22 m^3/s (7000 ft^3/s).

5. Historical Ice Jam Analysis

Ice jam flooding is particularly problematic for emergency management because change can occur quickly, and damage can be severe. It is well known that the formation of a breakup ice jam is a large ice discharge produced by a premature breakup of a competent ice cover. The cover breakup is influenced by the weather and hydrological conditions of the catchment. Analyzing a rare ice jam flooding event in a river in Hokkaido, Shen and Liu (2003) suggested that the combination of warm air temperature with rainfall in a catchment with snow accumulation is the condition that could lead to a breakup ice jam flooding. In this section, the historical ice jams in the Lower St. Regis River were analyzed to provide a method to forecast the occurrence of potential ice jam flooding.

Table 1 shows that there were 25 ice jam events on the St. Regis River between 1867 and 2012 (HDR, Inc. 2012). Except for the three ice jams that occurred in Hogansburg in 1876, 1935, and 1981, the rest were all located at Brasher Falls, approximately 12 miles upstream. This indicates that most of the time, the ice discharge from upstream of the study reach will not pass Brasher Falls. Two recent ice jam flooding occurred in 2018 and 2020. All five past ice jam events were analyzed based on the weather data from NOAA and the flow data from USGS station at Brasher Falls (Station No. 04269000), along with descriptions of these events. The discharge data is available between 1910 and 2020, while the stage data is only available between 2007 and 2020 at the Brasher Falls. The time interval of the discharge data is daily before 1990 and is 15 min. after 1990. The time interval of the stage data is 15 mins. The stage data before 2007 was estimated based on the rating curve established for the period between 2007 and 2020.

- **1867 Jam**

  Flow and weather data are not available for this event. A brief description of this event was given as “The St. Regis River became jammed with ice and flooded Akwesasne. It destroyed many homes, injured several people, and forced the evacuation of the village of St. Regis.” and “…, ice was by high water piled 25 feet high in the highway [at Hogansburg], and a new road had to be provided.” (HDR, Inc. 2012). This event prior to the dam construction implies that the ice jam occurred without the effect of the dam. The channel at Hogansburg is prone to the ice jam formation.

Table 3. Reported ice jam events on the St. Regis River (1867-2012) (HDR, Inc. 2012).

REPORTED ICE JAM EVENTS ON THE ST. REGIS RIVER (1867-2012)

Date	Location	Jam Type	Description	Damage	Source
February 1, 1867	Hogansburg, NY	Breakup	See Section 2.5.2	Homes damaged, several people injured, evacuations	USACE 2012
April 7, 1911	Brasher Falls, NY	NA	Maximum annual gage height of 10.1 feet affected by backwater from ice, reported at USGS gage St. Regis River at Brasher Center, on April 7, 1911. Discharge 16,240 cfs.	NA	USACE 2012
January 1, 1913	Brasher Falls, NY	NA	Maximum annual gage height of 9.7 feet, affected by backwater from ice, reported at USGS gage St. Regis River at Brasher Center, on January 18, 1913. Discharge 7,880 cfs.	NA	USACE 2012
March 27, 1914	Brasher Falls, NY	NA	Maximum annual gage height of 9.1 feet, affected by backwater from ice, reported at USGS gage St. Regis River at Brasher Center on March 27, 1914. Discharge 12,400 cfs.	NA	USACE 2012
March 31, 1916	Brasher Falls, NY	NA	Maximum annual gage height of 10.2 feet affected by backwater from ice, reported at USGS gage St. Regis River at Brasher Center, on March 31, 1916.	NA	USACE 2012
December 27, 1920	Brasher Falls, NY	NA	Maximum annual gage height of 10.17 feet, affected by backwater from ice, reported at USGS gage St. Regis River at Brasher Center, on December 27, 1920. Additional ice-affected gage height of 9.56 feet reported on December 15, 1920. Discharge of 5,600 cfs.	NA	USACE 2012
Januarys 12, 1924	Brasher Falls, NY	NA	Maximum annual gage height of 9.68 feet, affected by backwater from ice, reported at USGS gage St. Regis River at Brasher Center, on January 12, 1924.	NA	USACE 2012
March 27, 1928	Brasher Falls, NY	NA	Maximum stage not determined, but estimated to be more than 11 feet and affected by backwater from ice, reported at USGS gage St. Regis River at Brasher Center, on March 27, 1928. Discharge estimated at 8,000 cfs. Additional ice-affected gage heights of 10.08 feet reported on March 25, 1928 and 9.7 feet reported on March 14, 1928.	NA	USACE 2012
January 19, 1929	Brasher Falls, NY	NA	Gage height of 9.52 feet, affected by backwater from ice, reported at USGS gage St. Regis River at Brasher Center, on January 19, 1929. Additional ice-affected gage height of 10.22 feet (maximum for year) was reported on March 20. 1929.	NA	USACE 2012
January 21, 1935	Hogansburg, NY	Breakup	See Section 2.5.2	Homes and buildings damaged	USACE 2012; Bonaparte 1998
March 17, 1935	Brasher Falls, NY	NA	Maximum annual gage height of 10.24 feet, affected by backwater from ice, reported at USGS gage St. Regis River at Brasher Center on March 17, 1935.	NA	USACE 2012
April 6, 1937	Brasher Falls, NY	NA	Maximum annual gage height of 15.3 feet, affected by backwater from ice, reported at USGS gage St. Regis River at Brasher Center, on April 6, 1937.	NA	USACE 2012
February 7, 1938	Brasher Falls, NY	NA	Gage height of 9.64 feet, affected by backwater from ice, reported at USGS gage St. Regis River at Brasher Center, on February 7, 1938. Additional ice-affected gage height of 9.67 feet reported on March 22, 1938. Not the maximum gage height for year.	NA	USACE 2012
March 27, 1939	Brasher Falls, NY	NA	Maximum annual gage height of 9.44 feet, affected by backwater from ice, reported at USGS St. Regis River at Brasher Center, on March 27, 1939.	NA	USACE 2012

Date	Location	Jam Type	Description	Damage	Source
March 31, 1940	Brasher Falls, ny	NA	Maximum annual gage height of 10.36 feet, affected by backwater from ice, reported at USGS gage St. Regis River at Brasher Center, on March 31, 1940.	NA	USACE 2012
March 9, 1946	Brasher Falls	NA	Gage height of 9.39 feet, affected by backwater from ice, reported at USGS gage St. Regis River at Brasher Center on March 9, 1946. Not the maximum for the year.	NA	USACE 2012
March 26, 1967	Brasher Falls	NA	Gage height of 9.91 feet, affected by backwater from ice, reported at USGS gage St. Regis River at Brasher Center on March 26, 1947 (estimated discharge of 6,000 cfs). Additional ice-affected gage height of 12.5 feet (maximum for year) reported on April 7, 1947 (estimated discharge of 9,200 cfs).	NA	USACE 2012
March 17, 1948	Brasher Falls	NA	Maximum annual gage height of 10.35 feet, affected by backwater from ice, reported at USGS gage St. Regis River at Brasher Center, on March 17, 1948.	NA	USACE 2012
March 23, 1949	Brasher Falls	NA	Maximum annual gage height of 11.51 feet, affected by backwater from ice, reported at USGS gage St. Regis River at Brasher Center, on March 23, 1949.	NA	USACE 2012
March 12, 1952	Brasher Falls	NA	Maximum annual gage height of 9.22 feet affected by backwater from ice, reported at USGS gage St. Regis River at Brasher Center, on March 12, 1952.	NA	USACE 2012
February 22, 1954	Brasher Falls	NA	Gage height of 9.99 feet affected by backwater from ice, reported at USGS gage St. Regis River at Brasher Center on February 22, 1954.	NA	USACE 2012
December 30, 1954	Brasher Falls	NA	Gage height of 9.61 feet, affected by backwater from ice, reported at USGS gage St. Regis River at Brasher Center on December 30, 1954. Additional ice-affected gage heights of 12.31 feet (maximum for year) reported on March 11, 1955; 9.32 feet reported on March 23, 1955; and 9.24 feet reported on April 4, 1955.	NA	USACE 2012
February 26, 1981	Hogansburg, NY	Breakup	See Section 2.5.2	Firehouse severely damaged, roads flooded	Emery 1981
January 19, 1996	Winthrop, NY	Breakup	The National Weather Service reported on January 19, 1996 in a flood warning that there was an ice jam present on the St. Regis River at the Rt. 420 bridge near Winthrop, NY. The ice jam was causing the bridge to shift.	Bridge Closed	USACE 2012
January 13, 1997	Brasher Falls, NY	NA	An ice jam formed under the State Route 11 C / 50 Bridge causing sewer system problems next to the jam. As a result, North Street, Congress Street, and Vice Road were flooded. Homes were hit the hardest on Factory Street, North Church Street, and Converse Street. A State of Emergency was declared.	Homes flooded, sewer system damaged	USACE 2012

- **1934-35 Winter**

A brief description of this event was given as “An ice jam formed on the St. Regis River on Jan. 21, 1935 destroyed several homes and caused flooding adjacent to the river (USACE 2012)”. Figure 53 shows the flow and weather conditions during the week of the jam event. The ice jam occurred with a rapid increase in air temperature above the freezing point in addition to the rainfall.

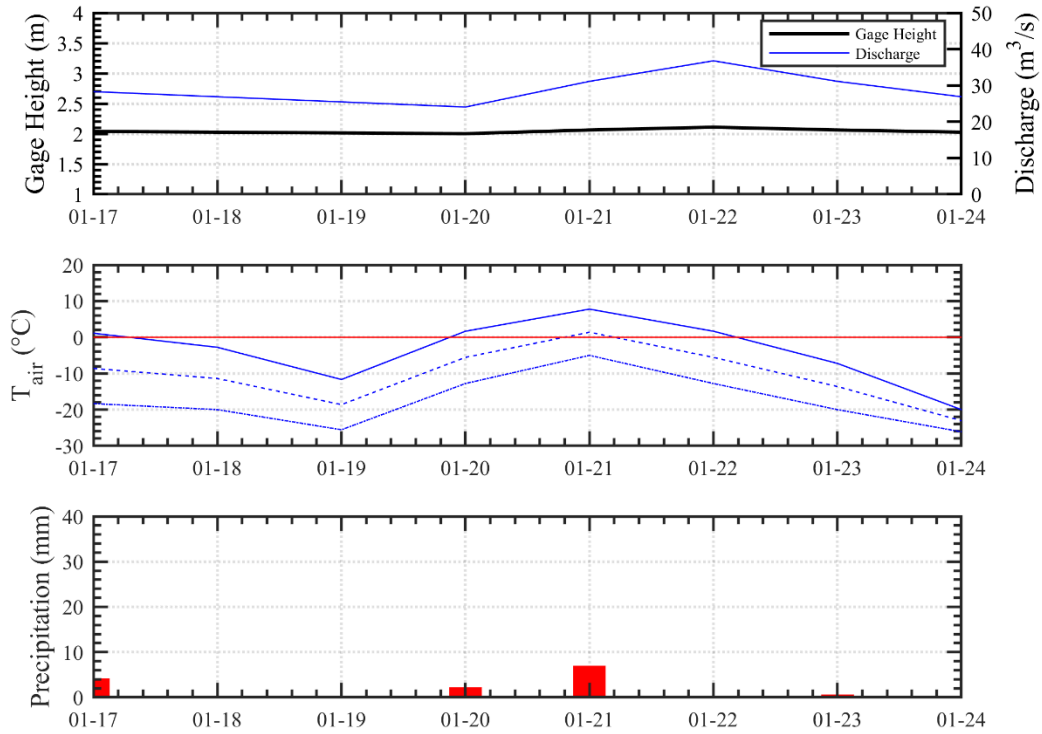

Figure 53. January 1935 flow and weather conditions.

- **1980-81 Winter**

The Feb. 26, 1981 ice jam caused severe flooding, power outages, and property damage in Hogansburg (HDR, Inc. 2012). Failure of the jam occurred at approximately 10:20 PM on the evening of Feb. 26 (Emery 1981). Figure 54 shows the weather and flow conditions in mid and late February. There was a warm period before Feb. 26. The jam might have formed from the warm rainfall on Feb. 20-21, then released after the three consecutive days of warm air temperature and moderate rainfall on Feb. 26. The ice jam formed in the sharp bend downstream of the dam. The failure of the jam in the evening was probably due to the collapse of the ice cover at the jam toe. The strength of that ice cover deteriorated due to the melting associated with the warm air temperature and rainfall. Photos of ice jam flooding in the Hogansburg area are given by the SRMT Environmental Division (Emery 1981). Figure 55 to Figure 58 show the photos of the ice conditions at Hogansburg as a result of the ice jam flooding.

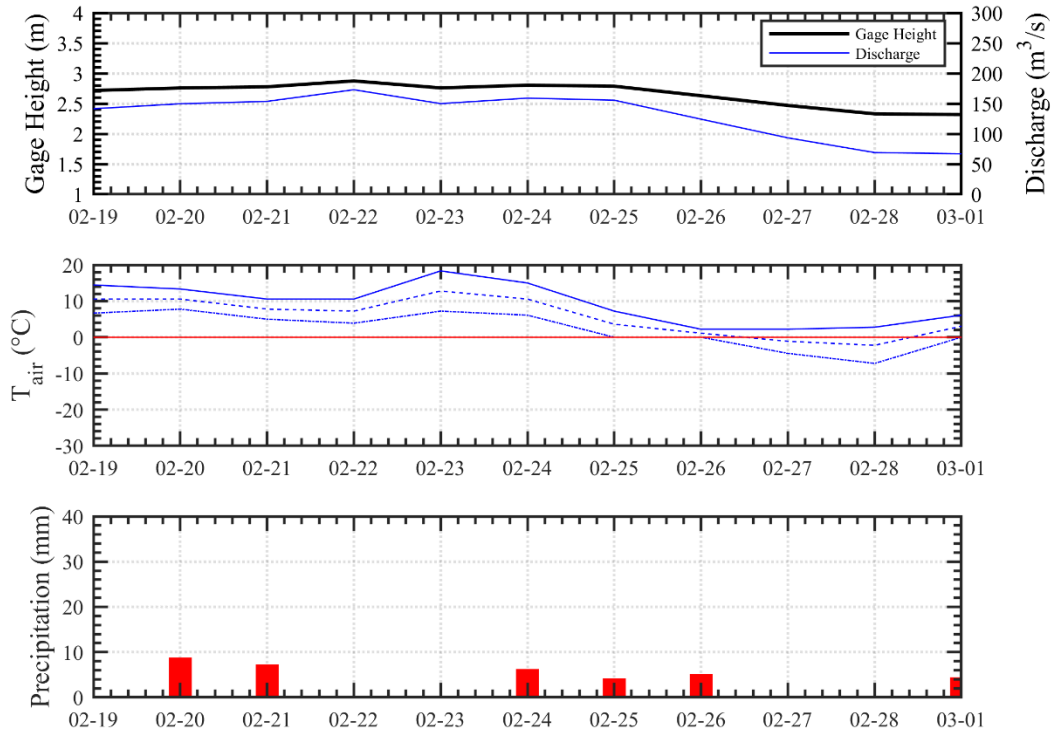

Figure 54. February 1981 flow and weather conditions.

Figure 55. Ice jam damage on the SRMT reservation on Feb. 26, 1981. (Emery 1981)

Figure 56. Ice deposited on the shoreline of the St. Regis River due to the ice jam flooding on Feb. 26, 1981. (Emery 1981)

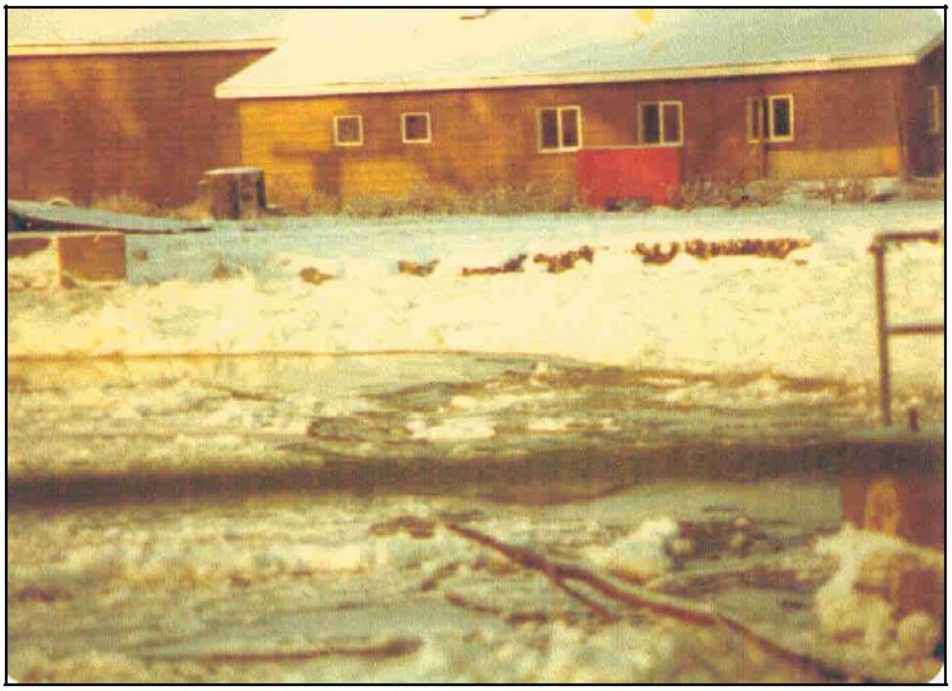

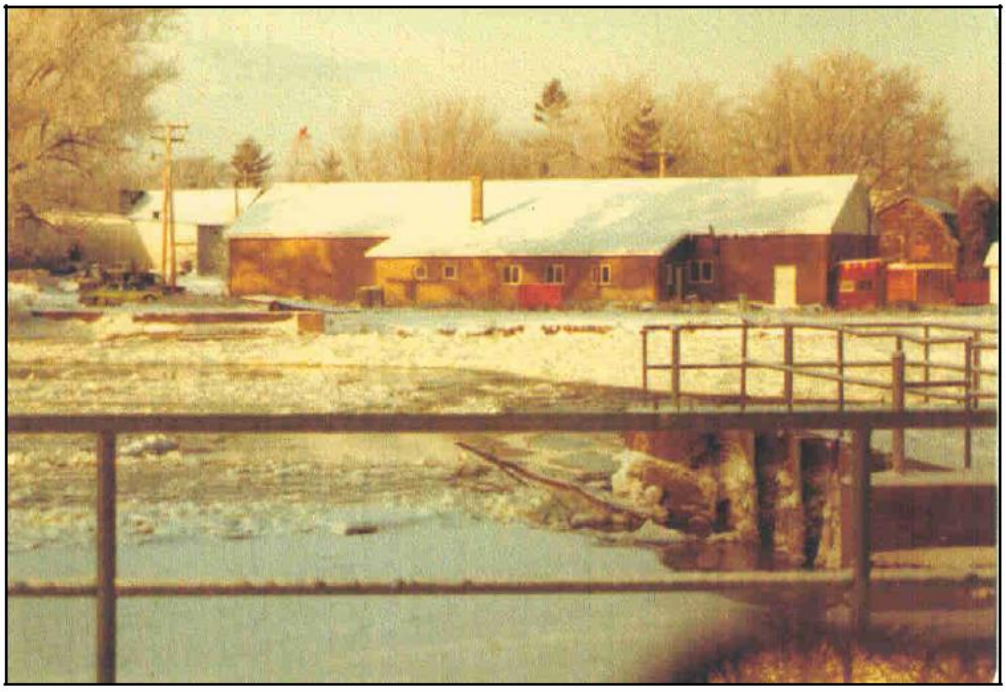

Figure 57. HAVFD station 1 on river left during the ice jam flooding on Feb. 26, 1981. (Emery 1981)

Figure 58. Ice deposited in front of the HAVFD station 1 as a result of the ice jam flooding on Feb. 26, 1981. (Emery 1981)

- **2017-18 Winter**

Figure 59 shows the flow and weather of the winter. The hydrograph indicates the ice cover breakup, jam formation, and release processes. This shows a mid-winter breakup jam occurred in mid-January. Another breakup occurred with a rainy warm period around Feb. 20, the jam formed in mid-January was released, and a new jam was formed. Both of these events occurred before spring.

The significant increase in air temperature and the heavy rainfall on Jan. 12 led to the considerable surface runoff in the catchment. This resulted in a rapid increase in river discharge. The breakup of ice cover occurred on the evening of Jan. 12 and caused the abrupt drop of the water level at the gauging station. This is a typical pattern of the water level change due to the reduction of the ice resistance on the flow when the ice cover breaks up. Following the breakup, a jam quickly formed and released downstream of the gauging station, which resulted in a rapid increase and decrease in the water level. The ice run reached the Hogansburg and formed an ice jam at the downstream of the dam site. The stage at the gauging station gradually decreased with the partial release of the channel storage of the jam, before the next cold spell, which frozen the surface ice accumulation in the channel.

Another warm period with warm air temperature and steady rainfall occurred between Feb. 20 and 22 resulted in approximately seven miles of ice cover breakup along with the release of the January jam. An ice jam formed again downstream of the dam site and caused severe flooding. It was reported that fifteen rescues were performed to remove trapped residents. Ninety-six people had evacuated and were staying in hotels or with family. Power had been knocked out at a substation for ten hours on Feb. 22, 2018. Figure 60 shows the 2018 February ice jam flooding at Hogansburg. (https://www.newyorkupstate.com/northern-ny/2018/02/flooding_ice_jams_in_north_country_see_video_photos_along_st_regis_river.html)

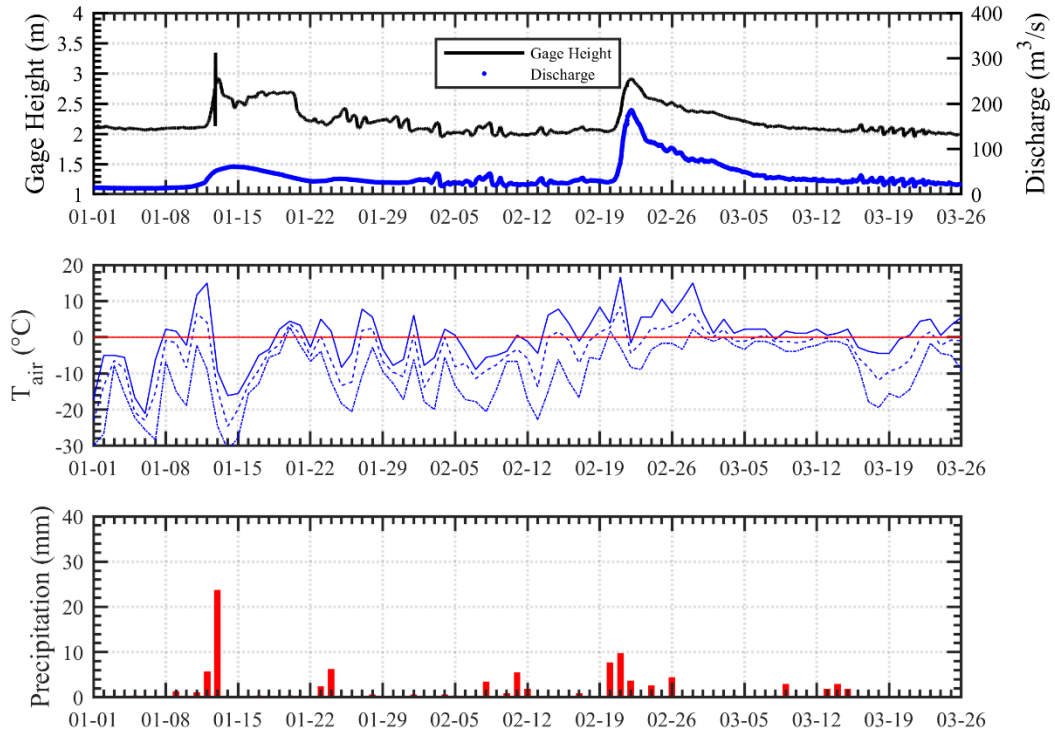

Figure 59. January - March 2018 flow and weather conditions.

Figure 60. 2018 Februry ice jam flooding at Hogansburg. Courtesy of SRMT Police. (https://www.newyorkupstate.com/northern-ny/2018/02/flooding_ice_jams_in_north_country_see_video_photos_along_st_regis_river.html)

- **2018-19 Winter**

This is a borderline case for a mechanical breakup in mid-March. Figure 61 shows the flow and weather of the winter. Heavy rain on the night of Mar. 13 was followed by a warm period between March 14 and 15 increased discharge and water level. However, this short period of the rainfall in the night did not lead to large surface runoff and rapid increases in discharge and water level to cause the cover breakup. The following two days were warm but no precipitation. The ice cover melted in place, as shown in Figure 62.

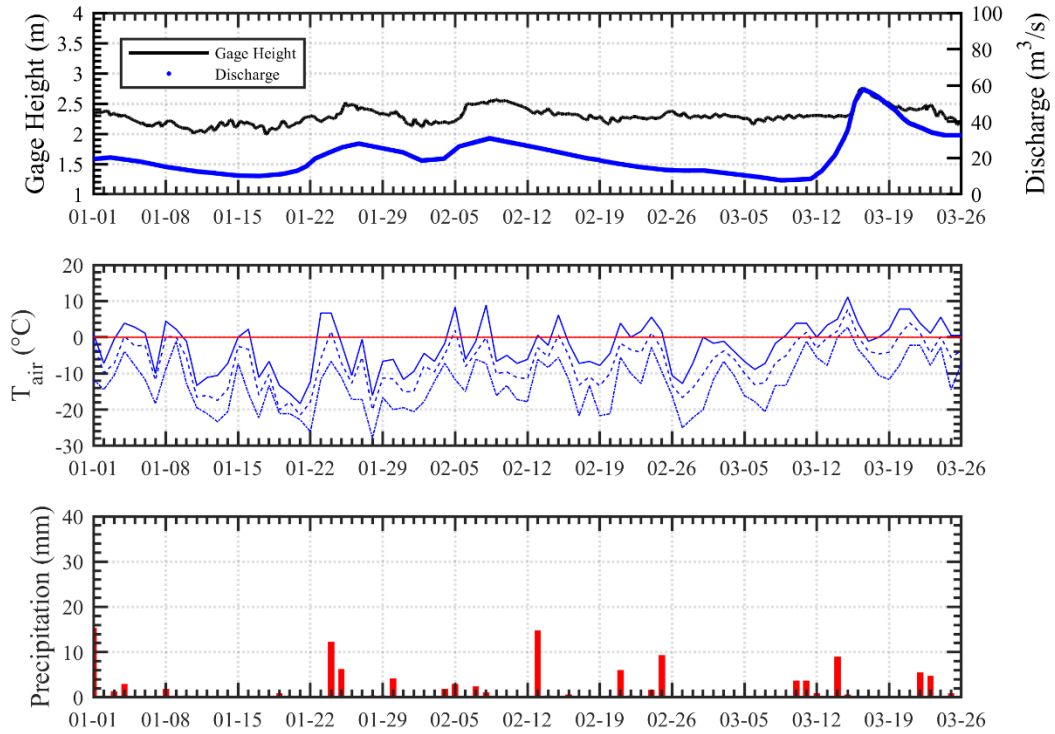

Figure 61. January - March 2019 flow and weather conditions.

Figure 62. Observed ice condition at the downstream of Helena Bridge, Mar. 15, 2019.

- **2019-20 winter**

Mid-winter cover breakup and ice jam flooding occurred this winter. Figure 63 shows the flow and weather of the winter. The increase of discharge due to rainfall and warm air temperature on Jan. 11 caused the breakup of ice cover between Helena and Hogansburg on the night of Jan. 12 when the surface runoff in the catchment from the upstream reach arrived Helena. An ice jam formed against the intact ice cover downstream of the Hogansburg Dam site. Two houses were evacuated due to the localized ice-jam flooding. Figure 64 shows the ice jam formation at the downstream of the dam site on Jan. 13. Comparing with the 2018 ice jam events, the damage caused by the 2020 ice jam was localized because of the relatively small amount of ice. The ice cover breakup reach was between Helena and Hogansburg on the night of Jan. 12, 2020. A rapid drop in the water level did not occur when the breakup of the ice cover occurred. The increase of the water level between Jan 18 and 22 was due to the ice jam formation immediately downstream of the gauge station observed by an on-site residence. This was different from the catastrophic 2018 Feb. jam flooding, which was originated from a long reach of ice cover breakup and the preceding ice jam formation in Jan. 2018. Figure 65 shows the ice condition at the Hogansburg project on Jan. 13, 20, 24, and 28, 2020. The jam consolidated and frozen in place during the cold spell of the following week. Ice cover formed again between Helena and Hogansburg. A large rainfall on Jan. 26 triggered the cover breakup again and reconsolidated the ice jam. The growing ice jam led to the continuous flood inundation of the properties along the banks. A long reach excavator was employed to remove the ice from the jam to help release the channel storage on Jan. 27. It brought about a temporary lowering of the backwater because the excavation area formed ice cover overnight due to the cold temperature. The crew resumed the work in the following day on Jan. 28 and further mitigated the flooding. Figure 66 to Figure 69 shows aerial photos on the ice condition at the Hogansburg project on Jan. 30.

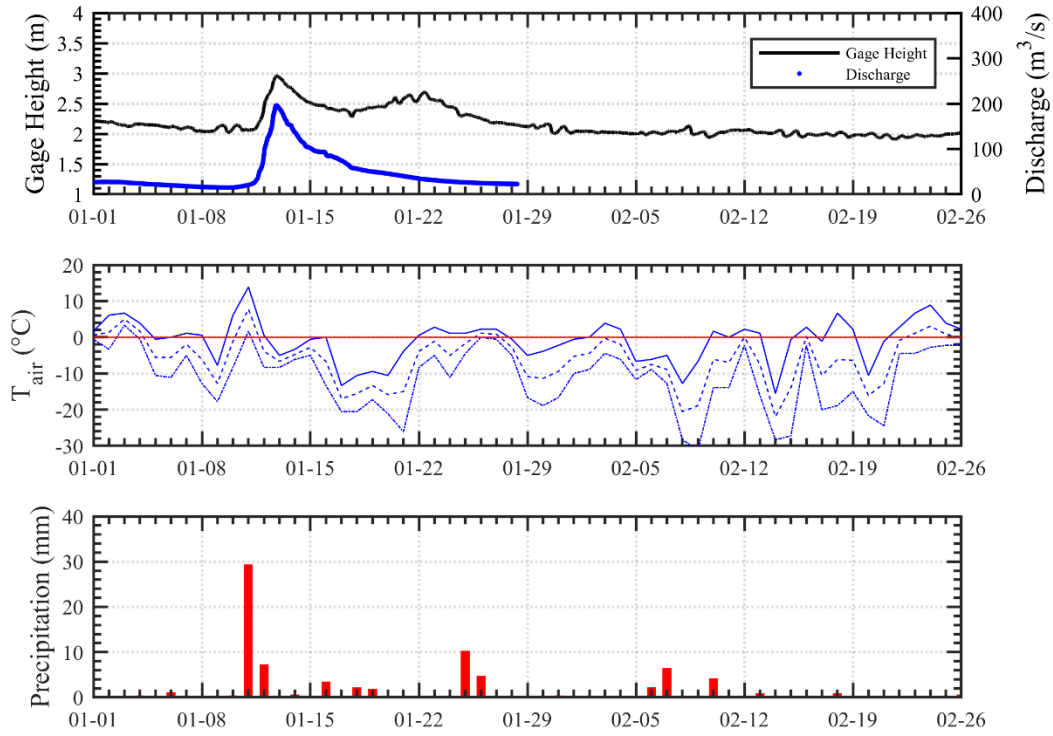

Figure 63. January - March 2020 flow and weather conditions.

Figure 64. Ice jam formation Jan. 13, 2020.

Figure 65. Ice conditions at the Hogansburg project, Jan. 2020.

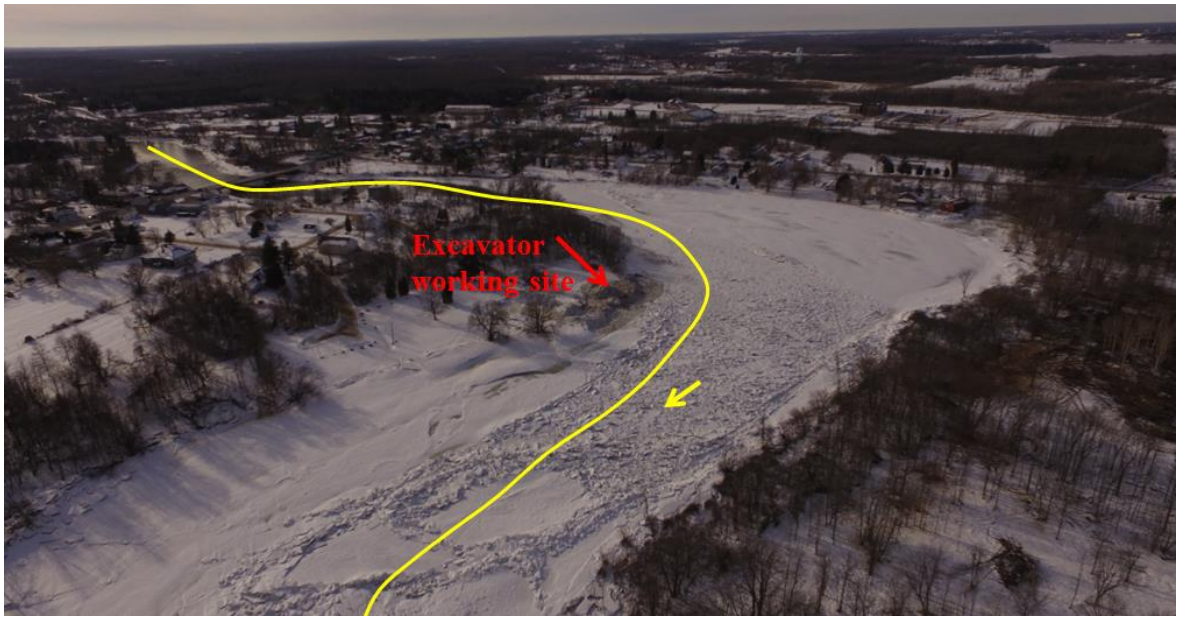

Figure 66. Ice condition at the Hogansburg on Jan. 30. The yellow line indicates the main flow path. Due to the high spots and shallow areas along the outer bank, the main flow path is closer to the inner bank. The effective ice passage in the sharp bend is limited. The ice discharge from the breakup of the upstream ice cover exceeds the ice transport capacity of the bend and form the ice jam at the bend exit against the ice cover downstream.

Figure 67. The aerial photo on the flow and ice condition at the bend entrance on Jan. 30. The ice cover extents to about 70% of the channel width and reaches the submerged island. The open water strip indicates the main flow path where the lateral growth of the ice cover ice stopped due to the high velocity except for very cold periods.

Figure 68. Aerial photo of the ice jam toe on Jan. 30. The red line indicates the ice jam front against the ice cover downstream.

Figure 69. The aerial photo on ice jam and the excavator working site on Jan. 30. Although the removal of the ice accumulation by excavator was a small fraction of the cross-section, it was close to the main flow path and increased the flow to downstream. As a result, it alleviated the high water level caused by the ice jam.

The above analysis on the past ice jam events suggested that the combination of warm air temperature with rainfall in the catchment with snow accumulation is the condition that could lead to a breakup ice jam flooding, especially when it occurred in mid-winter before March. This could be used to forecasts the ice jam flooding potential for emergency management. Although without sufficient data to provide meaningful statistical analysis, the historical data appears to show a worsened scale and frequency of ice jam flooding, which might be related to the occurrences of more extreme events related to climate change.

6. Potential Remediation Approach

The historical events indicate that once the mechanical breakup of ice cover occurs, the ice jam is likely to form at Hogasburg and increase the flooding potential. The removal of the dam increases the ice jamming potential at the downstream of the dam site and causes slightly higher backwater than that with the dam condition. The amount of ice entering the pool area downstream of the dam site plays an important role in the jamming and flooding potential. Removing the ice cover downstream of the dam site might provide some relief, but not practical. A possible mitigation scheme could be to install ice booms upstream of the dam site to reduce the ice supply and the rate of ice discharge to Hoganburg. Slow flowing cross sections are possible boom sites so that the movement of ice run could be held back (Shen et al. 1997, Tuthill and Lever 2006). The critical Froude number for the entrainment of surface ice pass the boom, or a surface ice accumulation is 0.09 (Shen and Ho 1986). The growth of the ice jam thickness will increase the water velocity underneath. When the water velocity exceeds a critical erosion velocity of about 1.5 m/s (Tuthill and Gooch, 1998), the ice rubbles will erode and transport to downstream. The ice boom might submerge due to excessive load from the ice accumulation, and the ice will spill over the boom to downstream.

The evaluation of the effectiveness of using ice boom to mitigate the ice jam flooding potential in the Hogansburg area is discussed in this chapter. Both one- and two-boom set-ups are examined. Freeze-up simulations are made first with the ice boom or booms in place to obtain the ice distributions in the domain. The frozen ice accumulation formed against the boom during the freeze-up would enhance the function of the boom. The breakup simulations will be made with the simulated freeze up results. However, the minimum cover thickness is increased to 0.43 m (17 inches) based on the observed cover thickness during the Feb. 2018 breakup jam event.

Figure 70 shows the simulated longitudinal profile of the open water flow condition with a typical freeze up discharge of 22.65 m^3/s (800 ft^3/s). Figure 71 shows the simulated Froude number distribution with the discharge of 22.65 m^3/s (800 ft^3/s) and the selected locations for both booms. Two ice boom locations are selected at the cross sections where the flow depth is large to allow thick ice accumulation, and the Froude number is less than 0.09. These boom locations are at 2.4 km and 7.98 km from Helena, respectively. The Froude number at the boom No.1 cross section is 0.065 and at the boom No.2 cross section is 0.035. In the booms simulations, a high critical line load of 5.3 kN/m for the ice boom is assumed to allow for the estimation of the required boom design load. Other boom parameters are listed in Table 4.

Table 4. Ice boom characteristics

	Critical Line Load (kN/m)	Buoyancy (kN/m)	Ice thickness for resurfacing (m)	Boom-ice friction coefficient (μ)
Pontoon Boom	5.3	2.15	0.55	1.0

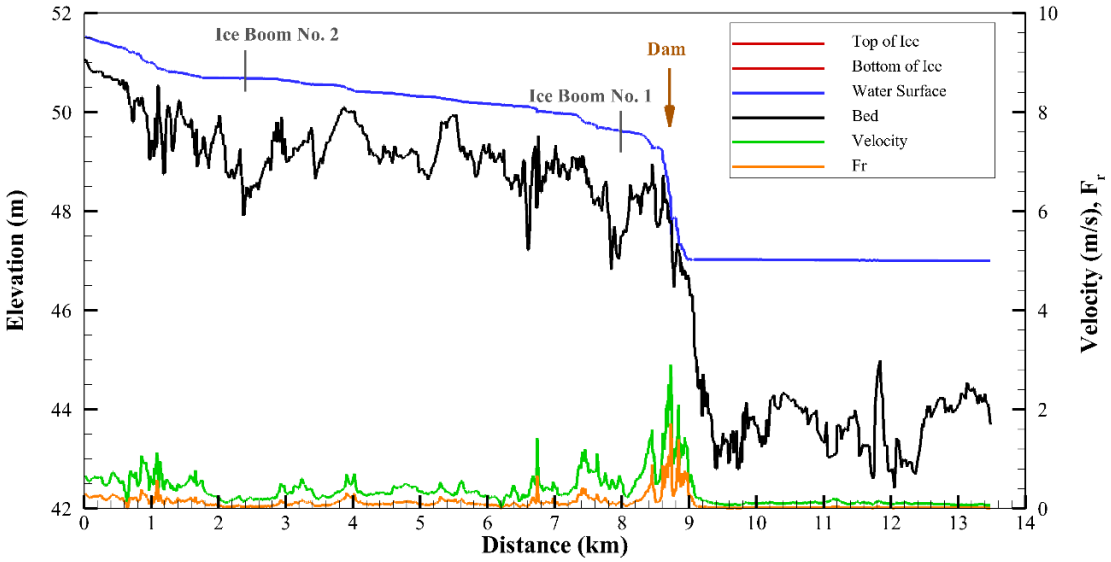

Figure 70. Simulated longitudinal profile of flow condition and selected ice boom locations (Q = 22.65 m^3/s).

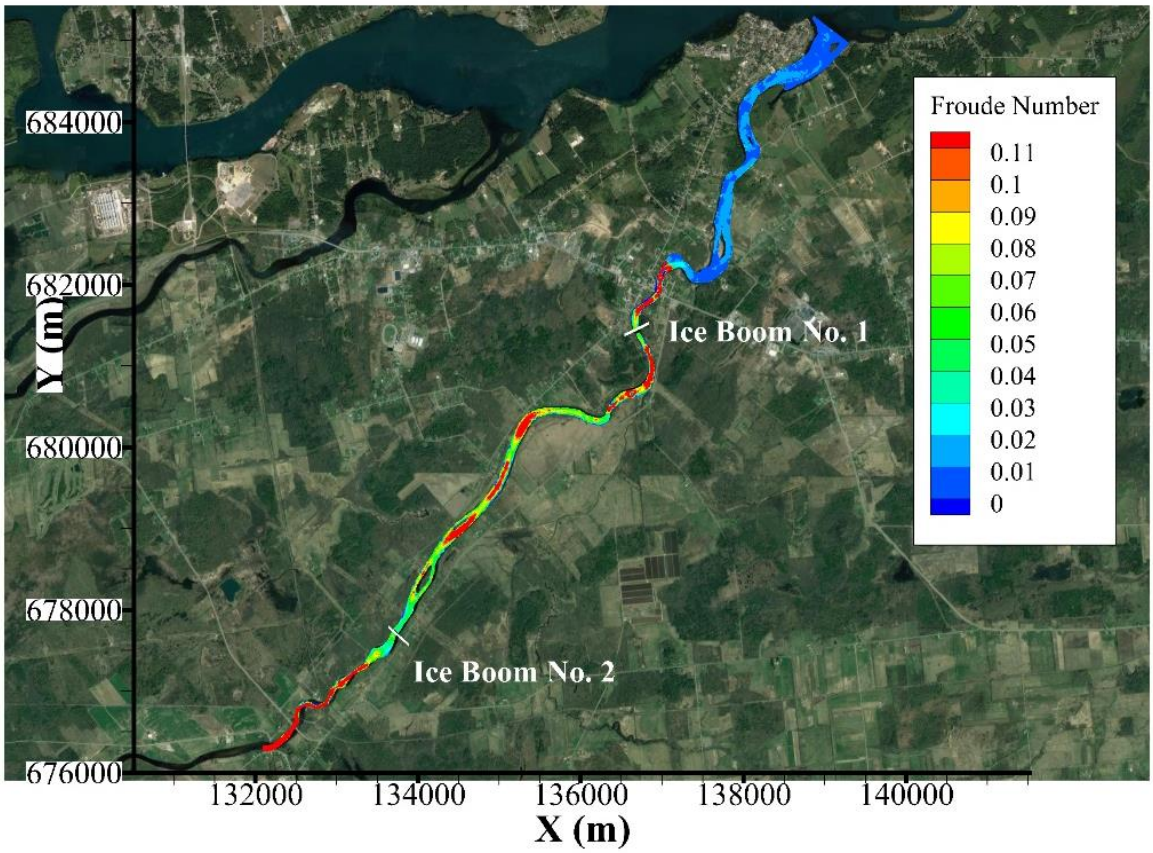

Figure 71. Simulated Froude number distribution and selected ice boom locations (Q = 22.65 m^3/s).

6.1 Freeze-up with Boom Installation

The flow and weather conditions of four winters after the dam removal are shown in Figure 72 to Figure 75. Table 5 summarizes the average discharge over the freeze-up period. A discharge of 22.65 m^3/s (800 ft^3/s) and an air temperature of -10°C are used for the freeze-up simulation without and with boom installations. Figure 76 shows the simulated flow and ice conditions of freeze up without the ice boom. Thick ice accumulation formed at the upstream of the former dam site. Figure 77 and Figure 78 show the simulated flow and ice conditions. The ice boom No. 1 located slightly upstream of the dam site reduced the surface ice discharge to downstream. The rapid area at the dam site remains open. The addition of the ice boom No. 2 reduces the ice volume between the two booms and the load on the first boom. Figure 79 shows the maximum ice load on the ice boom during the freeze-up period.

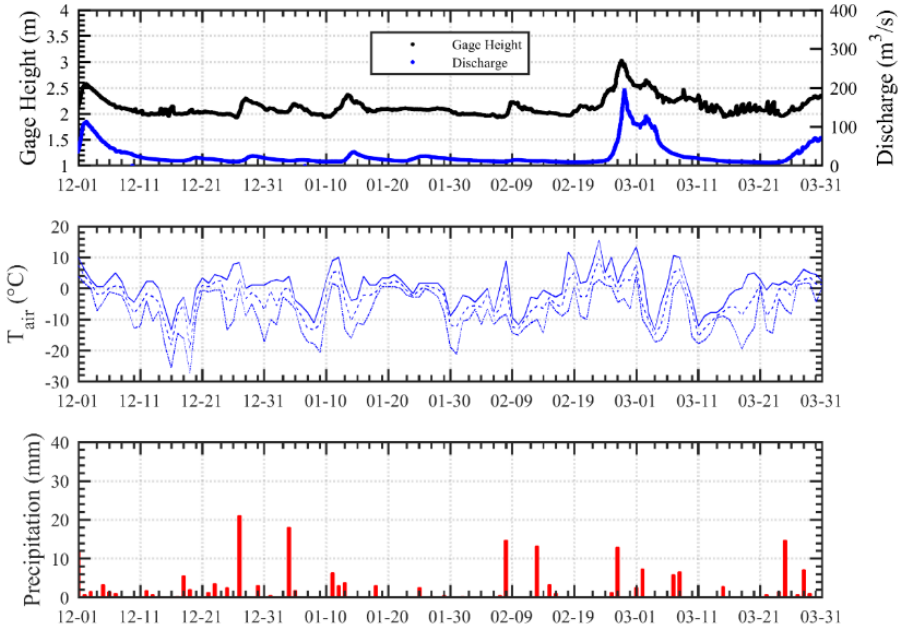

Figure 72. December 2016 - March 2017 flow and weather conditions.

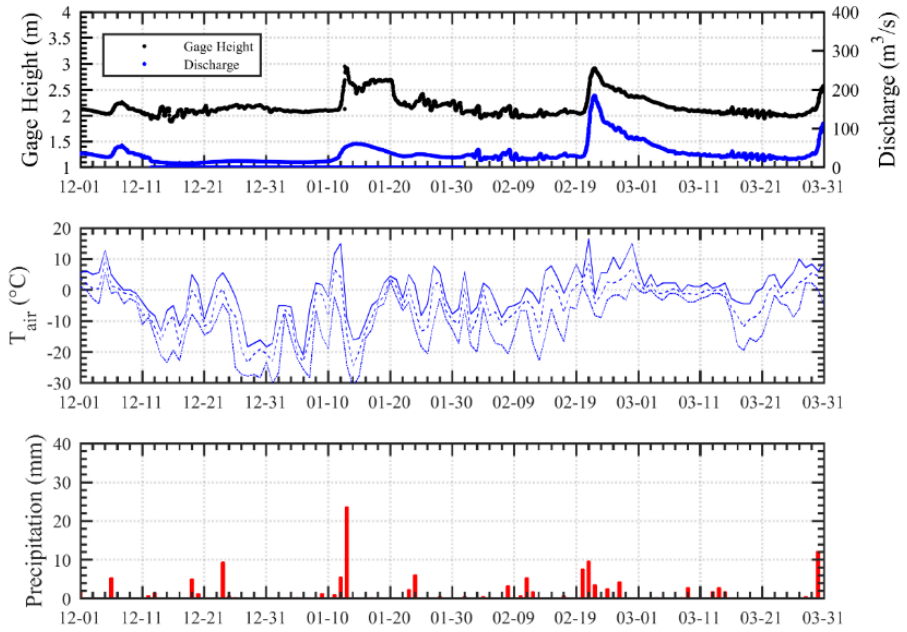

Figure 73. December 2017 - March 2018 flow and weather conditions.

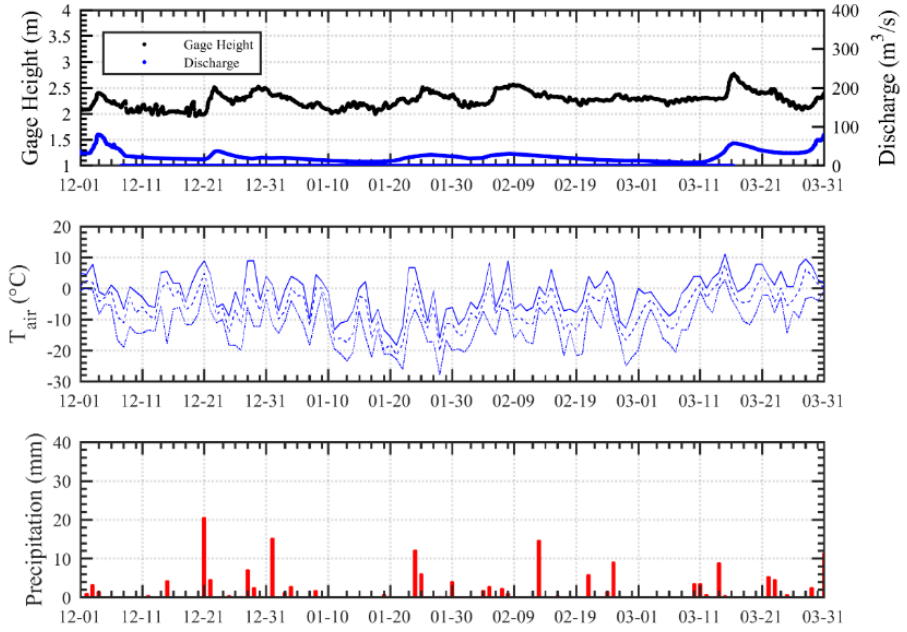

Figure 74. December 2018 - March 2019 flow and weather conditions.

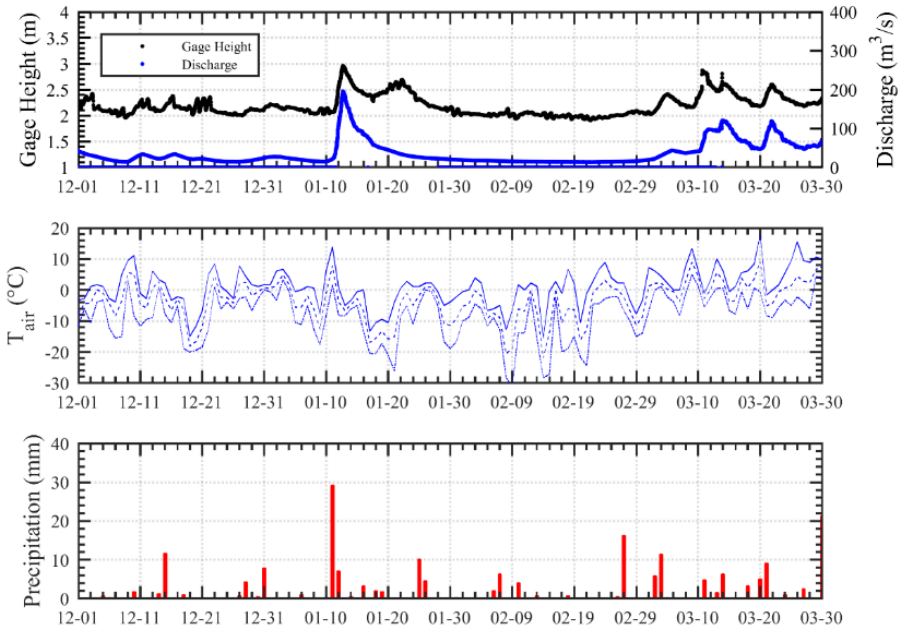

Figure 75. December 2019 - March 2020 flow and weather conditions.

Table 5. Freeze-up conditions 2016-2019 winters.

Winter	Q (cms)	Q (cfs)	Freeze-up Period
2016-17	15.2	536.8	12/15 - 1/10
2017-18	16.1	568.3	12/11 - 1/5
2018-19	20.5	724.4	12/25 to 1/10
2019-20	21.9	775.5	12/15 to 1/5

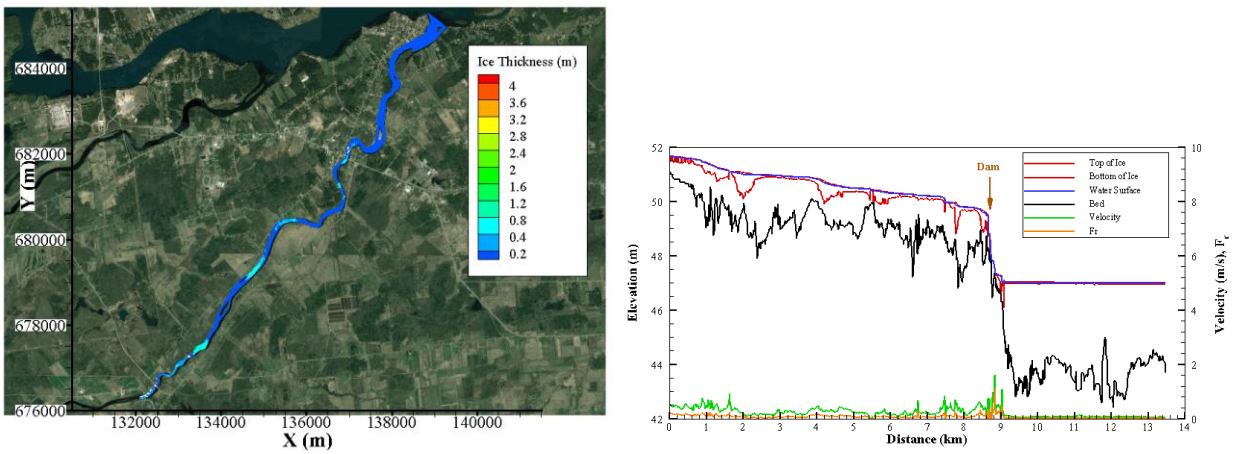

Figure 76. Simulated ice and flow conditions of freeze up without ice booms.

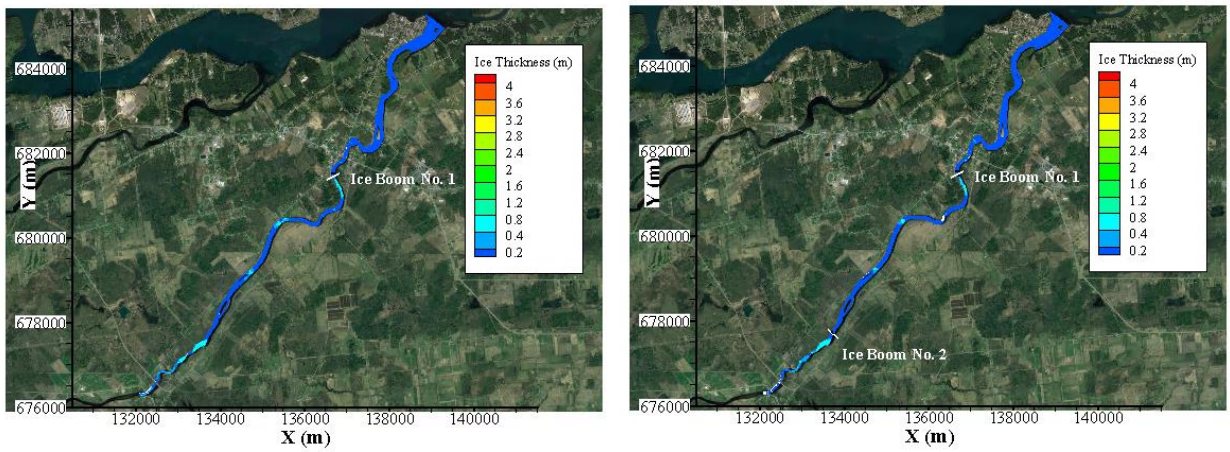

Figure 77. Simulated ice thickness distribution of freeze up. Left: One-ice-boom installation. Right: Two-ice-boom installation.

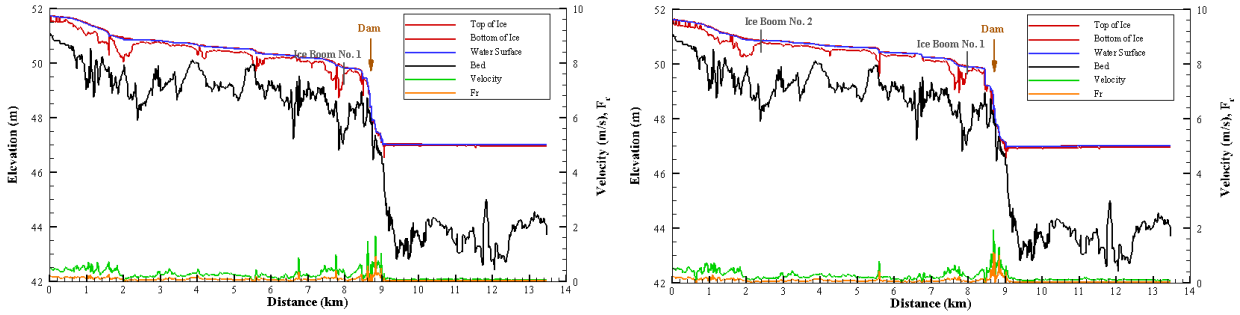

Figure 78. Simulated longitudinal profiles of freeze up flow and ice conditions. Left: One-ice-boom installation. Right: Two-ice-boom installation.

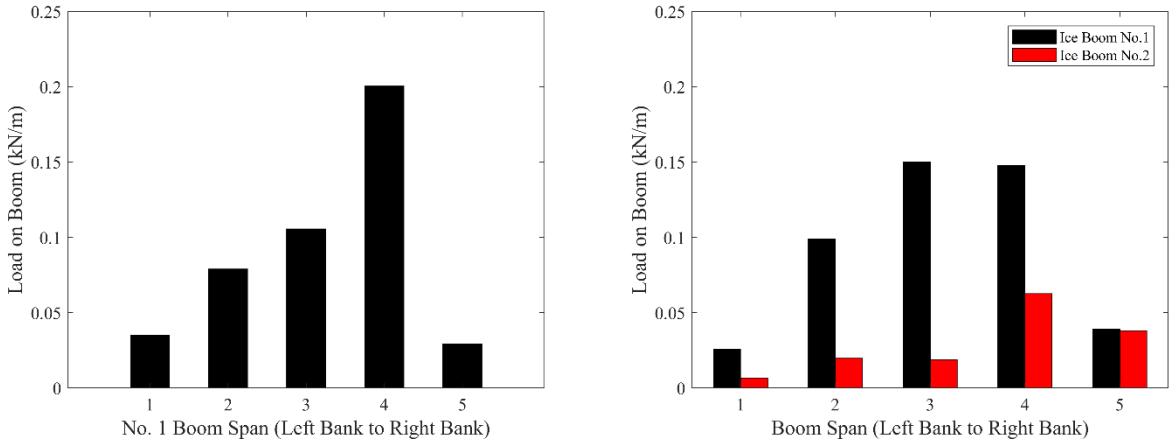

Figure 79. Simulated maximum ice load on boom spans. Left: One-ice-boom installation. Right: Two-ice-booms installation.

6.2 Breakup with Boom Installation

The observed discharge during the 2018 Feb. ice jam flooding event, as shown in Figure 80, is used as the inflow discharge at the upstream boundary. The minimum ice cover thickness from the freeze-up simulation results is increased to 0.43 m (17 inches). The initial ice thickness distribution for two-ice-boom scenarios are presented in Figure 81.

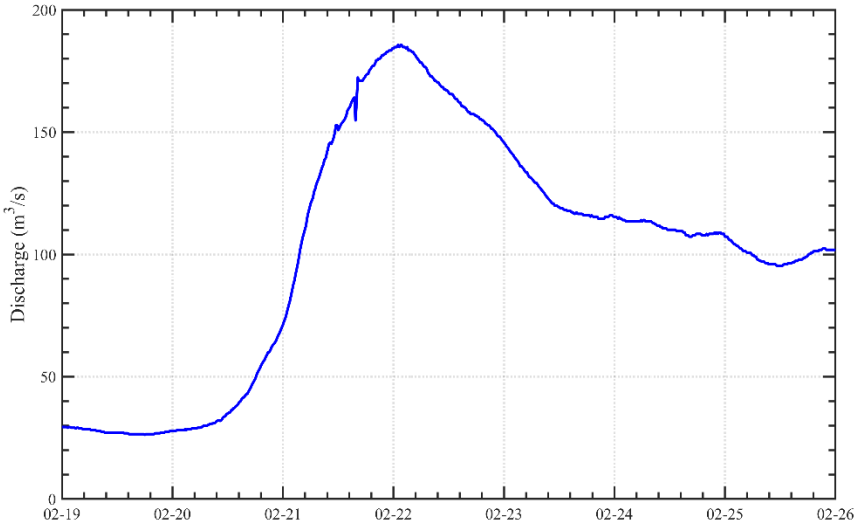

Figure 80. Observed discharge during the 2018 Feb. ice-jam flooding event. The sudden drop of the discharge at 15:45 on Feb. 21 indicated the occurrence of the ice cover breakup.

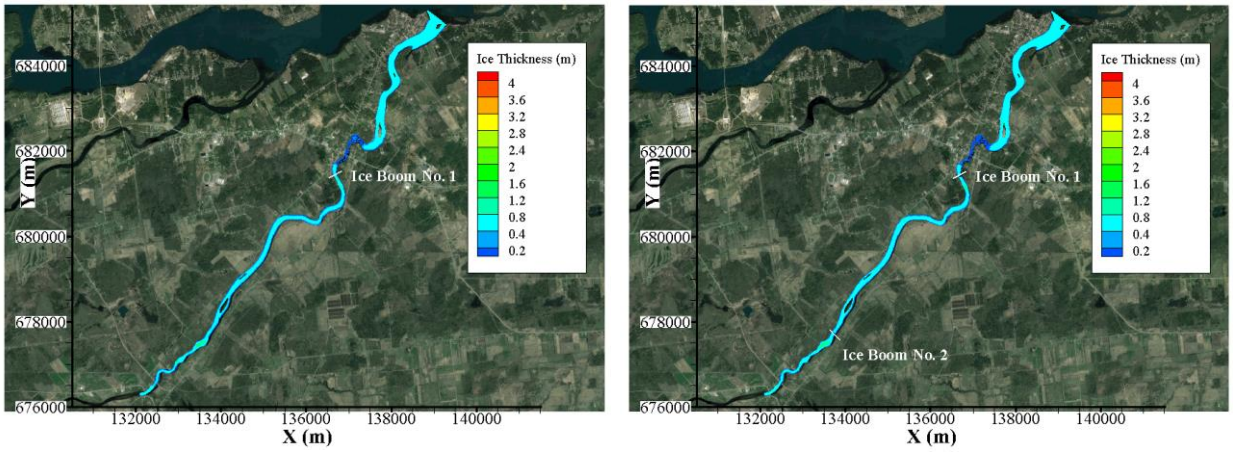

Figure 81. Initial ice cover distribution for breakup simulation. Left: one ice boom installation. Right: two ice booms installation.

6.2.1 One-boom installation

Figure 82 and Figure 83 show the simulated ice thickness distribution in the vicinity of the dam site and the simulation domain. Figure 84 and Figure 85 show the simulated water depth distribution. Figure 86 shows the simulated longitudinal profiles of ice and flow conditions. The ice jam formed against the ice boom after the breakup of the ice cover. The increasing flow discharge resulted in the erosion of the ice underneath the jam. The eroded ice floe led to the formation of the ice jam against the ice cover in the pool downstream of the dam site. The ice supply from the erosion of the bottom of the ice jam led to the growth of the ice jam and the increase in the water level at Hogansburg. In the upstream reach, some surface ice rested on the floodplain after the peak discharge receded. The boom reduced the ice supply to downstream and the size of the jam at Hogansburg. The ice accumulation at the ice boom led to an increase in water depth in the upstream reach. Ice jam did not form at the channel contraction 2.24 km downstream of the Helena.

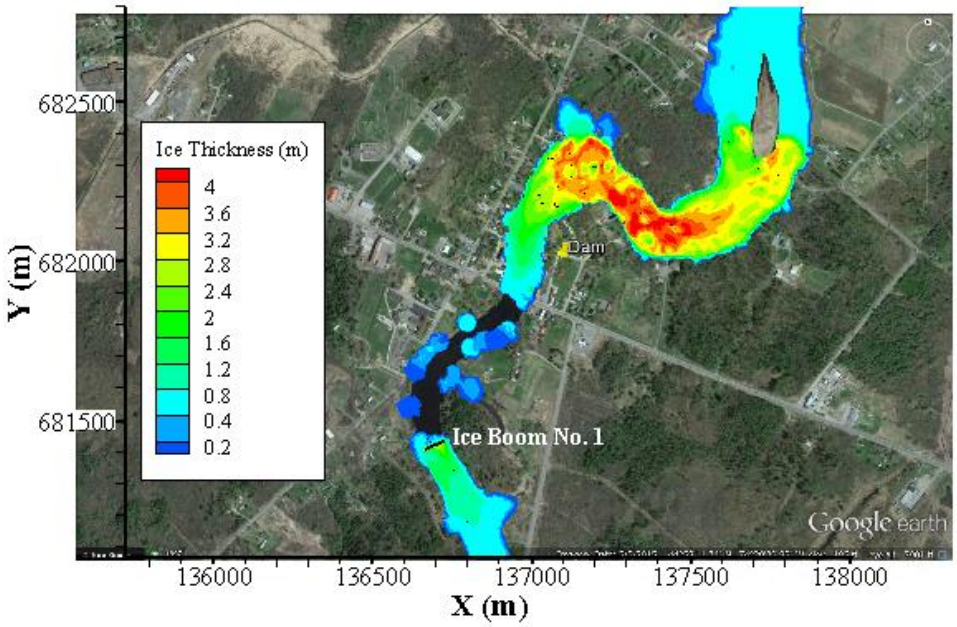

Figure 82. Simulated ice thickness distribution at Hogansburg, at 12 pm, Feb. 22, 2018 – One-ice-boom.

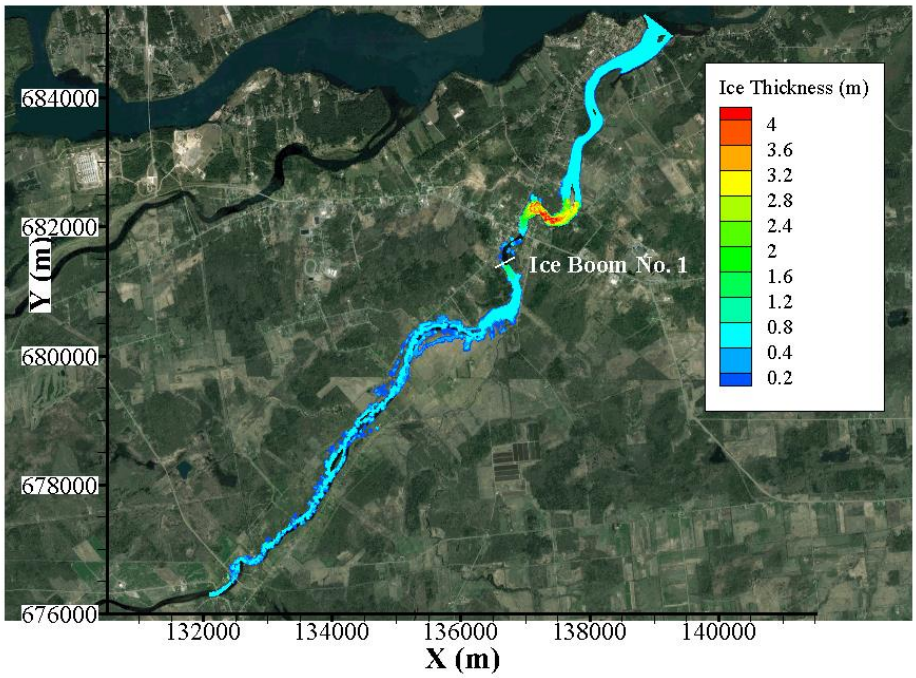

Figure 83. Simulated ice thickness distribution, at 12 pm, Feb. 22, 2018 – One-ice-boom.

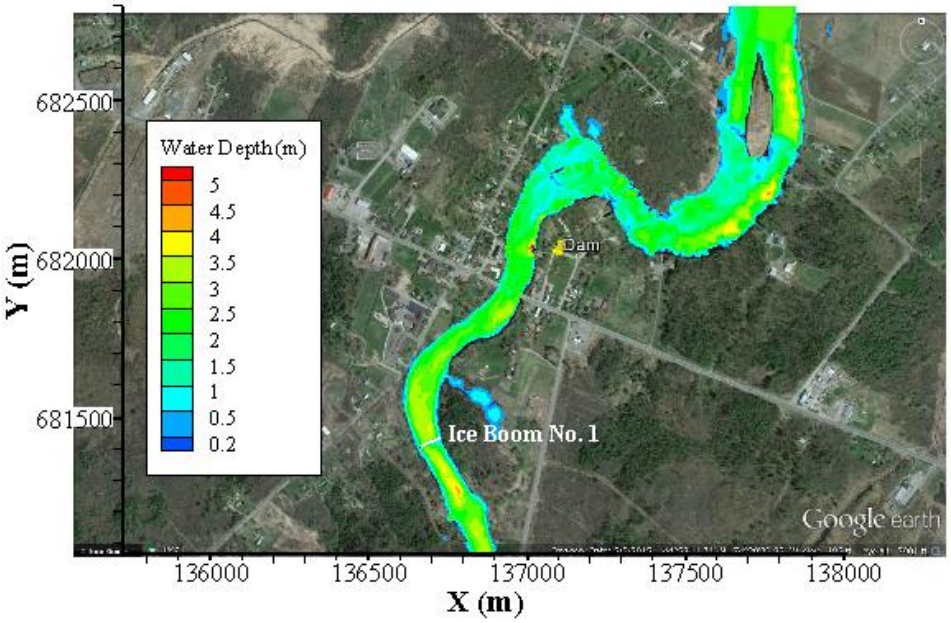

Figure 84. Simulated water depth distribution at Hogansburg, at 12 pm, Feb. 22, 2018 – One-ice-boom.

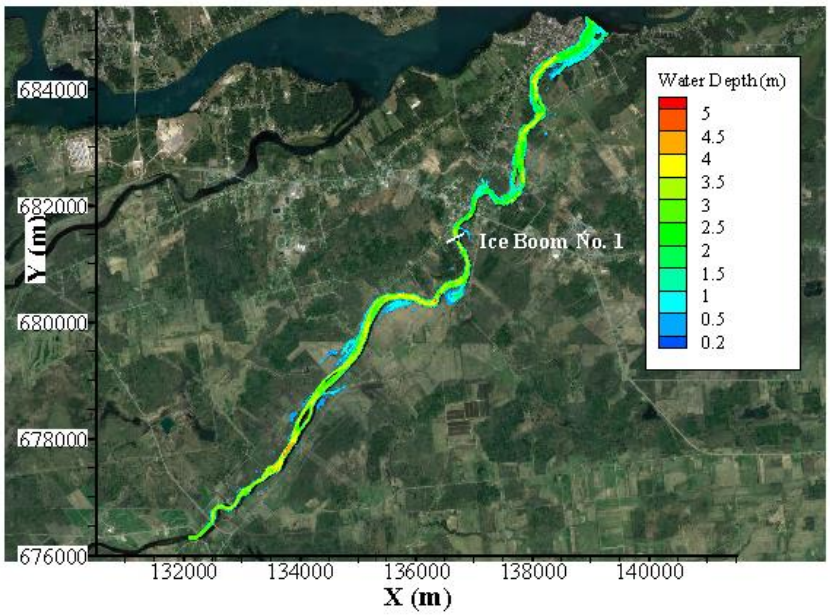

Figure 85. Simulated water depth distribution, at 12 pm, Feb. 22, 2018 – One-ice-boom.

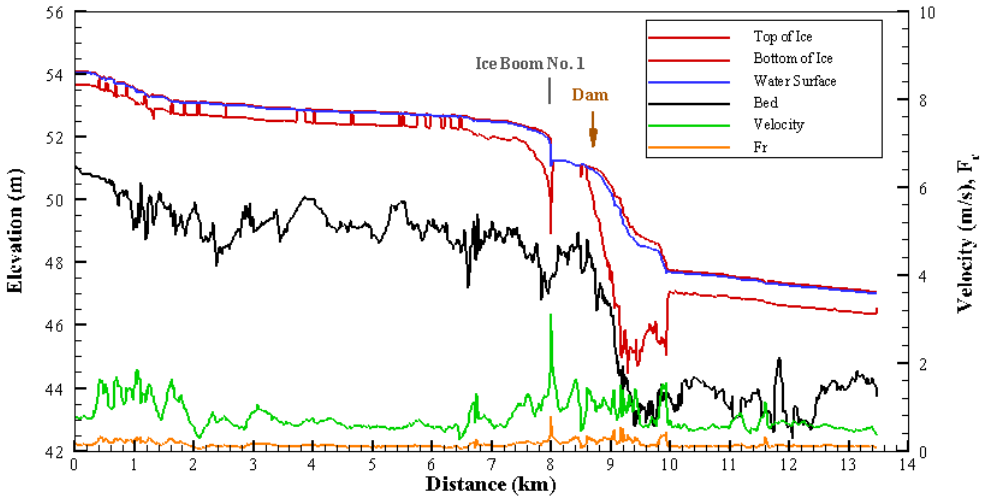

Figure 86. Simulated longitudinal profiles of flow and ice conditions, at 12 pm, Feb. 22, 2018 – One-ice-boom.

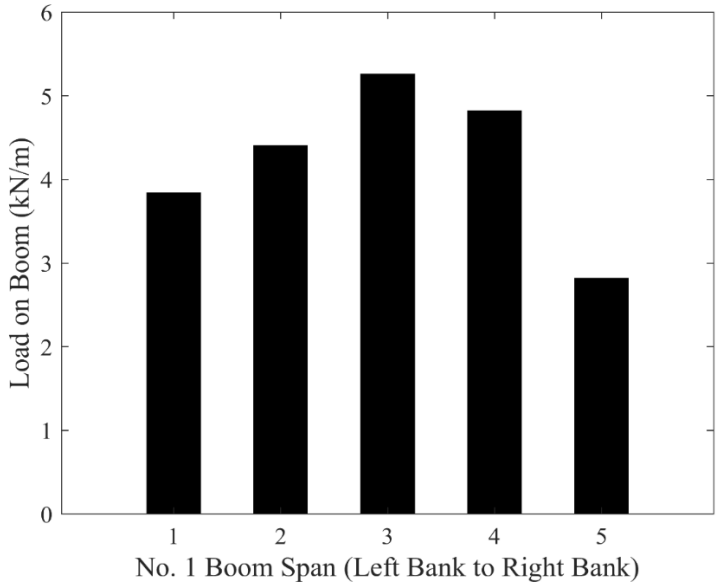

Figure 87. Simulated ice load on boom spans – One-ice-boom.

6.2.2 Two-boom installation

Figure 88 and Figure 89 show the simulated ice thickness distribution in the vicinity of the dam site and the simulation domain. Figure 90 and Figure 91 show the simulated water depth distributions. Figure 92 shows the simulated longitudinal profiles of ice and flow conditions. Ice jams formed against both ice booms after the breakup of the ice cover. Some ice rested on the floodplains after the peak discharge receded. The ice jam against boom No. 2 delayed the peak ice discharge from the peak water discharge to downstream. Hence, the erosion of the ice under the jam toe against boom No. 1 did not occur. The thick ice jam remained against the ice boom No.1. Flooding occurred between two ice booms. The backwater caused by the ice jam with the arrival of the peak discharge at boom No.1 resulted in the flow into the sub-channel. Some ice moved into the sub-channel and bypassed the ice boom No.1 back into the main channel. As a result, an ice jam formed in the sharp bend downstream of the dam site. However, the jam size is much smaller than the single boom case and much less flooding in the Hogensburg area.

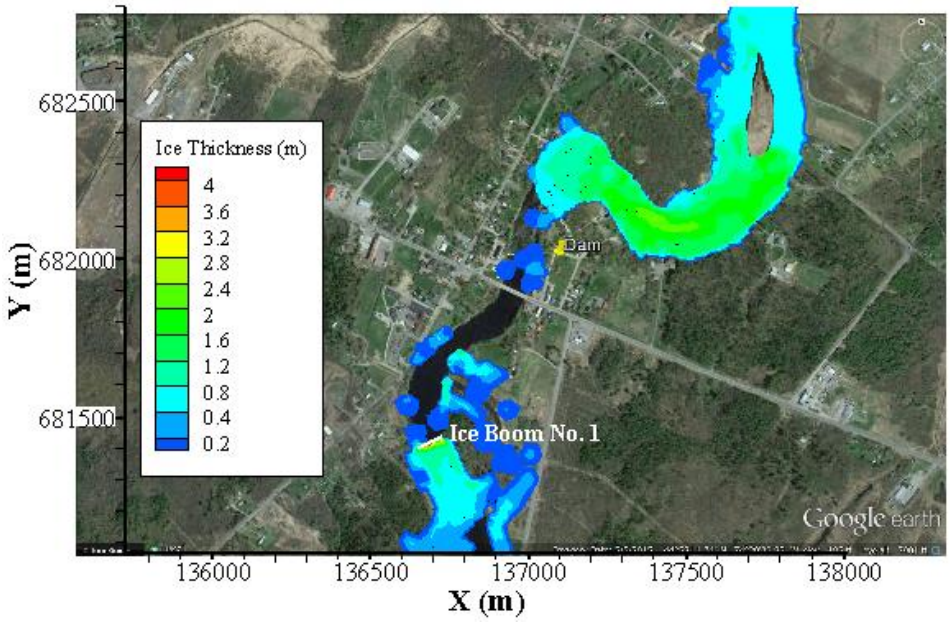

Figure 88. Simulated ice thickness distribution at Hogansburg, at 12 pm, Feb. 22, 2018 – Two-ice-booms.

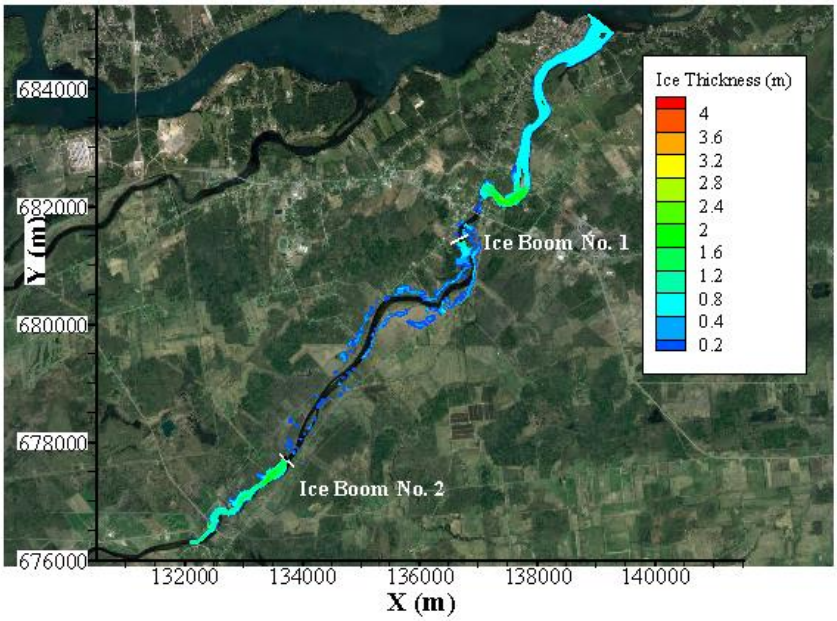

Figure 89. Simulated ice thickness distribution, at 12 pm, Feb. 22, 2018 – Two-ice-booms.

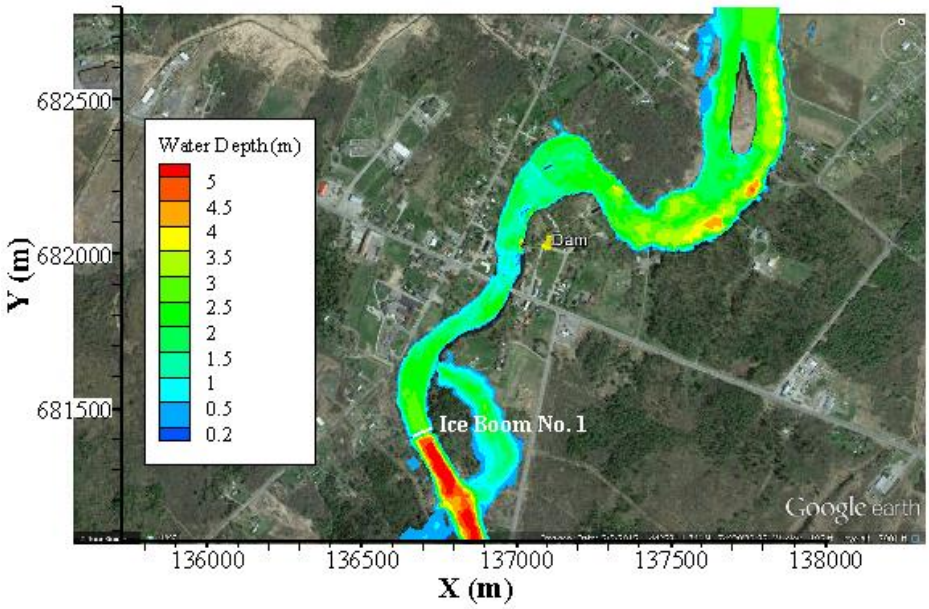

Figure 90. Simulated water depth distribution at Hogansburg, at 12 pm, Feb. 22, 2018 – Two-ice-booms.

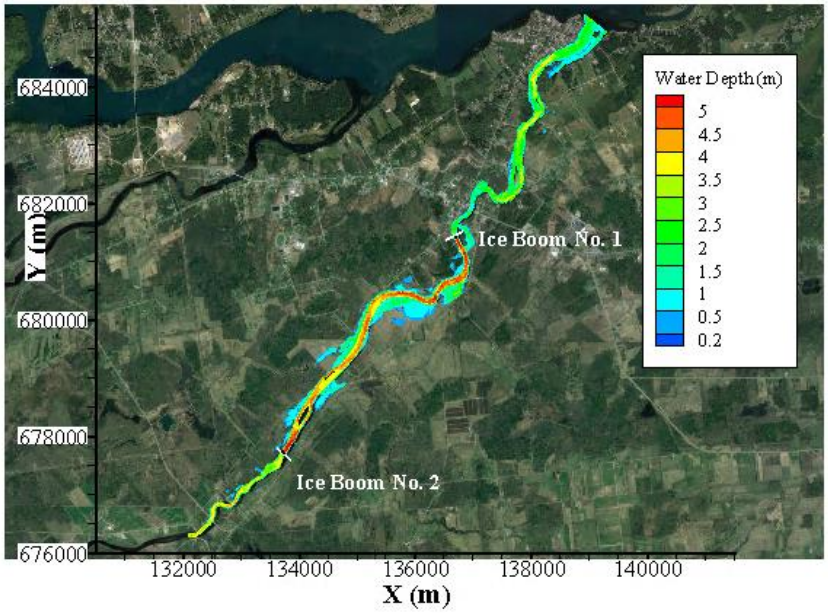

Figure 91. Simulated water depth distribution at Hogansburg, at 12 pm, Feb. 22, 2018 – Two-ice-booms.

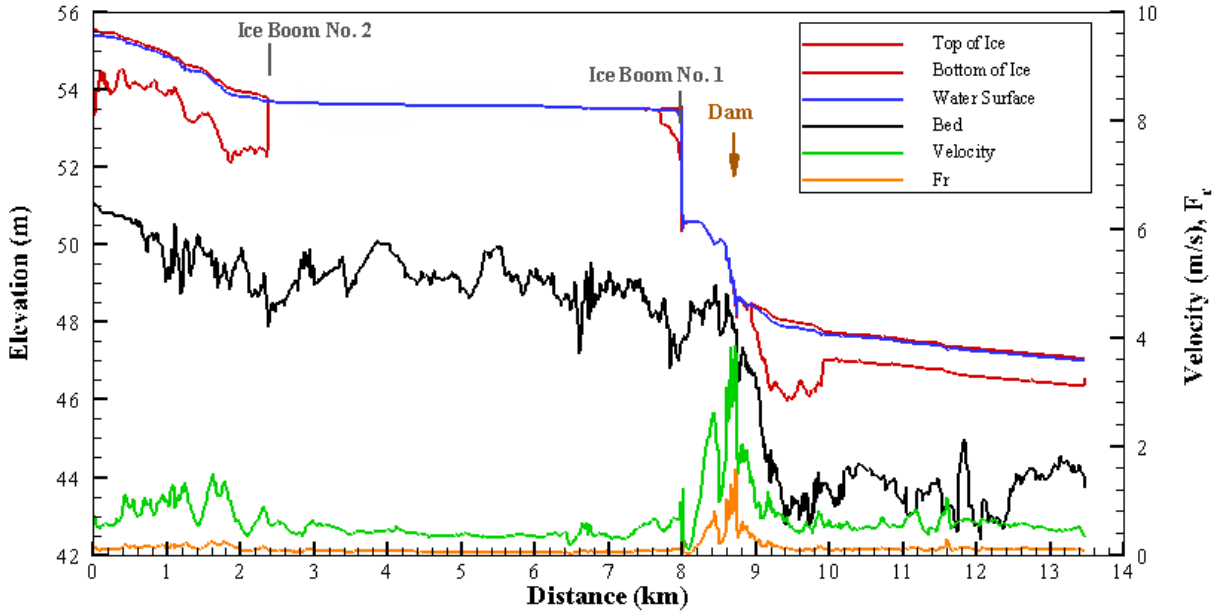

Figure 92. Simulated longitudinal profiles of flow and ice conditions, at 12 pm, Feb. 22, 2018 – Two-ice-booms.

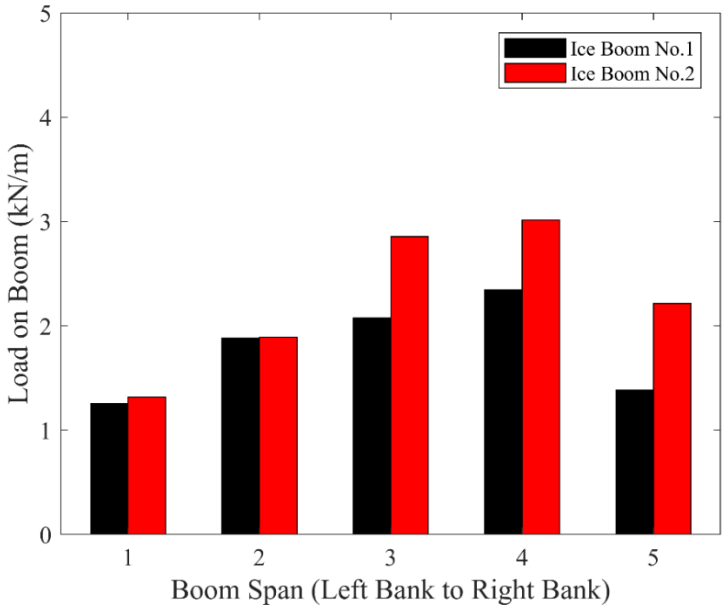

Figure 93. Simulated ice load on the ice booms – Two-ice-booms.

6.3 Summary

The effect of ice booms on the ice-jam flooding potential is evaluated by using the 2018 Feb. breakup discharge at the upstream boundary. Two ice booms are placed at 2.4 and 7.98 km from Helena, respectively. The ice booms produced ice accumulations during the freeze-up and

limited the surface ice supply to Hogansburg. Figure 94 shows the comparison of the simulated water levels with and without ice booms at 12 pm, Feb. 22, 2018. The simulated results indicate that the ice booms reduced the ice supply to Hogansburg. For the scenario with one ice boom installation, the ice jam formed against the boom after the breakup of the ice cover. However, the water velocity during the peak discharge was high enough to erode ice from the underside of the jam and transport to downstream. Minor localized flooding caused by the ice jam formation at Hogansburg. For the scenario with the two-ice boom installation, ice jams formed against both booms. The ice erosion did not occur at boom No.1 because the upstream ice jam attenuated the peak discharge. Both ice jams led to an increase in the water level in the upstream reach. The arrival of the peak discharge at ice boom No.1 and the backwater due to the ice jam caused flooding in the sub-channel. This diverted the ice and flow into the downstream and contributed to the ice jam formation at Hogansburg. The size of the ice jam at Hogansburg is small, so the ice-jam flooding did not occur there. However, flooding occurred in the reach between the two ice booms.

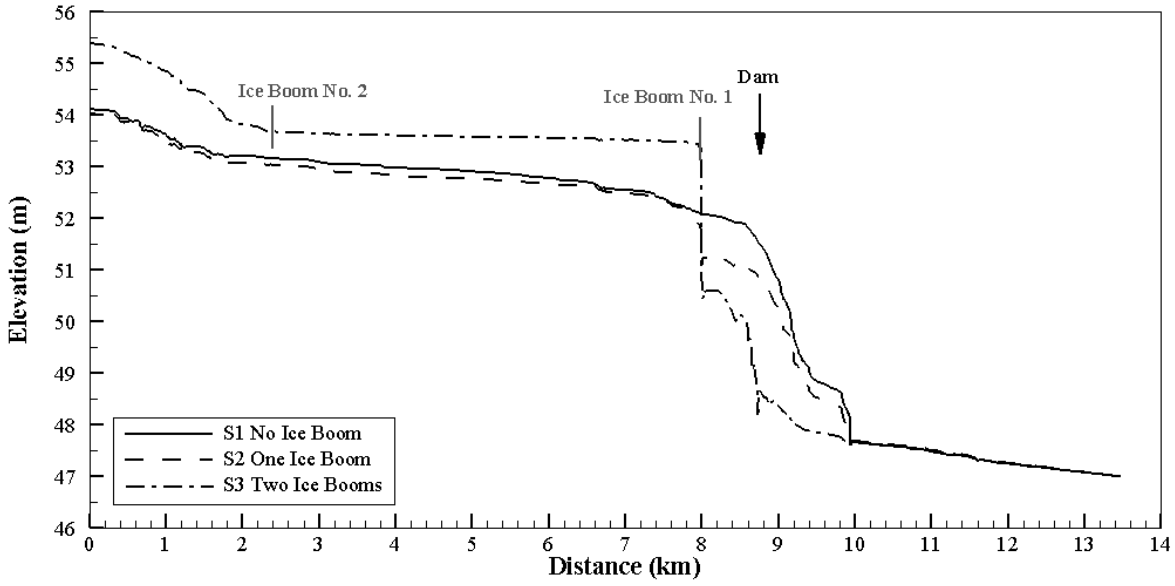

Figure 94. Comparison of the simulated water levels at 12 pm, Feb. 22, 2018.

The maximum water level and ice thickness at key locations shown in red circles in Figure 5 are summarized in Table 6. The maximum jam thickness at Hogansburg at locations indicated in Figure 95 are also included in Table 6.

Table 6. Summary of ice and flow conditions at the key locations.

Locations	Post-Dam Removal, No Ice Boom	
	$h_{i,max}$ (m)	$H_{w,max}$ (m)
Left Bank at Hogansburg	3.330	50.733
Right Bank at Hogansburg	3.091	50.881
Dam Site	1.972	51.495
NY 37 Bridge	1.021	51.769
NY 37C Bridge	0.353	53.948
Ice Jam at Hogansburg	5.340	49.295

Location	Post-Dam Removal, One Ice Boom	
	$h_{i,max}$ (m)	$H_{w,max}$ (m)
Left Bank at Hogansburg	2.537	50.180
Right Bank at Hogansburg	2.369	50.20
Dam Site	1.296	50.786
NY 37 Bridge	0.422	50.890
NY 37C Bridge	0.346	53.944
Ice Jam at Hogansburg	4.869	48.955

Location	Post-Dam Removal, Two Ice Boom	
	$h_{i,max}$ (m)	$H_{w,max}$ (m)
Left Bank at Hogansburg	0.451	48.664
Right Bank at Hogansburg	0.416	48.572
Dam Site	0.091	48.793
NY 37 Bridge	0.131	48.989
NY 37C Bridge	1.075	55.250
Ice Jam at Hogansburg	2.412	48.022

Note: $h_{i,max}$ is the maximum ice thickness; $H_{w,max}$ is the maximum water surface elevation.

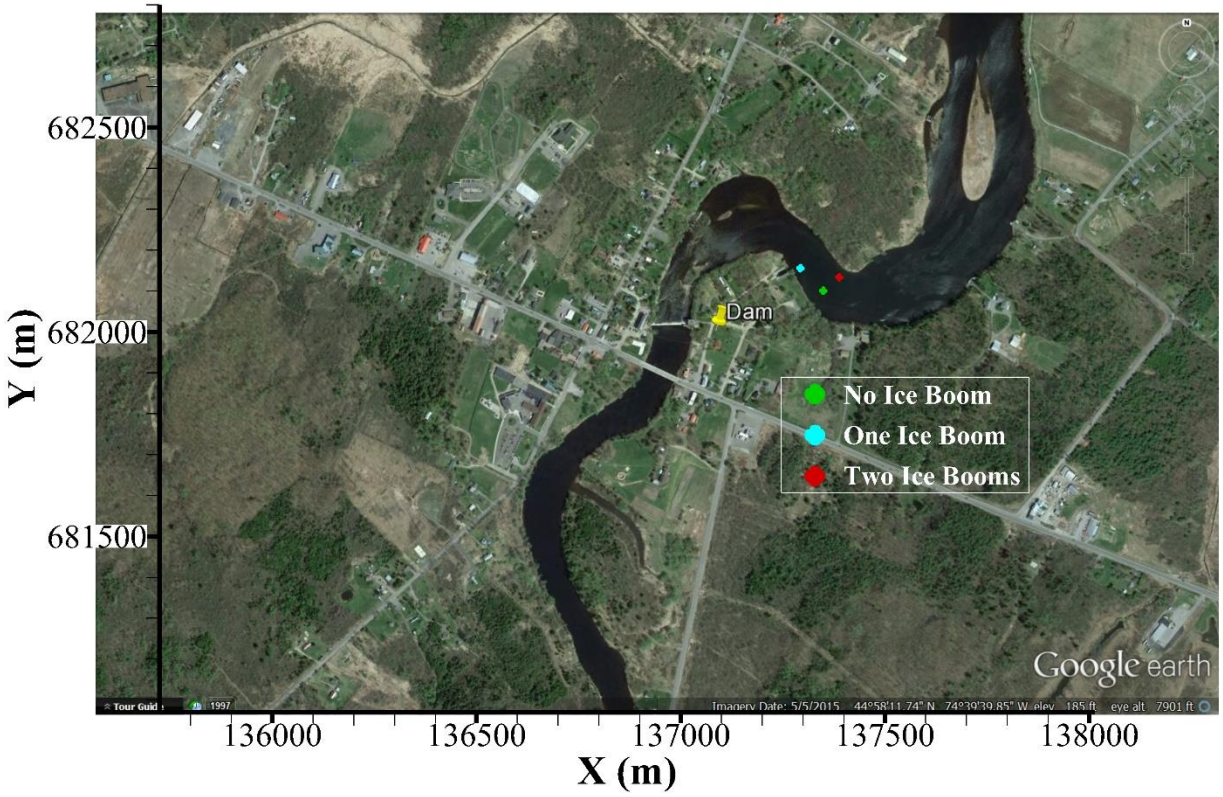

Figure 95. Locations of the maximum ice jam thickness at Hogansburg. – with or without booms.

7. Summary

This report presents a numerical model study on the ice transport and ice jam processes in the Lower St. Regis River for the pre- and post-dam removal conditions of the Hogansburg Dam. Past ice jam flooding events are reviewed to suggest a forecasting method for emergency management.

Diagnostic simulations for flow and ice movement characteristics are simulated first for four discharge conditions ranging from 24.07 m^3/s (850 ft^3/s) to 198.22 m^3/s (7000 ft^3/s). The simulation results indicate that under the low flow condition of 24.07 m^3/s (850 ft^3/s), the dam prevented the surface ice run to downstream, and the ice accumulation formed in the juxtaposition mode upstream of the dam. Under a higher flow condition with discharges of 39.64 m^3/s (1400 ft^3/s), 113.27 m^3/s (4000 ft^3/s), or 198.22 m^3/s (7000 ft^3/s), the ice run overtops the dam and forms a thick ice accumulation in the sharp bend downstream of the dam, and a thicker ice accumulation along the river upstream of the dam. The removal of the dam increased the flow and ice transport capacity. This increased the ice discharge to downstream to form a thicker ice jam in the sharp bend near the dam site. The effect of the dam on reducing the ice movement to downstream decreases as the flow discharge increases. The majority of the surface ice floes can overtop the dam and contribute to the thick ice jam formation in the bend at the downstream of the dam with high discharges. The dam removal further enhanced this process. However, the effect becomes less significant when the discharge becomes larger.

Observed historical ice jams are reviewed. The historical jam events showed that heavy rainfall during a warm spell would increase the discharge from the surface runoff in the catchment. This rapid increase of discharge is likely to trigger the breakup of the ice cover and cause the ice jam flooding.

The effect of the ice boom installation upstream of Hogansburg as a potential method to mitigate the ice-jam flooding potential is evaluated. The installation of ice booms helps to slow the surface ice transport and reduce the ice supply to Hogansburg. One ice boom can hold some surface ice and decrease the ice supply. However, the erosion of the ice at the underside of the jam against the boom can occur at high discharge conditions. As a result, the ice jam can still form and lead to an increase in water level at Hogansburg. A two-ice-boom could effectively limit the ice supply to Hogansburg, even though flow and ice can divert to the sub-channel and return to the river near Hogansburg. The size of the ice jam and flooding in Hogansburg is limited.

References

CH2M (Jacobs). 2015. Basis of Design: Decommission and Removal of the Hogansburg Hydroelectric Dam, SRMT 14-48, Report prepared for Saint Regis Mohawk Tribe.

David, T. 2016. Removal of the Hogansburg: Dam Reclaiming Tribal Lands and Natural Resources. ESRI, https://www.arcgis.com/apps/Cascade/index.html?appid=21952c937eb84b08addedd2ee0a933ff .

David, T. 2018. St. Regis River Ice Observations. Feb. 23, 2018.

Emery, E. 1981. Flood Waters Cause Evacuation of 8 Families. The Massena Observer, Feb. 26, Vol. 96, No. 10,506. Massena, New York.

Fisher Associates, 2015. Bathymetric and topographic survey data.

Fisher Associates, 2017. Supplemental bathymetric and topographic survey data.

Foltyn, E.P. and Tuthill, A.M. (1996) Design of Ice Booms, Cold Regions Technical Digest, No. 96-1, USA Cold Regions Research and Engineering Laboratory, Hanover, New Hampshire.

HDR Engineering, Inc., 2012. Hogansburg Hydroelectric Project (FERC No. 7518) Draft Historical Ice Jam Review Study Report submitted by Erie Boulevard Hydropower, L.P. (Erie).

Huang, F. and Shen, H.T., 2016. A Preliminary Study on Ice Jamming Potential Post Removal of the Hogansburg Dam, report submitted to St. Regis Mohawk Tribe.

Jantzen, T., Mitchell, R., and Monge, Z., 2018. Hogansburg Hydroelectric Dam: Upstream Conditions Analysis, 661101.03.C4.T4, Technical Memo submitted to St. Regis Mohawk Tribe.

Shen, H.T., 2010. Mathematical Modeling of River Ice Processes, Cold Regions Science and Technology, 62(1), 3-13, 2010.

Shen, H.T., and Ho, C.F., 1986. Two Dimensional Simulation of Ice Cover Formation in a Large River, Proceedings, IAHR Symposium on Ice, Vol. I, Iowa City, Aug. 547-558.

Shen, H.T., Lu, S.-A., and Crissman, R.D., 1997. Numerical Simulation of Ice Transport over the Lake Erie-Niagara River Ice Boom, Cold Regions Science and Technology, 26, 17-33.

Shen, H.T. and Liu, L., 2003. Shokotsu River Ice Jam Formation, Cold Regions Sc. and Tech., 37(1), 35-49.

Shen, H.T., Su, J., and Liu, L., 2000. SPH Simulation of River Ice Dynamics, Journal of Computational Physics, 165(2), 752-770.

St. Regis Mohawk Tribe (SRMT-Environmental Division), 2015. 2015-2016 Hogansburg Dam removal project. Technical Report.

Thew Associates., 2016. Map Showing As-Built Conditions for the Decommissioning of the Hogansburg Hydroelectric Development St. Regis River. Dec. 14.

Tuthill, A.M., and Gooch, G., 1998. A Physical Model Study of Ice Retention Booms. Proceedings, 14th International Symposium on Ice, Potsdam, N.Y., 61-68.

Tuthill, A.M., and Lever, J.H., 2006. Design of Breakup Ice Control Structures, ERDC/CRREL TR-06-7, US U.S. Army Cold Regions Research and Engineering Laboratory, Hanover, New Hampshire 03755-1290, 43p.